MOLECULAR MODELING OF POLY(2-ETHYL-2-OXAZOLINE)

A Thesis
Presented to
The Academic Faculty

by

Ayanna M. Bernard

In Partial Fulfillment
of the Requirements for the Degree
Doctor of Philosophy in the
School of Chemical & Biomolecular Engineering

Georgia Institute of Technology
August 2008

MOLECULAR MODELING OF POLY(2-ETHYL-2-OXAZOLINE)

Approved by:

Professor Peter Ludovice, Advisor
School of Chemical & Biomolecular Engineering
Georgia Institute of Technology

Professor Arthur Ragauskas
School of Chemistry & Biochemistry
Georgia Institute of Technology

Professor Yulin Deng
School of Chemical & Biomolecular Engineering
Georgia Institute of Technology

Professor Amyn Teja
School of Chemical & Biomolecular Engineering
Georgia Institute of Technology

Professor William Koros
School of Chemical & Biomolecular Engineering
Georgia Institute of Technology

Date Approved: July 7th 2008

Dedicated with Love to the Life and Legacy of

Deryck M. A. Bernard

1950 - 2008

ACKNOWLEDGEMENTS

This work would not have been possible without the grace of God and the help of those He has placed along the way.

I would like to thank my advisor Dr. Pete Ludovice for his guidance, my committee for their valuable input and my groupmates past and present for their help and support. I would also like to acknowledge the neighborly kindness and helpful nature of research groups such as the Breedveld, Nair, Khol, Beckham, Jones and Henderson groups. I must also thank Jae Kyu Cho who performed rheology experiments.

My parents, Deryck and Myrna and my sister, Denyse, have been my support and my most trusted advisors through everything. In addition I have been blessed with relatives and friends who each in their own way help to make the journey a bit easier.

This work is funded by the Institute of Paper Science and Technology, and for this I am grateful.

TABLE OF CONTENTS

LIST OF TABLES

LIST OF FIGURES

LIST OF SYMBOLS

Summary

PEOX	Poly(2-ethyl-2-oxazoline)
pH	Potential hydrogen

Chapter 1

PEOX	Poly(2-ethyl-2-oxazoline)
THF	Tetrahydrofuran
LCST	Lower critical solution temperature
PNIPAM	Poly(isopropyl acrylamide)
PVME	Poly(vinyl methyl ether)
pH	Potential hydrogen
PVPD	Poly(vinyl pyrrolidone)
Pro	Proline
C	Carbon
N	Nitrogen
PMOX	Poly(2-methyl-2-oxazoline)
°C	Degrees Celsius
M	Molar
NaCl	Sodium chloride
MD	Molecular dynamics
F	Force
U	Potential energy function
R	Position
t	Time
NVT	Canonical ensemble (N, V and T are conserved)

N	Number of moles
V	Volume
T	Temperature
MM	Molecular mechanics
SD	Steepest Descent
CG	Conjugate Gradient
TN	Truncated Newton
θ	Incident angle
d	Inter-planar spacing
λ	Wavelength of the incident beam
n	Order of diffraction
MOE®	Molecular Operating Environment

Chapter 2

PEOX	Poly(2-ethyl-2-oxazoline)
kg mol^{-1}	Kilograms per mole
°C	Degrees Celsius
THF	Tetrahydrofuran
SEC	Size Exclusion Chromatography
M_w	Weight average molecular weight
M_n	Number average molecular weight
M_w/M_n	Polydispersity
nm	Nanometers
HPLC	Hight performance liquid chromatography
μm	Micrometers
dn/dc	Refractive index increment
$< s^2 >^{1/2}$	Root mean square radius of gyration

R_g	Radius of gyration
M_w	Molecular weight
R(θ)	Rayleigh ratio
A_2	Second virial coefficient
K	Kelvin
c	Concentration
n_o	Refractive index of the solvent
λ_o	Wavelength of the incident light
θ	Detector angle
N_A	Avogadro's number
η_{red}	Reduced viscosity
η_{inh}	Inherent viscosity
$[\eta]$	Intrinsic viscosity
η	Viscosity of the solution
η_s	Viscosity of the solvent
M	Molecular weight
MHS	Mark Houwink Sakurada
K	MHS constant
a	MHS constant
θ	Theta
M	Molar
c*	Overlap concentration
c**	Crossover concentration from extremely dilute to dilute
g	Grams
dL	Deciliters
NaCl	Sodium chloride

Chapter 3

T	Absolute temperature
ΔG	Free energy of mixing
ΔH	Enthalpy of mixing
ΔS	Entropy of mixing
LCST	Lower critical solution temperature
PVDP	Poly(vinyl pyrrolidone)
PNIPAM	Poly(isopropyl acrylamide)
C	Carbon
N	Nitrogen
PEOX	Poly(2-ethyl-2-oxazoline)
THF	Tetrahydrofuran
WAXD	Wide angle x-ray diffraction
MOE®	Molecular Operating Environment
U	Potential energy
MMFF	Merck Molecular Force Field
P1	Space group P1
$\mathring{A}$	Angstrom
g cm^{-3}	Grams per cubic centimeter
ps	picoseconds
NVT	Canonical ensemble (N, V and T are conserved)
N	Number of moles
V	Volume
T	Temperature
MD	Molecular dynamics
NPA	Nosé Poincaré Andersen
MM	Molecular Mechanics

K	Kelvin
E_{str}	Bond stretch energy
E_{ang}	Bond angle bend energ
E_{oop}	Out-of-plane energy
E_{tor}	Torsion energy
E_{vdw}	Van der Waals energy
E_{ele}	Electrostatic energy
$^{\circ}$	Degrees
R_v	Viscomectric radius
$[\eta]$	Intrinsic viscosity
M	Molecular weight
N_A	Avogadro's number

Chapter 4

PEOX	Poly(2-ethyl-2-oxazoline)
LCST	Lower critical solution temperature
PNIPAM	Poly(isopropyl acrylamide)
PVPD	Poly(vinyl pyrrolidone)
$^{\circ}$	Degrees
MD	Molecular dynamics
MM	Molecular Mechanics
g cm^{-3}	Grams per cubic centimeter
K	Kelvin
ε	Dielectric constant
c	Concentration
ns	Nanosecond
ps	Picosecond

NaCl	Sodium chloride
R_g	Radius of gyration
$\mathring{A}$	Angstrom
C=O	Carboxyl
THF	Tetrahydrofuran

Chapter 5

poly(DADMAC)	Polydimethyldiallylammonium chloride
C-PAM	Cationic polyacryamide
PEO	Poly(ethylene oxide)
PEOX	Poly(2-ethyl-2-oxazoline)
MCC	Microcrystalline cellulose
°C	Degrees Celsius
kg mol^{-1}	Kilograms per mole
MB	Methylene blue
nm	Nanometers
$mol\ L^{-1}$	Moles per liter
rpm	Revolutions per minute
UV	Ultra violet
A	Absorbance
b	Path length
c	Concentration
$mg\ L^{-1}$	Milligrams per liter
ϵ	Absorbtivity
S_{MB}	Specific surface area
km^2kg^{-1}	Square kilometers per kilogram
N_g	Amount of methylene blue adsorbed at the monolayer

$kg\ kg^{-1}$	Kilograms per kilogram
a_{MB}	Surface area occupied by 1 methylene blue molecule
$\mathring{A}^2$	Squared angstroms
N	Avogadro's number
M_{MB}	Molecular weight of methylene blue
$g\ mol^{-1}$	Grams per mole
$kg\ mol^{-1}$	kilograms per mole
wt%	Percent by weight
R^2	Coefficient of determination
C	Equilibrium concentration
BET	Brunauer-Emmett-Teller
M	Molar
$mg\ g^{-1}$	Milligrams per gram

SUMMARY

Poly(2-ethyl-2-oxazoline) (PEOX) is a nonionic, synthetic polymer which is soluble in both organic solvents and water. It is biocompatible, heat stable and blends well with other polymers leading to its use in a variety of applications such as adhesives, photo resists, inks, coatings, compatibilizing agents in personal care products and in drug delivery agents.

Hydrogen bonding between the PEOX carbonyl group and water molecules facilitates the dissolution of PEOX in water and was hypothesized to result in conformational behavior besides a typical random coil of the polymer chain to and account for the negative entropy of mixing for PEOX in water.

The ordering of water molecules around PEOX was further hypothesized to facilitate the adsorption of PEOX to surfaces through increased entropy of the water molecules upon adsorption. PEOX adsorption onto cellulose could produce a useful papermaking additive which does not interfere with various other additives that interact with cellulose through electrostatic interactions.

The shape of PEOX in water was investigated experimentally to determine whether it forms a rigid rod helix. Viscometry measurements of PEOX in water show that its shape scales similar to a random coil and that its molecules collapse in the presence of sodium chloride.

Investigation into the molecular structure of PEOX through molecular scale simulations have revealed that although a rigid helical conformation does not exist, the potential exists for PEOX to have secondary helical structure in both water and other solvents. Without the rigid predicted structure, however, it is not surprising

that PEOX does not adsorb well on cellulose.

We originally hypothesized that PEOX formed a conformation other than a random coil which was stabilized by hydrogen bonds and only in water. This investigation has shown that in fact helical conformations exist which could be present in solvents other than water. Although the structure may not be entirely stabilized by water molecules, the side chain carbonyl groups of PEOX provide the opportunity for hydrogen bond bridges and complex networks of water. Comparing this folded helical conformation to a random coil conformation reveals that the random coil produces a lower energy system in water and can account for the network of water molecules which would explain the negative entropy of mixing observed for PEOX.

The conformation that we found with secondary helical structure is similar to a folded peptide or poly(N-substituted glycine) (peptoid) and may be present in both water and in organic solvents such as THF since it is a conformational phenomenon and not dependent on inter-chain hydrogen bonding. Although these helices are a structural possibility, random coils are more energetically favorable in vacuum and in aqueous solution. Helical peptoids, however, have added large chiral groups which stabilize secondary helical structure thus altered side groups with sufficient steric influence on poly(oxazolines) may actually stabilize helical configurations.

CHAPTER I

INTRODUCTION

1.1 Motivation and Objectives

The highly developed experimental techniques in polymer science provide insight into polymer properties that helps to make polymers invaluable materials in everyday life. Molecular modeling of these materials quantifies how and why they have their specific properties, which makes it a powerful predictive tool that can accelerate the discovery of new applications for polymers by exploring their behavior. Polymer solutions are no exception. This work explores the aqueous solution properties of poly(2-ethyl-2-oxazoline) (PEOX) with the intent that once its properties are better understood, it will find more extensive and valuable applications.

Poly(2-ethyl-2-oxazoline) is a tertiary amide polymer which belongs to the group of polymers known as poly(oxazolines). Poly(oxazolines) are useful in a variety of applications including steric stabilizers and biocompatible materials for drug delivery [12, 50, 4] . PEOX is used as an adhesive, as a compatibilizing agent in personal care products and is also used in polymer systems and in various block co-polymers and micelles for drug delivery [8, 51, 56].

PEOX is soluble in both a wide range of organic solvents and in water [8]. This study is done to investigate the structure of PEOX in water where hydrogen bonding between the PEOX carbonyl (C=O) group found on the PEOX side chain, shown in Figure 1.1, is hypothesized to facilitate the dissolution of PEOX in water and may result in a helical conformation or other behavior besides a typical random coil of the polymer chain.

In aqueous solution PEOX molecules are believed to be surrounded by a network

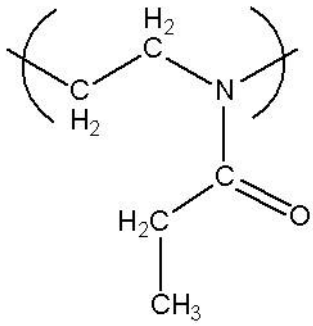

Figure 1.1: Primary Structure of Poly(2-ethy-2-oxazoline)

of water molecules. If this is true, the adsorption of PEOX on a surface will be facilitated by an increase in entropy due to the release of the water molecules which are no longer held to the polymer chain by hydrogen bonds.

Paper manufacture employs numerous colloidal particles such as fines, fibers and fillers in an aqueous suspension along with other additives and contaminants. This suspension is deposited onto a moving wire or fabric on which the water is drained and the solids are dried and formed into the paper sheet. It is important to the paper making process that the fine particles are retained on the wire and are not wasted through loss during drainage. This retention is accomplished by the use of various polymers which cause the aggregation of the fine particles to form larger ones [36]. Most of these colloidal particles are negatively charged and most of the polymers employed for retention and other purposes in the paper making process are positively charged as shown in Figure 1.2. Charge competition is therefore an important factor to consider in the choice of retention aid systems and other paper process additives.

This study probes the possibility of a rigid helical conformation which, if adsorbed onto a surface, would not result in a significant drop in entropy whereas a typical random coil polymer would significantly decrease the entropy of the system upon adsorption. Adsorption of a rigid conformation accompanied by disorganization of

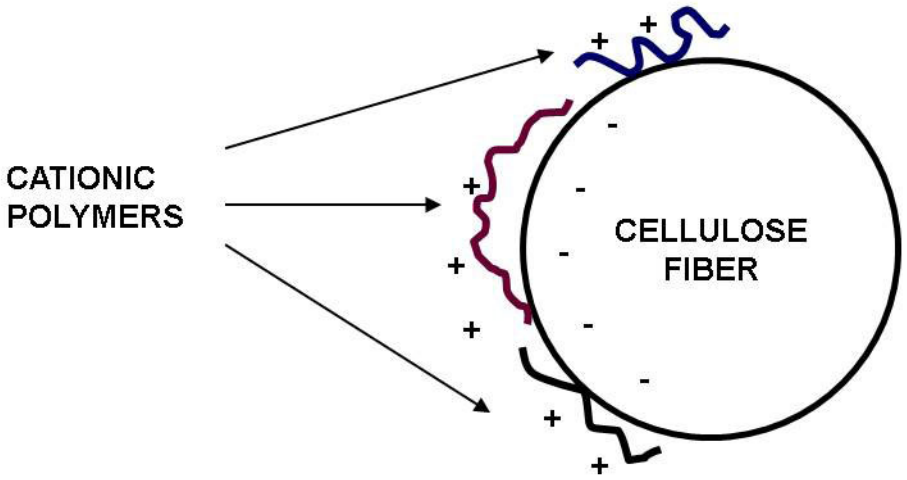

Figure 1.2: Adsorption of Cationic Polymers on Cellulose

water molecules was proposed to allow the adsorption of PEOX on cellulose fibers in the wet end processes of paper manufacture. Once adsorbed, it may contribute to the retention of particles or have other favorable effects on the process or final product without being a competitor for the charge sites employed by other polymers used in paper chemistry.

This work will begin to shed light on the interactions involved in PEOX aqueous solution behavior. Understanding this behavior not only leads to the prediction of how effective a paper making additive it will make, but also provides a basis for expanding how PEOX may be used more effectively in its other current and future applications.

The dissolution of PEOX in water causes a pronounced decrease in entropy of the system [5]. Such decreases in entropy of mixing usually occur in water soluble polymers with relatively rigid structures, rather than a more flexible random coil

conformation in solution. This rigidity, coupled with the organization of hydrogen bonded water molecules adjacent to the polymer result in the net decrease in entropy upon dissolution. This behavior has been found to occur in peptides and peptoids [58, 19] and given the similarity of the PEOX backbone to that of a peptide or peptoid, the following hypotheses were tested:

Hypothesis 1: PEOX forms a helix in aqueous solution

1. Hydrogen bonding between the C=O group on the side chain and water molecules facilitates a helical conformation

2. Helical conformation is not present in solvents, such as tetrahydrofuran (THF), which do not exhibit hydrogen bonding with PEOX

Hypothesis 2: This helical conformation is responsible for its tendency to adsorb onto polar surfaces

The overarching goal of this work was to develop techniques for modeling of polymer solution properties and to combine knowledge from simulation and experiment to predict and interpret polymer behavior and properties. More in depth understanding of polymer behavior on the molecular level helps to predict and explain macroscopic behavior in order to discover additional uses and develop tailored polymer systems for various applications.

More specifically, the goal was to develop a model of the conformation of poly(2-ethyl-2-oxazoline) in order to predict its usefulness in wet end paper processing through prediction of the mechanism by with PEOX could adsorb on cellulose.

Investigations were done into the aqueous solution properties of poly(2-ethyl-2-oxazoline) through light scattering and rheology experiments and in order to determine its shape and size and more specifically determine whether it forms a rigid rod

helix. The applicability of PEOX in paper making was investigated by adsorption experiments.

The conformation of PEOX in water was investigated through molecular dynamics and molecular mechanics computer simulations in Molecular Operation Environment (MOE®), which is a molecular simulation package of the Chemical Computing Group, and comparison of simulation results to experimentally obtained properties, such as molecular radii. The relationships between the radius of gyration and the molecular weight and intrinsic viscosity and molecular weight yielded insight into the shape of the polymer chain in water.

The behavior of PEOX in an organic solvent without proton donators (tetrahydrofuran) served as a reference by which the role of hydrogen bonding and the arrangement of water molecules relative to the polymer chain play a role in its conformation in water. The simulation of a non-hydrogen bonding environment was achieved by simple molecular simulations in vacuum.

The adsorption properties of PEOX on cellulose fibers were also investigated by adding the polymer to aqueous pulp suspensions and measuring the extent of adsorption using ultraviolet (UV) spectroscopy to measure polymer concentration in the solution and comparing original polymer concentration.

1.2 Water Soluble Polymers

1.2.1 Overview of Water Soluble Polymers

In order to dissolve in water, polymers must possess either a polar or an ionizable group which is hydrophilic. The arrangement of water molecules around a dissolved polymer is complex due to the combined effects of the hydrophilic groups and the hydrophobic groups which make up the remainder of the polymer. The range of polymers which utilize these interactions in order to be water soluble is quite extensive and based on their individual properties they are utilized in many applications.

PEOX falls into the category of nonionic water soluble polymers which utilize a polar hydrophilic group in order to dissolve in aqueous solution.

Water soluble nonionic polymers are commonly used to tailor the properties of coatings and emulsions by acting as thickening agents and dispersants. They are also finding uses as biocompatible polymers for example in micelles for drug delivery. Even with their many uses, the mechanism by which these polymers are solvated by water molecules is not completely understood.

Polymers when combined with water tend to produce various interesting interactions. In many cases the water molecules reorganize around hydrophobic groups for example poly(isopropyl acrylamide) (PNIPAM) and poly(vinyl methyl ether) (PVME) [49]. PNIPAM is a linear nonionic polymer which when it is dissolved in water, the water molecules reorganize around its hydrophobic isopropyl group. PNIPAM is also known to undergo a coil-globule transition with increasing temperature to a more compact conformation in water [18, 27]. Usually these transitions and changes in conformation are due to changes in solvent properties such as temperature, pH or salt content.

The salting out effect, which is well known in the study of protein behavior [2, 7], is another aspect of water soluble polymer behavior. Proteins form complex folded structures which are stabilized by hydrogen bonding between hydrophilic amino acid groups. These structures limit the interactions between hydrophilic groups. When salt ions are added to a dissolved protein, the water molecules are attracted by the ions and become less available to the hydrophillic protein segments. This results in increases hydrophobic interactions between protein molecules and leads to rearrangement of structures, agglomeration of molecules and ultimately to the protein becoming insoluble or salting out.

Poly(vinyl pyrrolidone) (PVPD), for example, in aqueous solution is surrounded by regularly arranged water molecules which are bound by hydrogen bonds to its

the amide group. These interactions account for decreases in the heat of mixing of aqueous PVPD solutions when salt is added [41]. PNIPAM also salts out and its LCST decreases the addition of salt [44].

1.2.2 Adsorption

Many water soluble polymers are adsorbed onto surfaces [45, 20, 34, 53]. In order for adsorption to occur the overall free energy should decrease. The loss in entropy upon adsorption is typically balanced by and interaction between the polymer and the surface which produces a favorable enthalpic change.

Adsorption of polymers from aqueous solution is generally facilitated by hydrogen bonding between the polymer and hydroxyl surface groups, hydrophobic interactions between non polar segments and hydrophobic surfaces, electrostatic interaction between charged groups and surfaces or by binding between ionic groups. Even weak interactions may facilitate adsorption if there are enough of them and for this reason higher molecular weight polymers often adsorb more readily.

1.2.3 Peptides and Peptiods

Integral to our approach in this study, is the comparison of PEOX structure to that of a peptide or N-substituted glycine (peptoid) polymer. Peptides have long been discovered to have various helical secondary structures which form the basis for various tertiary and quaternary structures[38, 39]. These helical structures are as a result of the peptide backbone conformational states, and are stabilized by hydrogen bonding between various peptide residues. Some residues which appear to have a random conformation, actually have some degree of ordered structure in the form of the left-handed poly (Pro) II conformation, which is stabilized by networks of water molecules which hydrogen bond with the backbone[46].

Peptoids have a similar structure to peptides but the backbone nitrogen atom of a peptoid is substituted, making peptoids generally incapable of hydrogen bonding with

themselves. Even without inter-chain hydrogen bonding of a peptide, some peptoids are found to have secondary helical structure and form tertiary structures consisting of helical bundles [19, 3, 30, 35]. Without the influence of interchain hydrogen bonding, helices in peptoids are sterically stabilized and not as susceptible to solvents conditions as are peptides and proteins [43].

The approach in this study of PEOX conformation is significantly based on the observation that poly (oxazolines) share the C-C-N backbone of a peptide or peptoid and may therefore share some of their conformational tendencies. The major conformational differences between PEOX and a peptide are the location of the carbonyl group, which is on the side chain for PEOX and on the backbone for a peptide and the substitution of the backbone nitrogen in PEOX which causes PEOX to not have a proton donating site. This is important, since peptide helices tend to be stabilized by hydrogen bonds between polymer segments. We hypothesized that helical structures of PEOX could be stabilized by hydrogen bond interactions in water.

1.3 Poly(2-ethyl-2-oxazoline)

PEOX is a relatively new synthetic polymer which has only been investigated to a limited extent, and has not been extensively modeled by computer simulation. It is a nonionic tertiary amide formed by the cationic ring opening polymerization of 2-ethyl-2-oxazoline [42].

There have been a few solution characterization studies [47, 8, 6] of PEOX in various solvents in order to investigate its behavior in these solvents and, to a limited extent, enable inferences to be made about its molecular shape in solution.

As mentioned, PEOX is soluble in a range of organic solvents [8] including alcohols in which hydrogen bonding is also a critical factor [5]. The solution behavior of PEOX in tetrahydrofuran (THF), a non hydrogen bonding solvent, was investigated by Sung and Lee using static light scattering and viscometry[47]. This study showed that

PEOX forms a random coil in THF at room temperature. In addition they proposed that PEOX contracts to form a "random Gaussian globule" i.e. a more compact conformation than is typical for a random coil. This contraction of the polymer is attributed to interactions between the carbonyl carbon in the side chain and the backbone nitrogen.

Viscosity measurements indicate that water is nearly a theta solvent for PEOX at room temperature, which means that the polymer chains behave almost ideally [8]. PEOX also exhibits lower critical solution temperature behavior in water[6, 5, 9]. This LCST behavior was determined by the decrease in second virial co-efficient with increasing temperature and is attributed to hydrogen bonding between the PEOX molecules and the water molecules [6, 5]. The excess enthalpy and excess entropy of mixing are both negative and have magnitudes which increase with molecular weight [5]. Both C.H. Chen and F.P. Chen attribute these properties to partial organization of the PEOX-water system through specific hydrogen bonding interactions between the carbonyl oxygen on the PEOX side chain and water molecules in solution. This claim is supported by the work of F.P. Chen and co-workers through infrared spectra which show a preferential interaction between the carbonyl oxygen and water molecules. This preferential interaction is evidenced by shifts in relative transmission peaks between non-hydrogen bonding solvent and deuterium oxide[6]. C.H. Chen compared PEOX with PMOX poly(2-methyl-2-oxazoline) which is identical in structure to PEOX except for the ethyl group on the side chain being substituted with a methyl group. They found that PMOX had a negative entropy of mixing with a larger magnitude than PEOX suggesting that water molecules are more highly ordered around PMOX which has the shorter alkyl group. This increased order around PMOX is due to the greater polarity of its carbonyl group and to a less bulky hydrophobic alkyl group interfering with hydrogen bonding of the carbonyl on the side chain with water molecules.

Aqueous PEOX solutions become turbid above 60°C. With the addition of NaCl the cloud point is decreased by as much as 1-2°C for a 0.3 M NaCl solution [33]

Adsorption of PEOX onto silica was investigated in a study by Chen, Wilson et al.[5]in both water and ethanol. The adsorption energy in water was found to be higher than in ethanol. This was attributed to specific solvent effects due to hydrogen bond bridges between silanol groups and the polymer in the water and related to the negative entropy of mixing of PEOX in water. This study has centered on testing the hypothesis that these observed behaviors in water are the result of a helical conformation.

PEOX is used as an adhesive [8, 13, 37]. Both the melt and the solution may be used in adhesion applications since PEOX is very water soluble and softens at 110°C to 120°C to form an easily processed melt with a thermal stability up to 380°C [8, 22]. PEOX combines well with many other polymers to form polymer blends [22, 23, 24, 9] and is therefore used to enhance many polymeric systems. The combination of being water soluble, heat stable and blending well with other polymers lend PEOX to be useful in a variety of applications. One example is as an additive in toner formulations for printing where heat stability and adhesion properties are useful [11].

Due to its biocompatible nature[12] PEOX is available for use in a variety of medical and personal care roles [21, 54]. PEOX has been used in drug delivery applications [31, 56, 17, 55]. There are various micellar systems used to deliver drugs [29, 56]. These polymeric drug delivery systems usually consist of a lyophilic centers to harbor hydrophobic drugs and enable them to evade recognition and get directly to pathological sites such as tumors. These systems consist of block co-polymers which self assemble into a hydrophobic core and a hydrophilic exterior. These micellar drug delivery systems have been shown to improve the stability and efficiency of anti-cancer drugs [48]. In addition to being hydrophilic, PEOX is also a pH responsive polymer which enables very specific control of drug delivery and release at the appropriate site

through pH cues [56, 17, 31]. Due to its dispersant properties and water solubility it is also used as a compatibilizing agent in personal care products [52].

PEOX is also used in photo resists [26] inks and coatings [25, 32, 14, 28, 40].

The usefulness and applicability of PEOX and other alkyl-oxazoline polymers in these and other applications will be expanded by continuing studies on the more efficient synthesis of oxazoline polymers and co-polymers [16, 15].

1.4 Molecular Modeling Techniques

This study has employed very traditional molecular modeling tools. The behavior of PEOX in aqueous solution was simulated by adding water molecules explicitly to a periodic cell around the structure of interest. Following equilibration by molecular dynamics and molecular mechanics, the properties of the system were analyzed.

The effects of changes in electrolyte concentration were examined through investigating the effect of changing the dielectric constant of the system. The dielectric constant reflects the extent to which the solvent can concentrate electrostatic lines of flux. Decreasing the dielectric constant was used to simulate the screening of the electrostatic effect of the water molecules on the polymer that would occur with the addition of salt.

1.4.1 Molecular Dynamics

In molecular dynamics (MD) simulation Newton's second law of motion is integrated using numerical integration methods. Newton's second law is given by

$$F = -\frac{dU}{dR} = m\frac{d^2R}{dt^2} \tag{1.1}$$

where F is the force, U is the potential energy function, R is position, m is mass and t is time. MD demonstrates the motion of particles in a molecular system over a specified time period. The goal of molecular simulation is to sample the phase space

which a molecular system occupies. In MD the system is assigned a temperature which provides energy for particles in the system to sample as many of the possible conformational states as possible. Statistical mechanics is used to calculate the bulk physical properties of the system based on the atomic positions and velocities of the simulation [1]

In this study MD is done using the NVT ensemble method which keeps the number of molecules, volume and temperature constant.

1.4.2 Molecular Mechanics

Molecular Mechanics (MM) generally refers to the minimization of the potential energy surface. The potential energy is calculated using a force field (potential energy function). MM algorithms find the gradient of the potential energy function and use the gradient to determine molecular coordinates which minimize the potential energy. In this work the MM algorithms used were Steepest Descent (SD), Conjugate Gradient (CG), and Truncated Newton (TN).

1.4.3 Force Field

The force field describes the atomic characteristics and interaction parameters which are used to calculate the potential energy of the system such as the bond lengths, bond angles atomic charges. In this study the Amber forcefield developed by Kholman and co-workers [10, 57] is used to model PEOX solution behavior because of its ability to simulate hydrogen bonding well and its common application to protein and peptide modeling since PEOX is viewed to have commonalities with peptide structure.

1.4.4 Wide Angle X-Ray Diffraction

X-ray diffraction is used in the analysis of the crystal structure of materials through the observation of the scattered intensity of an x-ray beam which was incident on

the sample in question. The scattered intensity is observed as a function of the incident angle of the beam, the scattered angle, the polarization of the beam and the wavelength or energy of the beam. The scattered angle is a function of the intermolecular distances, and by comparing the scattered intensity for various distances inferences can be made about the structure of solids. Observable diffraction angles obey the Bragg equation which relates the incident angle of the radiation (θ) to the inter-planar spacing (d) as follows:

$$\sin\theta = n\frac{\lambda}{2d} \tag{1.2}$$

where λ is the wavelength of the incident beam and n is the order of diffraction (an integer). The x-ray diffraction patterns of various PEOX structures were obtained by using the x-ray diffraction utility in the MOE®simulation package.

Through these simulation techniques, insight into the structure of PEOX and its interactions with water molecules were obtained and compared with experimental information to expand the overall understanding of how and why PEOX dissolves in water.

1.5 References

[1] Allen, M. P. and Tildesley, D. J., *Computer simulation of liquids*. Oxford [England]; New York: Clarendon Press ; Oxford University Press, 1987.

[2] Arakawa, T. and Timasheff, S. N., "Mechanism of protein salting in and salting out by divalent cation salts: balance between hydration and salt binding," *Biochemistry*, vol. 23, no. 25, pp. 5912–5923, 1984.

[3] Baldauf, C., Günther, R., and Hofmann, H.-J., "Helices in peptoids of alpha and beta peptides," *Physical Biology*, vol. 3, no. 1, p. S1, 2006. 1478-3975.

[4] Bernard, R., Loge, G. W., and Krylova, K., "Separation media including oxazoline polymers," 2005.

[5] Chen, C. H., Wilson, J. E., Davis, R. M., Chen, W., and Riffle, J. S., "Measurement of the segmental adsorption energy of poly(2-ethyl-2-oxazoline) on silica in water and ethanol," *Macromolecules*, vol. 27, no. 22, pp. 6376–6382, 1994.

[6] Chen, F., Ames, A., and Taylor, L., "Aqueous solutions of poly(ethyloxazo1line) and its lower consolute phase transition," *Macromolecules*, vol. 23, no. 21, pp. 4688–4695, 1990.

[7] Chi, E. Y., Krishnan, S., Randolph, T. W., and Carpenter, J. F., "Physical stability of proteins in aqueous solution: Mechanism and driving forces in nonnative protein aggregation.," *Pharmaceutical Research*, vol. 20, no. 9, pp. 1325–36, 2003.

[8] Chiu, T. T., Thill, B. P., and Fairchok, W. J., "Poly (2-ethyl-2-oxazoline): A new water-and organic soluble adhesive," *by JE Glass, ACS*, p. 425, 1986.

[9] Christova, D., Velichkova, R., Loos, W., Goethals, E. J., and Prez, F. D., "New thermo-responsive polymer materials based on poly(2-ethyl-2-oxazoline) segments," *Polymer*, vol. 44, no. 8, p. 2255, 2003.

[10] Cornell, W. D., Cieplak, P., Bayly, C. I., Gould, I. R., Merz, K. M., Ferguson, D. M., Spellmeyer, D. C., Fox, T., Caldwell, J. W., and Kollman, P. A., "A second generation force field for the simulation of proteins, nucleic acids, and organic molecules," *Journal of the American Chemical Society*, vol. 117, no. 19, pp. 5179–5197, 1995.

[11] Fuller, Timothy J. Xerox Corp., U., "Processes for the preparation of toner compositions.," 1993.

[12] Gaertner, F. C., Luxenhofer, R., Blechert, B., Jordan, R., and Essler, M., "Synthesis, biodistribution and excretion of radiolabeled poly(2-alkyl-2-oxazoline)s," *Journal of Controlled Release*, vol. 119, no. 3, p. 291, 2007.

[13] Hanrot, A., "Polyethyloxazoline adhesives and application of water-soluble adhesives to paper," 2007.

[14] Hood, D. K., "Coating composition for forming an inkjet-printable coating on a substrate," 2007.

[15] Hoogenboom, R. and Fijten, Martin W. M.and Thijs, H. M. L. S. U. S., "Poly(2-oxazoline)s: Potential candidates for personal care applications.," in *234th ACS National Meeting*, (Boston, MA, United States), 2007.

[16] Hoogenboom, R., Fijten, M. W. M., Paulus, R. M., Thijs, H. M. L., Hoeppener, S., Kickelbick, G., and Schubert, U. S., "Accelerated pressure synthesis and characterization of 2-oxazoline block copolymers," *Polymer*, vol. 47, no. 1, p. 75, 2006.

[17] Hsiue, G.-H., Wang, C.-H., Lo, C.-L., Wang, C.-H., Li, J.-P., and Yang, J.-L., "Environmental-sensitive micelles based on poly(2-ethyl-2-oxazoline)-b-poly(l-lactide) diblock copolymer for application in drug delivery," *International Journal of Pharmaceutics*, vol. 317, no. 1, p. 69, 2006.

[18] Hu, Y., Xiaohu, Y., and Rongshi, C., "Investigation of solution properties of poly(n-isopropylacrylamide) in water with its thermohistory," *Journal of Polymer Science Part B: Polymer Physics*, vol. 38, no. 9, pp. 1188–1192, 2000.

[19] Huang, K., Wu, C. W., Sanborn, T. J., Patch, J. A., Kirshenbaum, K., Zuckermann, R. N., Barron, A. E., and Radhakrishnan, I., "A threaded loop conformation adopted by a family of peptoid nonamers," *J. Am. Chem. Soc.*, vol. 128, no. 5, pp. 1733–1738, 2006.

[20] Ishimaru, Y. and Lindstrm, T., "Adsorption of water-soluble, nonionic polymers onto cellulosic fibers," *Journal of Applied Polymer Science*, vol. 29, no. 5, pp. 1675–1691, 1984.

[21] Jensen, S. D., "Peroxide/poly(2-ethyl-2-oxazoline) gel compositions of good stability for bleaching of teeth, hair, laundry," 20060208. 2007.

[22] Keskkula, H. and Paul, D. R., "Miscibility of polyethyloxazoline with thermoplastic polymers," *Journal Of Applied Polymer Science*, vol. 31, no. 5, pp. 1189–1197, 1986.

[23] Keskkula, H. and Paul, D. R., "Thermal-behavior of polyethyloxazoline," *Journal Of Applied Polymer Science*, vol. 31, no. 3, pp. 941–950, 1986.

[24] Keskkula, H., Paul, D. R., Young, P., and Stein, R. S., "Diffusion of miscible polymers in multilayer films," *Journal Of Applied Polymer Science*, vol. 34, no. 5, pp. 1861–1877, 1987.

[25] Khoultchaev, K. K., Ho, C. T., Xu, Z., and Liu, S. X., "Fast drying ink jet recording medium having an anionic surface layer and a cationic underlayer," 2007.

[26] Kim, M. S., Lee, H. J., and Park, C. S., "Manufacture of negative photoresist containing poly(2-ethyl-2-oxazoline) and azide photosensitizer," 2006.

[27] Kujawa, P. and Winnik, F. M., "Volumetric studies of aqueous polymer solutions using pressure perturbation calorimetry: A new look at the temperature-induced phase transition of poly(n-isopropylacrylamide) in water and d_2o," *Macromolecules*, vol. 34, no. 12, pp. 4130–4135, 2001.

[28] Kuwahara, K., Nanbu, H., Ibi, A., and Fukuyama, Y., "Polymer dispersant for pigment and nonaqueous pigment dispersion containing it," 2007.

[29] Kwon, G. S. and Okano, T., "Polymeric micelles as new drug carriers," *Advanced Drug Delivery Reviews*, vol. 21, no. 2, pp. 107–116, 1996.

[30] Lee, B. C., Zuckermann, R. N., and Dill, K. A., "Folding a nonbiological polymer into a compact multihelical structure," *J. Am. Chem. Soc.*, vol. 127, no. 31, pp. 10999–11009, 2005.

[31] Lee, S. C., Kang, S. W., Kim, C., Kwon, I. C., and Jeong, S. Y., "Synthesis and characterization of amphiphilic poly(2-ethyl-2-oxazoline)/poly(epsilon-caprolactone) alternating multiblock copolymers," *Polymer*, vol. 41, no. 19, pp. 7091–7097, 2000. 0032-3861.

[32] Liaw, J.-J., "Integrated semiconductor structure for static random access memory (sram) cells," 2007.

[33] Lin, L.-N., Brandts, J. F., Brandts, J. M., and Plotnikov, V., "Determination of the volumetric properties of proteins and other solutes using pressure perturbation calorimetry," *Analytical Biochemistry*, vol. 302, no. 1, p. 144, 2002.

[34] Lindstrom, T. and Glad-Nordmark, G., "Selective adsorption, flocculation, and fractionation of wood pulps with polyethyleneoxide," *Journal of Colloid and Interface Science*, vol. 94, no. 2, p. 404, 1983.

[35] Lucas, A., Huang, L., Joshi, A., and Dill, K. A., "Statistical mechanics of helix bundles using a dynamic programming approach," *J. Am. Chem. Soc.*, vol. 129, no. 14, pp. 4272–4281, 2007.

[36] Moore, G. and Pira, I., *Wet End Chemistry Strategies: A Literature Review.* Pira International, 1992.

[37] Mueller, G. and Ahmed, S., "Moisture-activable adhesive reinforcement strings and tear opening tapes for corrugated and cartonstock containers," 1999.

[38] Pauling, L., Corey, R. B., and Branson, H. R., "The structure of proteins - 2 hydrogen-bonded helical configurations of the polypeptide chain," *Proceedings Of The National Academy Of Sciences Of The United States Of America*, vol. 37, no. 4, pp. 205–211, 1951.

[39] Perutz, M. F., "New x-ray evidence on the configuration of polypeptide chains: Polypeptide chains in poly-[gamma]-benzyl-l-glutamate, keratin and haemoglobin," *Nature*, vol. 167, no. 4261, p. 1053, 1951.

[40] Pomplun, W. S. and Kerins, J. E., "Ion-trigger polymer coatings on water-sensitive polymer films," 2000.

[41] Rice, S. A. and Nagasawa, M., *Polyelectrolyte solutions, a theoretical introduction*. London, New York,: Academic Press, 1961.

[42] Rivas, B. L. and Ananias, S. I., "Ring opening polymerization of 2-ethyl-2-oxazoline.," *Polymer Bulletin*, vol. 18, no. 3, pp. 189–94, 1987.

[43] Sanborn, T. J., Wu, C. W., Zuckermann, R. N., and Barron, A. E., "Extreme stability of helices formed by water-soluble poly-n-substituted glycines (polypeptoids) with," *Biopolymers*, vol. 63, no. 1, pp. 12–20, 2002.

[44] Schild, H. G., "Poly(n-isopropylacrylamide): experiment, theory and application," *Progress in Polymer Science*, vol. 17, no. 2, p. 163, 1992.

[45] Shulga, A., Widmaier, J., Pefferkorn, E., Champ, S., and Auweter, H., "Kinetics of adsorption of polyvinylamine on cellulose fibers: I. adsorption from salt-free solutions," *Journal of Colloid and Interface Science*, vol. 258, no. 2, p. 219, 2003.

[46] Sreerama, N. and Woody, R. W., "Molecular dynamics simulations of polypeptide conformations in water: A comparison of alpha, beta, and

poly(pro)ii conformations," *Proteins: Structure, Function, and Genetics*, vol. 36, no. 4, pp. 400–406, 1999.

[47] Sung, J. and Lee, D., "Molecular shape of poly(2-ethyl-2-oxazoline) chains in thf," *Polymer*, vol. 42, pp. 5771–5779, 2001.

[48] Sutton, D., Nasongkla, N., Blanco, E., and Gao, J., "Functionalized micellar systems for cancer targeted drug delivery," *Pharmaceutical Research*, vol. 24, no. 6, p. 1029, 2007.

[49] Tamai, Y., Tanaka, H., and Nakanishi, K., "Molecular dynamics study of polymer-water interaction in hydrogels. 1. hydrogen-bond structure," *Macromolecules*, vol. 29, no. 21, pp. 6750–6760, 1996.

[50] Thill, B. P., "Blend of polycarbonate and polyamide compatibilized with a polyalkyloxazoline," 1989.

[51] Torgerson, P. M. and Midha, S., "Cosmetic and pharmaceutical compositions containing silicone grafted thermoplastic elastomeric copolymers," 1995.

[52] Torizuka, M., Suzuki, H., Fujiwara, K., Oda, T., Tanaka, N., and Rindo, K., "Emulsified, water-in-oil type composition and skin cosmetic preparation," 1997.

[53] Torn, L. H., Koopal, L. K., deKeizer, A., and Lyklema, J., "Adsorption of nonionic surfactants on cellulose surfaces: Adsorbed amounts and kinetics," *Langmuir*, vol. 21, no. 17, pp. 7768–7775, 2005.

[54] Trieu, H. H., Carls, T., Lim, R., Lange, E. C., Anderson, K. M., and Bruneau, A., "Interosteotic implant comprising a metallic or polymeric material for treatment of spinal disorders," 2007.

[55] Unger, E. C., Matsunaga, T. O., and Zutshi, R., "Liquid-filled nanodroplets containing lipids and antitumor drugs for cancer treatment," 20060207. 2007.

[56] Wang, C.-H., Wang, C.-H., and Hsiue, G.-H., "Polymeric micelles with a ph-responsive structure as intracellular drug carriers," *Journal of Controlled Release*, vol. 108, no. 1, p. 140, 2005.

[57] Wang, J., Cieplak, P., and Kollman, P., "How well does a restrained electrostatic potential (resp) model perform in calculating conformational energies of organic and biological molecules?," *J. Comput. Chem.*, vol. 21, pp. 1049–1074, 2000.

[58] Xu, H. and Berne, B. J., "Hydrogen-bond kinetics in the solvation shell of a polypeptide," *J. Phys. Chem. B*, vol. 105, no. 48, pp. 11929–11932, 2001.

CHAPTER II

EXPERIMENTAL CHARACTERIZATION OF PEOX SOLUTIONS

2.1 Introduction

The conformation of poly(2-ethyl-2-oxazoline) in water has only been investigated to limited extent [9, 7, 18, 6, 24] with conclusions being drawn about its solution behavior but not its shape.

Water is nearly a theta solvent for PEOX at room temperature as is indicated by viscometry [9]. The second virial co-efficient of aqueous PEOX solutions decreases with increasing temperature indicating lower critical solution temperature behavior and attributed to hydrogen bonding between the PEOX molecules and the water molecules [7, 6] . The excess enthalpy and excess entropy of mixing in water become increasingly negative as the molecular weight of PEOX increases due to the partial organization of the PEOX-water system through specific hydrogen bonding interactions between the carbonyl oxygen on the PEOX side chain and water molecules in solution [6]. Water molecules are more highly ordered around PMOX which has the shorter alkyl group due to the greater polarity of its carbonyl group and to a less bulky hydrophobic alkyl group interfering with hydrogen bonding of the carbonyl on the side chain with water molecules.

Static light scattering and dilute solution viscometry were employed in this study to compare observed behavior to a molecular model. Fractionation of the PEOX samples was used in an attempt to obtain narrow molecular weight distributions so that light scattering could be performed.

The salting out effect, where the decreased availability of water molecules to interact with hydrophobic groups causes increased hydrophobic interactions and precipitation, is well known in the study of protein behavior [1, 8]. The addition of salts to water soluble polymers has also been shown to cause changes in polymer conformation [10, 18, 22, 21]. For poly(oxazolines) "salting out" has been observed by decreases in the cloud point of aqueous PEOX solutions with the addition of NaCl [18] as well as the decrease in phase transition temperature, increase in phase transition enthalpy and decrease in the hydration layer around the polymer chains with addition of NaCl to poly(2-isopropyl-2-oxazoline) solutions [10]. Following the trend of these observations the effect of salt on PEOX conformation in water was also investigated by viscometry measurements to shed light on the important effects which drive its dissolution in water.

2.2 Methodology

2.2.1 Fractionation

PEOX samples were obtained from Sigma Aldrich with reported molecular weights 500, 200 and 50 kg mol^{-1} (denoted as 500K, 200K and 50K in this study). The 200 kg mol^{-1} sample was fractionated in order to obtain samples of narrow molecular weight distribution. Fractionation was done by the column elution technique [23, 5]. A column was packed with 0.5 mm diameter glass beads which were coated in PEOX by adding a 20% solution of PEOX in acetone to the beads and adding n-hexane in order to precipitate the polymer onto the beads. Adding non-solvent facilitated the deposition of higher molecular weight molecules onto the bead surface first and smaller molecular weights in the outermost layers [5]. Solvent of increasing strength was then eluted down the column under gravity at room temperature (24°C) starting with 100% non-solvent n-hexane and increasing solvent power to 100% excellent solvent tetrahydrofuran (THF). Ten or more fractions were collected and the polymer

extracted by solvent evaporation.

Size Exclusion Chromatography (SEC) was performed in THF in order to determine the weight average molecular weight (M_w) and number average molecular weight (M_n) and the polydispersity (M_w/M_n) or molecular weight distribution of the three manufacturer's samples and of the fractions which were extracted.

2.2.2 Static Light Scattering

Static multi-angle light scattering was done at room temperature ˜24°C using Wyatt Technology Corporation's light scattering equipment on PEOX samples and fractions at a wavelength of 690nm. HPLC-grade water was used instead of deionized water and all samples were filtered through a 0.1 μm Whatman®syringe filter. The refractive index increment (dn/dc) was measured using the Wyatt Technology Corporation Waters 2410 Refractive Index Detector. The refractive index increment was found by plotting the refractive index vs. a range of concentrations for each molecular weight for a series of concentrations and finding the gradient. A Zimm plot [13, 26] was used to calculate the root mean square radius of gyration $< s^2 >^{1/2}$ or R_g and molecular weight M_w.

The Rayleigh ratio, R(θ), which is the ratio of the intensity of scattered to incident light, is related to the second virial coefficient (A_2), the radius of gyration R_g and polymer weight average molecular weight M_w. by:

$$\frac{Kc}{R(\theta)} = \frac{1}{M_w}\left[1 + \frac{16\pi^2 n_o^2}{3\lambda_o^2} R_g^2 \sin^2\left(\frac{\theta}{2}\right)\right] + 2A_2 c \tag{2.1}$$

where c is the concentration of the polymer solution, n_o is the refractive index of the solvent, λ_o is the wavelength of the light incident on the sample, θ is the detector angle and

$$K = \frac{4\pi^2 n_o^2}{N_A \lambda_o^4}\left(\frac{dn}{dc}\right)^2 \tag{2.2}$$

where N_A is Avogadro's number.

The Zimm method [13, 26] was used to find R_g, A_2 and M_w. From equation **??**, when θ=0

$$\frac{Kc}{R(\theta)} = 2A_2c + \frac{1}{M_w} \tag{2.3}$$

and when c=0

$$\frac{Kc}{R(\theta)} = \frac{1}{M_w}\left[1 + \frac{16\pi^2 n_o^2}{3\lambda_o^2} R_g^2 \sin^2\left(\frac{\theta}{2}\right)\right] + \frac{1}{M_w} \tag{2.4}$$

Therefore from a plot of Kc/R(θ) vs. $\sin^2\theta/2$ + kc, where k is an arbitrary constant which adjusts the appearance of the Zimm plot, the θ=0 line has a slope proportional to A_2, the c=0 line has a slope proportional to R_g^2 and the two lines intercept at $1/M_w$..

2.2.3 Dilute Solution Viscometry

The rheologic behavior of dilute aqueous PEOX solution at 25C was investigated using a Cannon Fenske viscometer. The elution time for PEOX solutions of various concentrations ranging from 0.02-0.8 g/dL were measured in a water bath. As with light scattering HPLC-grade water was used and all samples were filtered through a 0.1 μ m syringe filter. The reduced and inherent viscosities (η_{red} and η_{inh}) were calculated and subsequently the intrinsic viscosity ([η]) of each sample.

$$\eta_{red} = (\eta/\eta_s - 1)/c \tag{2.5}$$

$$\eta_{inh} = (ln(\eta/\eta_s))/c \tag{2.6}$$

Where η is the viscosity of the solution, η_s is the viscosity of the solvent and c is the solution concentration. The ratio η/η_s is obtained from the ratio of the solution

elution time to solvent elution time. When the reduced and inherent viscosities are plotted verses concentration, the intrinsic viscosity is obtained by the extrapolation of either curve to c=0. The intrinsic viscosity gives a measure of the solute contribution to the solution viscosity.

The intrinsic viscosity of a polymer solution is related to the molecular weight (M) by the Mark Houwink Sakurada (MHS) relation [15]:

$$[\eta] = KM^a \tag{2.7}$$

where K and a are constants for each polymer-solvent combination. On a logarithmic plot of $[\eta]$ verses M, the slope a, for a typical random coil polymer, is between 0.5 and 0.8. If a $>$ 0.8 the polymer is considered to be semi-flexible and if a $<$ 0.5 it is considered collapsed. At the θ condition ($A_2 = 0$) a = 0.5 and for a rigid rod a = 2.

Viscometry was also done in 0.5M and 1M NaCl solutions to investigate the effect of salt on the conformation of PEOX in water.

2.2.4 Effect of Temperature on Viscosity

In proteins the viscosity is temperature dependent due to the effects of temperature on molecular structure and therefore viscosity [19, 20]. The viscosity of PEOX 500kg/mol samples in water with viscosity of approximately 2cp was measured with increasing temperature from 20 to 50°C) using a Paar Physica rheometer.

2.3 Results and Discussion

2.3.1 Fractionation

The molecular weights and molecular weight distributions of the manufactured PEOX samples and some of the fractions obtained are shown in Table 2.1 The lowest molecular weight distributions obtained from fractionation ranged from 1.7 to 2.2.

The fractions obtained are identified as E or F and all have lower polydispersities than the starting sample (200K). The samples also increase in molecular weight as

the fraction number increases which corresponds to increasing solvent power with increasing fraction number.

Table 2.1: Molecular weight and polydispersity (M_w/M_n) of PEOX samples from size exclusion chromatography along with refractive index increment (dn/dc)

Sample I.D.	$M_n \times 10^{-3}$ ($gmol^{-1}$)	M_w×10-3 (g/mol)	M_w /M_n	dn/dc (cm^3g^{-1})
50K	95	710	7.5	0.194
200K	450	2420	5.4	0.184
500K	615	2619	4.3	0.182
E12	312	629	2.0	
E13	549	1175	2.1	
E14	949	1628	1.7	
E15	1276	2840	2.2	
F5	157	279	1.8	
F7	236	490	2.1	
F8	341	691	2.0	

2.3.2 Static Light Scattering

The values of the derivative of the refractive index of the polymer solution with respect to the concentration dn/dc used to produce the Zimm plots, and molecular weights determined from SEC are shown in Table 2.1. Static light scattering was done primarily to obtain the radius of gyration for PEOX of different narrowly defined molecular weights. The Zimm plots obtained were not regular and reproducible due to the broad molecular weight distribution of both the original samples and the best fractions obtained. Figure 2.1 shows the regular pattern of a typical Zimm plot which was obtained for a monodisperse poly (styrene) standard in THF as well as the Zimm plot for the PEOX fraction with the narrowest polydispersity, E14, in THF.

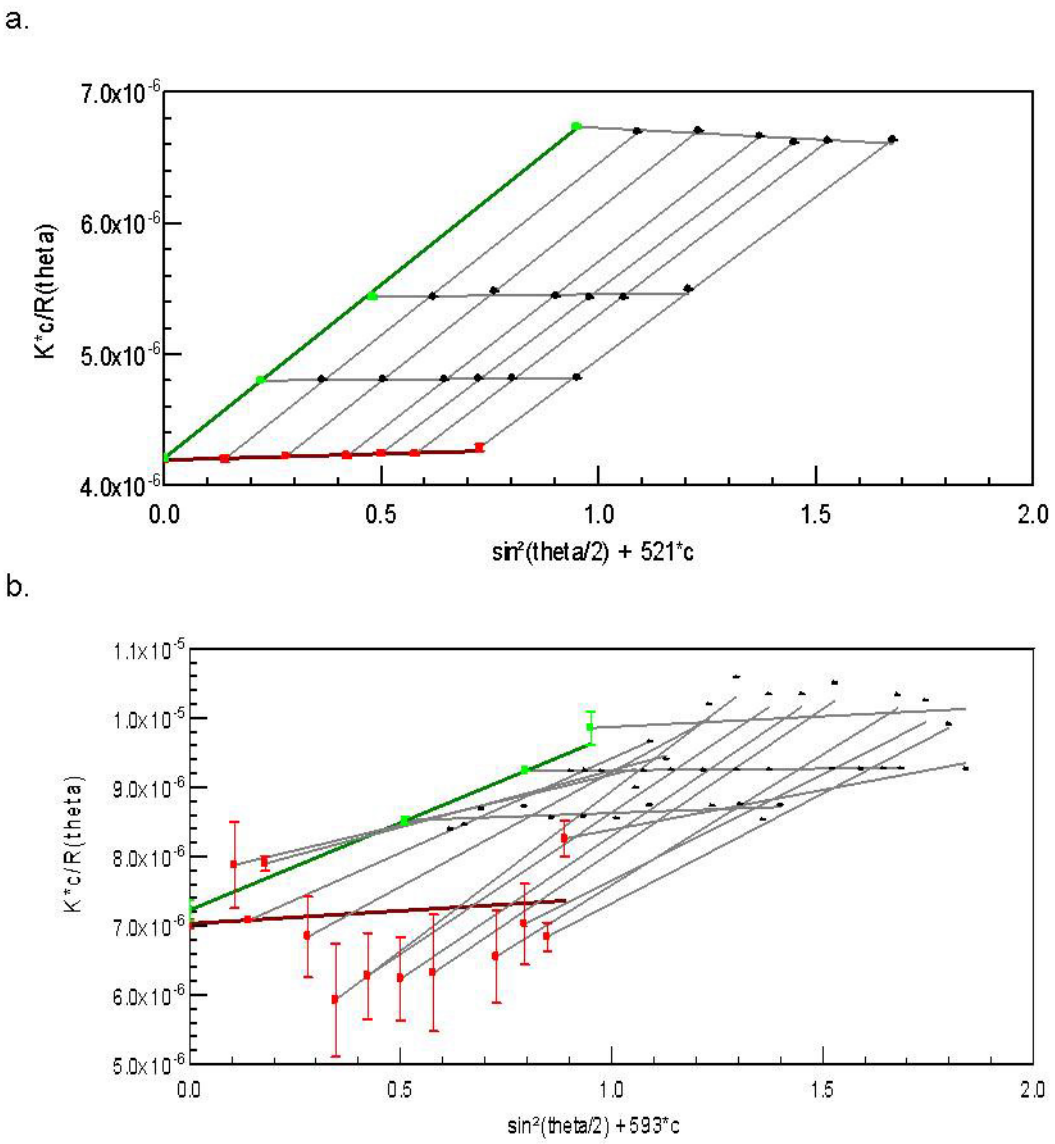

Figure 2.1: Zimm plots for a. a narrow poly(styrene) standard and b. PEOX fraction E14 both in THF

The mean squared radius of gyration is related to M by:

$$< R_g^2 >^{1/2} \propto M^a \tag{2.8}$$

For a random coil at the θ condition, a = 0.5 [14] and for an extended conformation

such as a rigid rod a = 1 [14]. This scaling should determine if PEOX is adopting a helix in solution since a helix should scale similar to a rigid rod. The radii of gyration for the manufactured samples have been previously reported between 14 an 21nm but with an unlikely a of 0.14 [2], however, due to the irregularities in the light scattering results, dilute solution viscometry measurements were deemed more appropriate for determination of polymer structure.

2.3.3 Dilute Solution Viscometry

The relative and inherent viscosities for PEOX of nominal molecular weights 50, 200 and 500 kg mol^{-1} are plotted in Figures 2.2 through 2.4. It can be observed that there is a change in slope for the reduced and inherent viscosities verses molecular weight. These changes in slope generally occur in response to a change in concentration regime.

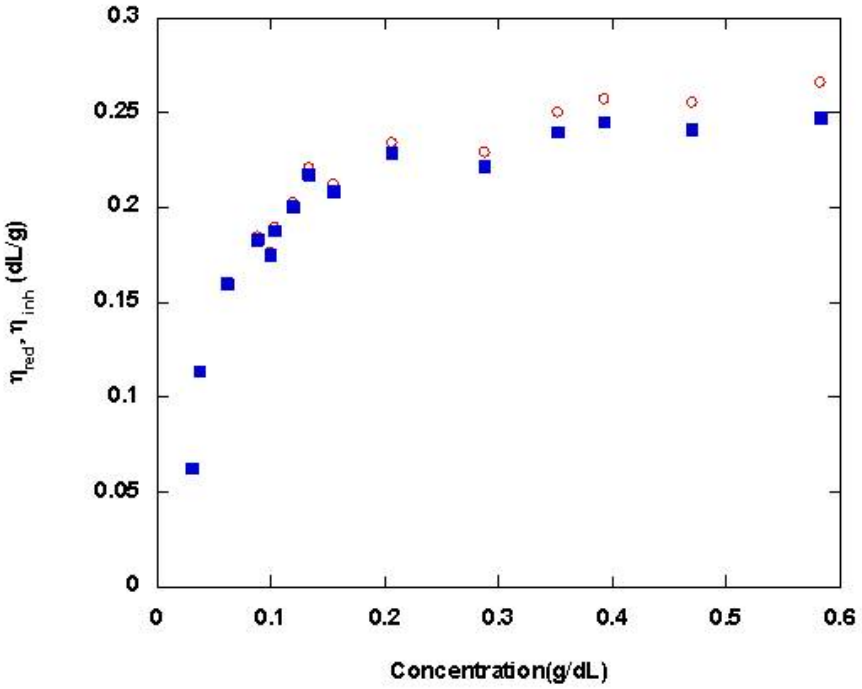

Figure 2.2: Reduced (open circles) and inherent (filled squares) viscosity verses concentration for 50kg mol^{-1}sample

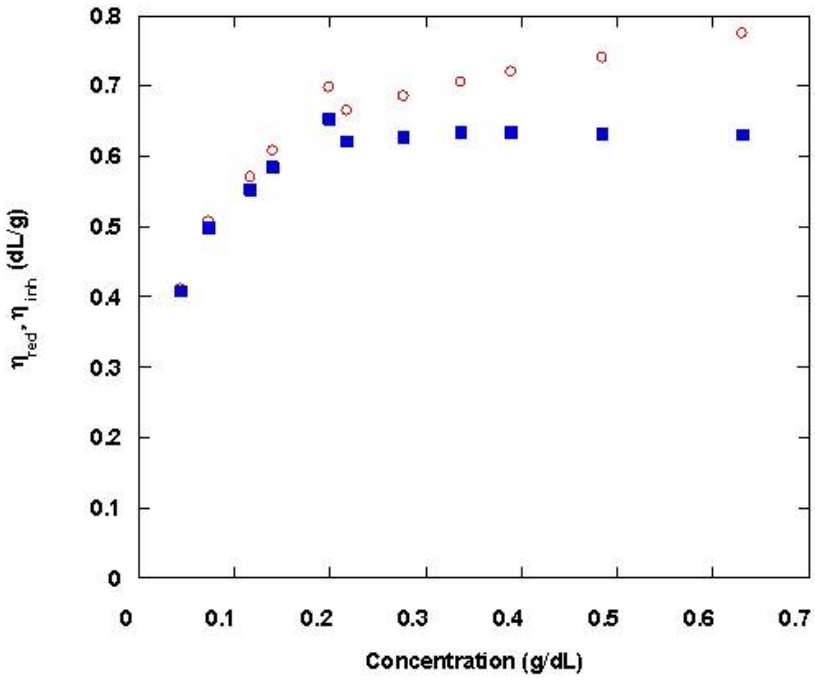

Figure 2.3: Reduced (open circles) and inherent (filled squares) viscosity verses concentration for 200kg mol^{-1}sample

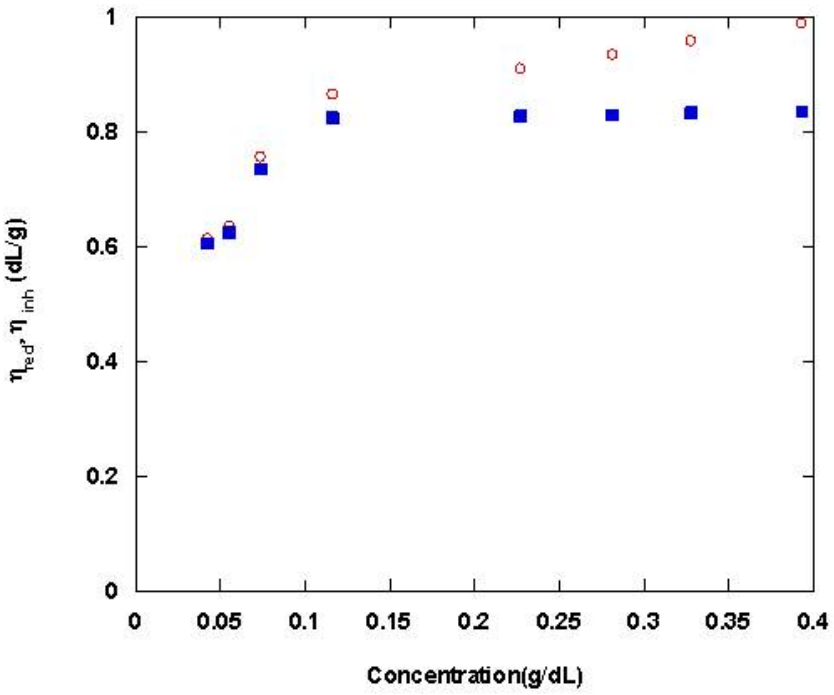

Figure 2.4: Reduced (open circles) and inherent (filled squares) viscosity verses concentration for 500kg mol^{-1}sample

The concentration regime represented by the observed change is from the extremely dilute to the dilute regime. This critical concentration c** was identified by Donods and co-workers [16, 17, 11, 12] and corresponds with the first permanent contacts between macromolecules in the solution [4, 3]

The more well known regime change is from dilute to semi-dilute solution and this change occurs at a concentration c*>c** close to $1/[\eta]$. The intrinsic viscosity values and calculated overlap concentration c* for the PEOX samples are shown in Table 2.2 along with estimated values of c**.

As shown in Table 2.2 the critical concentration c*, calculated from obtained from the measured intrinsic viscosity, lies well beyond the concentration range examined so the critical concentration which lies near to 0.2g/L for the 3 samples is therefore c**.

Table 2.2: Intrinsic viscosity and critical overlap concentrations of PEOX samples

Sample I.D.	$[\eta]$ (dL/g)	c*(1/$[\eta]$) (g/dL)	c** (g/dL)
50K	0.23	4.3	0.2
200K	0.63	1.6	0.2
500K	0.81	1.2	0.2

c* tends to be about ten times greater than c** [16] this is true in this case since the c* values in Table 2.2 about a factor of ten greater than the c** values. The observation of this regime change during dilute solution viscometry is attributed to the adsorption of polymer onto the capillary of the viscometer, causing an artificial increase in the viscosity for lower concentrations which are sensitive to this effect [25]. It is proposed by Yang and coworkers [25] that this effect could be corrected by measuring the solvent elution time after running polymer solution through the capillary and without rinsing or drying the viscometer. This way the effect of adsorbed polymer will be canceled out. This procedure however did not yield a significant difference in the resulting curves shown in Figures 2.2 through 2.4.

The dependence of $[\eta]$ on molecular weight is shown in Figure 2.5 and yields the MHS relation:

$$[\eta] = 5.7 \times 10^{-4} M^{0.56 \pm 0.17} \tag{2.9}$$

This result shows agreement with values reported in literature particularly for the exponent. The MHS relation obtained by Chiu and co-workers is [9]:

$$[\eta] = 6.5 \times 10^{-4} M^{0.56} \tag{2.10}$$

An exponent of 0.5 is predicted for a random coil near the θ condition by extensive polymer theory and experiment and approaches 0.6 for a solvent system at the theta

condition. PEOX therefore scales with a random coil in aqueous solution at 25°C.

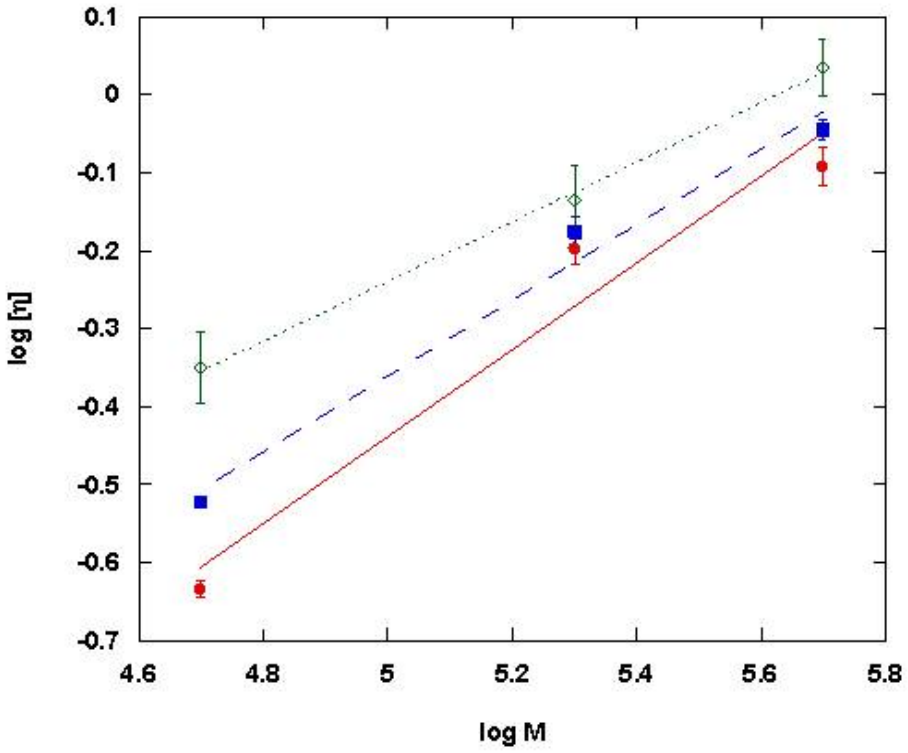

Figure 2.5: Log of intrinsic viscosity as a function of the log of the molecular weight for PEOX in HPLC water (filled circles), 0.5M $NaCl_{(aq)}$ (filled squares) and 1M $NaCl_{(aq)}$ (open diamonds). The error bars are the 95% confidence interval.

The effect of NaCl on the viscosity of PEOX in aqueous solution yielded the following MHS relations for 0.5 and 1 M solutions of NaCl.

$$0.5M : [\eta] = 1.6 \times 10^{-3} M^{0.48 \pm 0.09} \tag{2.11}$$

$$1.0M : [\eta] = 1.1 \times 10^{-2} M^{0.35 \pm 0.03} \tag{2.12}$$

The exponent decreases with the addition of salt to the solution signaling a reduction in the polymer volume upon addition of ions which appear to interfere with the hydrogen bonds which facilitate the expansion and dissolution of PEOX. This is salting-out effect was previously observed through cloud point experiments of Lin et al [18].

This mirrors the behavior of poly(2-isopropyl-2-oxazoline) (PIPOX) as outlined by Diab and coworkers [10] who observed a salt induced reduction in solvation power for PIPOX in water. This effect is believed to be due to the increased availability of carbonyl groups with increased molecular weight.

2.3.4 Effect of Temperature on Viscosity

Figure 2.6 shows the viscosity of PEOX in water verses temperature. This relationship is linear as for DI water indicating that PEOX aqueous solutions behave as Newtonian fluids without significant conformational changes with increasing temperature.

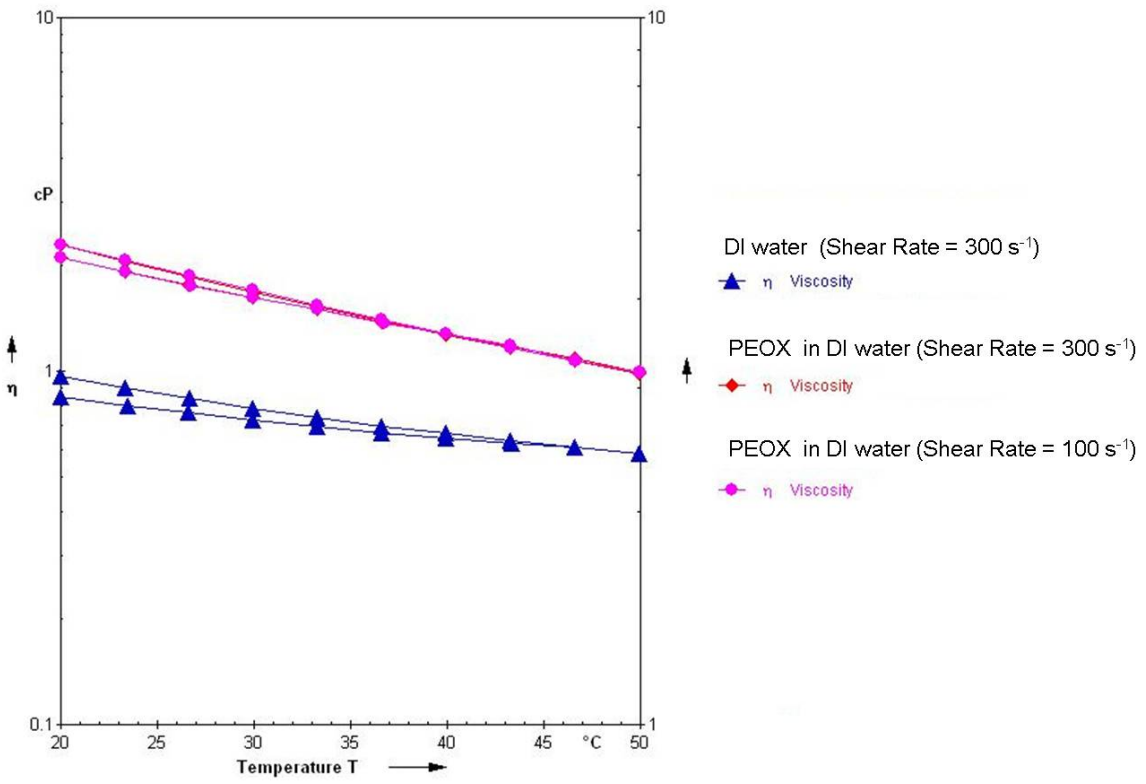

Figure 2.6: Viscosity as a function of temperature for PEOX of molecular weight 500kg/mol at shear rates of 100 and $300s^{-1}$ compared with the viscosity of deionized water

2.4 Conclusions

Based on viscometry measurements PEOX appears to adopt a random coil conformation in aqueous solution which collapses to a more compact conformation with the addition of sodium chloride salt which reduces the ability of water to solvate the polymer. Contrary to the proposed hypothesis, PEOX does not form a rigid helical conformation in water.

2.5 References

[1] Arakawa, T. and Timasheff, S. N., "Mechanism of protein salting in and salting out by divalent cation salts: balance between hydration and salt binding," *Biochemistry*, vol. 23, no. 25, pp. 5912–5923, 1984.

[2] Bernard, A. M., Callander, D., and Ludovice, P. J., "Conformation of poly(2-ethyl-2-oxazoline) in aqueous solution," *PMSE Preprints*, vol. 94, pp. 383–385, 2006.

[3] Brostow, W. and Drewniak, M., "Computer simulations of chain conformations in dilute polymer solutions under shear flow," *Journal of Chemical Physics*, vol. 105, no. 16, pp. 7135–7139, 1996.

[4] Brostow, W., Drewniak, M., and Medvedev, N. N., "Chain overlap and entanglements in dilute polymer solutions: Brownian dynamics simulation," *Macromolecular Theory and Simulations*, vol. 4, no. 4, pp. 745–758, 1995.

[5] Cantow, M. J. R., "Polymer fractionation," 1967.

[6] Chen, C. H., Wilson, J. E., Davis, R. M., Chen, W., and Riffle, J. S., "Measurement of the segmental adsorption energy of poly(2-ethyl-2-oxazoline) on silica in water and ethanol," *Macromolecules*, vol. 27, no. 22, pp. 6376–6382, 1994.

[7] Chen, F., Ames, A., and Taylor, L., "Aqueous solutions of poly(ethyloxazo1ine) and its lower consolute phase transition," *Macromolecules*, vol. 23, no. 21, pp. 4688–4695, 1990.

[8] Chi, E. Y., Krishnan, S., Randolph, T. W., and Carpenter, J. F., "Physical stability of proteins in aqueous solution: Mechanism and driving forces

in nonnative protein aggregation.," *Pharmaceutical Research*, vol. 20, no. 9, pp. 1325–36, 2003.

[9] Chiu, T. T., Thill, B. P., and Fairchok, W. J., "Poly (2-ethyl-2-oxazoline): A new water-and organic soluble adhesive," *by JE Glass, ACS*, p. 425, 1986.

[10] Diab, C., Akiyama, Y., Kataoka, K., and Winnik, F. M., "Microcalorimetric study of the temperature-induced phase separation in aqueous solutions of poly(2-isopropyl-2-oxazolines)," *Macromolecules*, vol. 37, no. 7, pp. 2556–2562, 2004.

[11] Dondos, A., "Relation between the quality of the solvent and the number of statistical segments of a polymer at the onset of excluded-volume and complete excluded-volume behaviour," *Polymer*, vol. 33, no. 20, p. 4375, 1992.

[12] Dondos, A., Tsitsilianis, C., and Staikos, G., "Viscometric study of aggregation phenomena in polymer dilute solutions and determination of the critical concentration c**," *Polymer*, vol. 30, no. 9, p. 1690, 1989.

[13] Doty, P. M., Zimm, B. H., and Mark, H., "An investigation of the determination of molecular weights of high polymers by light scattering," *The Journal of Chemical Physics*, vol. 13, no. 5, p. 159, 1945.

[14] Flory, P. J., *Principles of Polymer Chemistry*. Cornell University Press, 1953.

[15] Fujita, H., *Polymer solutions*. Amsterdam: Elsevier, 1990.

[16] Gosa, K. L., Papanagopoulos, D., and Dondos, A., "Study of the conformational transition of polystyrenepoly(methyl methacrylate) block copolymers with temperature using measurements of the c** critical concentration," *Colloid & Polymer Science*, vol. 282, no. 1, pp. 84–87, 2003.

[17] Gosa, K. L., Uricano, V., Pierri, E., Papanagopoulos, D., and Dondos, A., "Study of the critical concentration c** in dynamic and static state," *Macromolecular Chemistry and Physics*, vol. 201, no. 6, pp. 621–626, 2000.

[18] Lin, P., Clash, C., Pearce, E. M., Kwei, T. K., and Aponte, M. A., "Solubility and miscibility of poly(ethyl oxazoline)," *Journal of Polymer Science Part B: Polymer Physics*, vol. 26, no. 3, pp. 603–619, 1988.

[19] Monkos, K., "Viscosity of bovine serum albumin aqueous solutions as a function of temperature and concentration," *International Journal of Biological Macromolecules*, vol. 18, no. 1-2, p. 61, 1996.

[20] Monkos, K., "Viscosity analysis of the temperature dependence of the solution conformation of ovalbumin," *Biophysical Chemistry*, vol. 85, no. 1, p. 7, 2000.

[21] Paz, Y., Kesselman, E., Fahoum, L., Portnaya, I., and Ramon, O., "The interaction between poly(n-isopropylacrylamide) and salts in aqueous media: The "salting-out" phenomenon as studied by attenuated total reflection/fourier transform infrared spectroscopy," *Journal of Polymer Science Part B: Polymer Physics*, vol. 42, no. 1, pp. 33–46, 2004.

[22] Schild, H. G., "Poly(n-isopropylacrylamide): experiment, theory and application," *Progress in Polymer Science*, vol. 17, no. 2, p. 163, 1992.

[23] Sung, J. and Lee, D., "Molecular shape of poly(2-ethyl-2-oxazoline) chains in thf," *Polymer*, vol. 42, pp. 5771–5779, 2001.

[24] Xia, X., Hu, Z., Gao, J., Qin, D., Durst, H. D., and Yin, R., "Light scattering study of the self-association behavior of long chain branched poly(2-ethyloxazoline) in solvents," *Langmuir*, vol. 18, no. 22, pp. 8302–8308, 2002.

[25] Yang, H., Zhu, P., Peng, C., Ma, S., Zhu, Q., and Fan, C., "Viscometric study of polyvinyl alcohol in nacl/water solutions ranged from dilute to extremely dilute concentration," *European Polymer Journal*, vol. 37, no. 9, p. 1939, 2001.

[26] Zimm, B. H., "Molecular theory of the scattering of light in fluids," *The Journal of Chemical Physics*, vol. 13, no. 4, pp. 141–145, 1945.

CHAPTER III

CONFORMATIONAL ANALYSIS OF ISOLATED PEOX

3.1 Introduction

Previous investigations have shown that the PEOX possesses a pronounced negative entropy of mixing when dissolved in water[3]. At higher temperatures, the unfavorable entropic term ($T\Delta S$)of the free energy of mixing ($\Delta G = \Delta H - T\Delta S$) overcomes the favorable negative enthalpic term (ΔH)resulting a temperature below which mixing will always occur or a lower critical solution temperature (LCST). Negative entropies of mixing usually occur in water soluble polymers that maintain a relatively rigid structure in an aqueous solution. Polymers with a rigid structure have a significantly smaller entropy increase when dissolved than polymers that adopt a flexible random coil conformation in solution. This rigidity, coupled with an increase in the ordering of hydrogen bonded water molecules adjacent to the polymer can result in a net decrease in entropy upon dissolution. This behavior is common in globular proteins, but does occur in some synthetic polymers such as Poly(vinyl pyrrolidone) (PVDP) [20] and poly(isopropyl acrylamide) PNIPAM [21]. Given the similarity of the PEOX backbone to that of a peptide we hypothesized that PEOX formed a helical structure similar to that of a protein.

The monomer structures of a peptide, a peptoid and a poly(oxazoline) are compared in Figure 3.1. Peptide structures have been very intensely examined and many are well defined. In 1951 Pauling et al. reported 2 helical structures of polypeptides [19], one with 3.7 residues per turn and one with 5.1 residues per turn. The bond lengths and angles of peptides proposed in this study became widely accepted and have been improved largely through X-ray diffraction techniques. As shown in Figure

3.1, the peptide has an electron donating oxygen atom bonded to the backbone of the chain and a hydrogen atom which is bonded to a highly electronegative nitrogen atom on the backbone. Hydrogen bonding between these two groups facilitates helical conformations in polypeptides and proteins. These secondary helical structures in turn form sections of more complex tertiary and quaternary structures of proteins. Peptoids are similar to peptides but the backbone nitrogen atom of a peptoid is substituted and therefore peptoids are incapable of hydrogen bonding with themselves due to the lack of a proton donating group. In spite of this, some peptoids are found to have secondary helical structure and form tertiary structures consisting of helical bundles [15, 1, 16, 17].

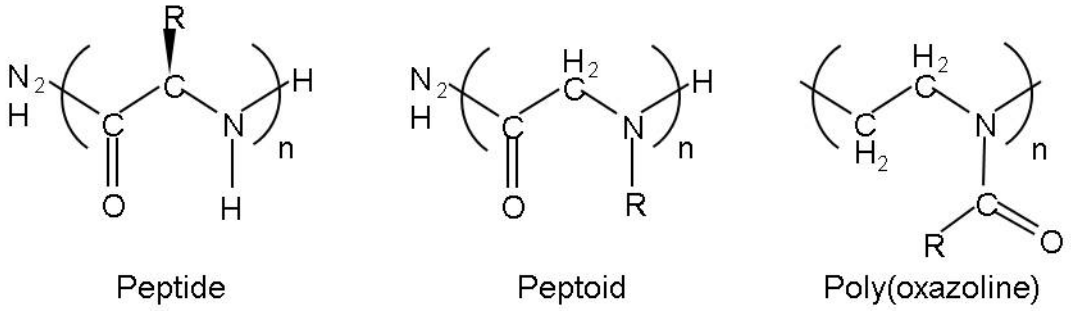

Figure 3.1: Comparison of peptide, peptoid and PEOX structures

PEOX has a similar C-C-N backbone to peptides and peptoids, but like peptoids, there is no hydrogen bonding possible between chain segments. For peptoids, however, the conformational properties of the backbone result in helical structures and we hypothesized that the same is possible for poly(oxazolines). The carbonyl group is found on the side chain for poly(oxazolines), but on the backbone for peptides and peptoids. This limits the structural similarities of PEOX with peptides and

peptoids, particularly peptides, in aqueous solution, because hydrogen bonding with water molecules aids in the stabilization of helices.

Given the lack of an amide hydrogen to hydrogen bond with the backbone carbonyl oxygen, we hypothesized that the helical structure of PEOX was stabilized by hydrogen bonding with the surrounding water. Since PEOX has no hydrogen bonding proton donator, solvent stabilization of an ordered structure, such as a helix could not occur in a solvent that is lacking a proton donator. This is consistent with the previous observation that PEOX adopts a random coil conformation in THF [24]. This molecular modeling study investigates whether PEOX forms a helix by examination of various conformations.

There has been some investigation of PEOX structure through spectrographic studies. The structure of PEOX in the solid state was found to be amorphous by wide angle x-ray diffraction (WAXD) [5]. In studies of the interaction between a metal salt and PEOX in polyelectrolytes where metal salts are dissolved in the polymer, polar groups on the polymer chain are observed to coordinate with the metallic cation [5, 22]. This coordination results in the cation acting as a crosslinker between the groups on the polymer chain. These links change the distance between the groups which they engage. These changes in inter and intra chain distance may be measured by observing their effect on the WAXD profile.

Quantum calculations on PEOX monomer and dimer units [22]reveal a tendency for the carbonyl groups to coordinate with silver cations and cause the side chains to move closer together. This coordination of carbonyl groups in the presence of positive charges, lends credence to the hypothesis that coordination occurs in the presence of water molecules.

The dihedral or torsion angles of a polymer determine its overall shape. In the case of PEOX we hypothesized a particular importance of the side chain torsions because of their influence on the orientation of the carbonyl group, which is the only

hydrogen bonding site on the molecule. The following study considers the conformations of PEOX and looks for the existence of possible helical conformations through a systematic search of the conformational space PEOX could occupy and by examining the stability of structures with repeating backbone torsion angles.

3.2 Methodology

In order to characterize the molecular structure of PEOX a series of computer experiments were conducted using Molecular Operation Environment®(MOE), a molecular simulation package of the Chemical Computing Group in Montreal, Canada. Simulations in vacuum were considered to represent the effects of non-polar solvent conditions.

3.2.1 Conformational Search

A model compound, shown in Figure 3.2 and similar to a dimer of PEOX, was used to investigate the torsion angles on the backbone as well as the torsion angles on the side chain. The side chain contains the carbonyl group which is suspected of contributing significantly to a potential helical configuration or other organized structure through coordination with water molecules. The backbone consists of a series of C-C bonds each followed by two C-N bonds. The model compound used for conformational analysis consists of two such C-N bonds and one C-C bond. The side chain contains two rotational bonds and the model compound contains two side chains. This gives a total of 7 torsion angles in the model compound.

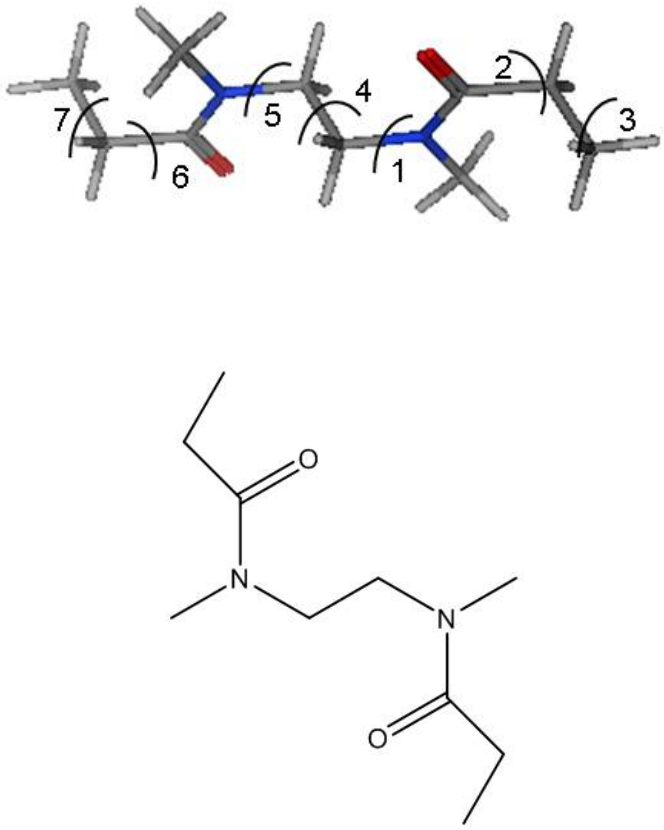

Figure 3.2: PEOX model compound

This model compound was built in MOE®and relaxed by energy minimization to a root mean squared gradient of 0.1. A systematic search of the possible conformations was then performed which produced a database of the most probable conformations. These conformations were then minimized and the minimized conformations were sorted according to a Boltzman distribution of the potential energy (U)[18]. Conformation calculations were performed using the Amber force field [6] as provided in MOE because of its ability to model hydrogen bonding interactions and the similarity between PEOX and peptide residues, as Amber was designed primarily for modeling proteins. The same operation was also conducted with the MMFF

force field [8, 9, 10, 14, 11, 12, 13], which is considered suitable for most small organic molecules to determine if the choice of force field would significantly affect the calculations.

3.2.2 Solvated Conformational Search

The systematic conformational search finds the torsion angles of the polymer in isolation but in order to investigate the molecular shape of PEOX in water the model compound had to be solvated in water and equilibrated. To achieve this, the conformations obtained by searching in vacuum were solvated in cubic periodic cells, with P1 symmetry and sides of length 20, to which water molecules were added randomly to achieve a density of 1g cm^{-3} as shown in Figure 3.3. The PEOX model compound was fixed and the water was allowed to equilibrate by 50ps of NVT molecular dynamics simulations (MD) using the Nos Poincar Andersen (NPA) algorithm [23, 2] at 300K and molecular mechanics (MM). When fixed, the PEOX was not allowed to move during equilibration or contribute to the calculated energy. The PEOX was then unfixed and the entire system allowed to equilibrate using MD.

The conformations of the solvated and equilibrated structures were then sorted according to a normalized Boltzman distribution of the total potential energy.

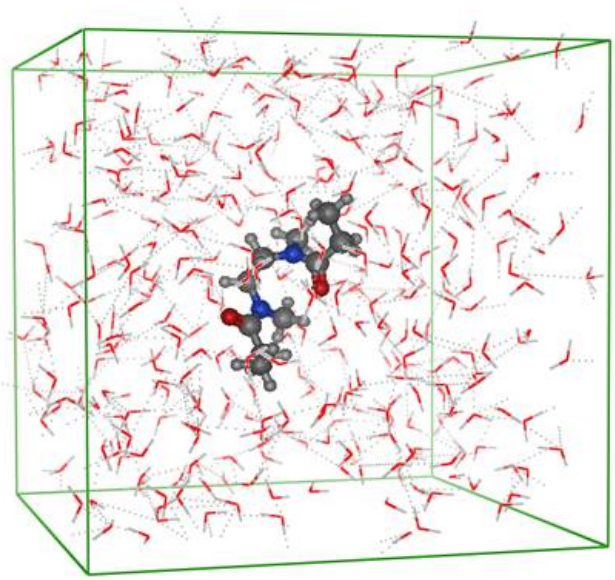

Figure 3.3: Solvated PEOX model compound

3.2.3 Helical Conformations

The angles which emerged as energetically favorable from the Boltzman distribution of the unsolvated conformational search were used to build a series of likely helical PEOX structures with 10 repeat units. These helices were then relaxed by running NVT MD for 1ns at 300K and the torsion angles along final structure were compared with angles along the starting structure. A stable helix was identified as having repeating backbone torsion angles.

Helices of various lengths ranging from 20 to 600 repeat units were built and relaxed using NPA MD for 1ns at 300K followed by energy minimization to a gradient of 0.0001.

3.2.4 Random Coil Conformations

Random coils of corresponding lengths to the simulated helices were built for the same range of polymer lengths as the helices and equilibrated using an identical scheme of

MD and MM as was described above for the helices.

The potential energy using the Amber force field consists of the following contributions:

$$U = E_{str} + E_{ang} + E_{oop} + E_{tor} + E_{vdw} + E_{ele} \tag{3.1}$$

Where E_{str} the bond stretch energy, E_{ang} the bond angle bend energy, E_{oop} the out-of-plane energy and E_{tor} the torsion energy are bonded energy terms and E_{vdw} the Van der Waals energy and E_{ele} the electrostatic energy are the non-bonded energy terms.

3.2.5 Wide Angle X-ray Diffraction

In order to determine which of the structures investigated (random coil or helical) corresponded with the WAXD patterns available in literature [5], PEOX crystals were simulated by placing 4, 20 repeat unit chains into a periodic crystal cell of P1 symmetry to obtain a density of 1.14 g cm^{-3} as reported [4]. The structure was minimized and equilibrated by 500ps of NPA MD using the Amber force field. MD was performed for both a random coil and a helix and at temperatures ranging from 300K to 700K.

3.3 Results and Discussion

3.3.1 Conformational Search

Table 3.1 summarizes the approximate values of the probable angles of the 7 considered torsions identified in Figure 3.2. These angles were found using both Amber and MMFF.

3.3.2 Solvated Conformational Search

The angles which emerged as most energetically popular from the initial conformational search were also the most energetically popular after being solvated and so

Table 3.1: Approximate values of torsion angles from conformational search

Torsion Angle #	1	2	3	4	5	6	7
	90	0	-90	-60	90	0	-90
Angle(degrees)	-90	180	180	70	-90	180	180
			90	180			90

were further considered as prospective angles for all structures. This is demonstrated in Figures 3.4 through 3.7 which show the population distributions for torsions 1, 2, 3 and 4 from both the conformational search and solvated conformational search.

Torsion 1, shown in Figure 3.4, is more broadly distributed for the solvated conformations but remains centered around 90 and -90 degrees. A similar trend is true for the other angles. Since the model compound is 2 repeat units long, torsion1 is similar to 5, 2 similar to 6 and 3 similar to 7.

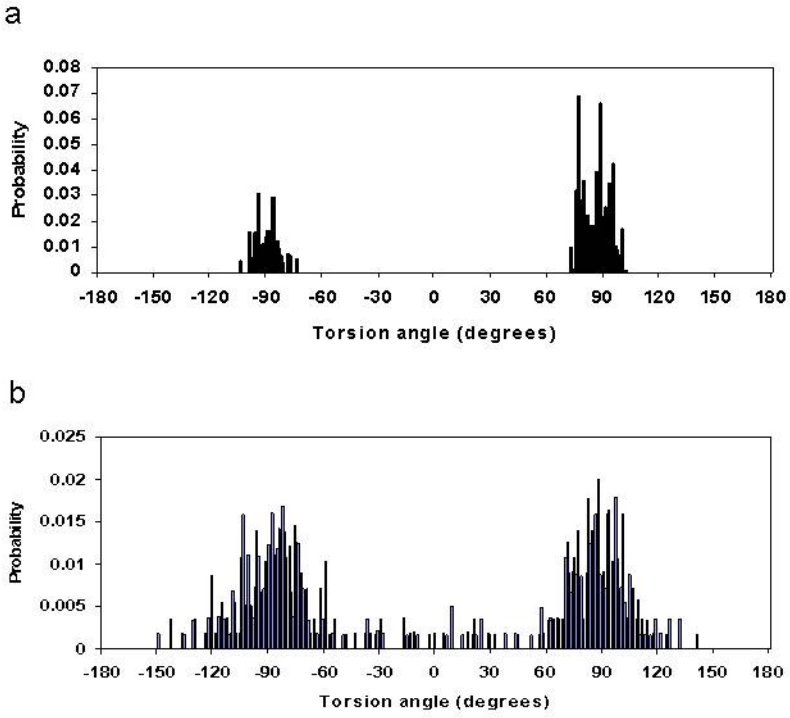

Figure 3.4: Boltzman distributions for torsion 1 a. unsolvated, b. solvated

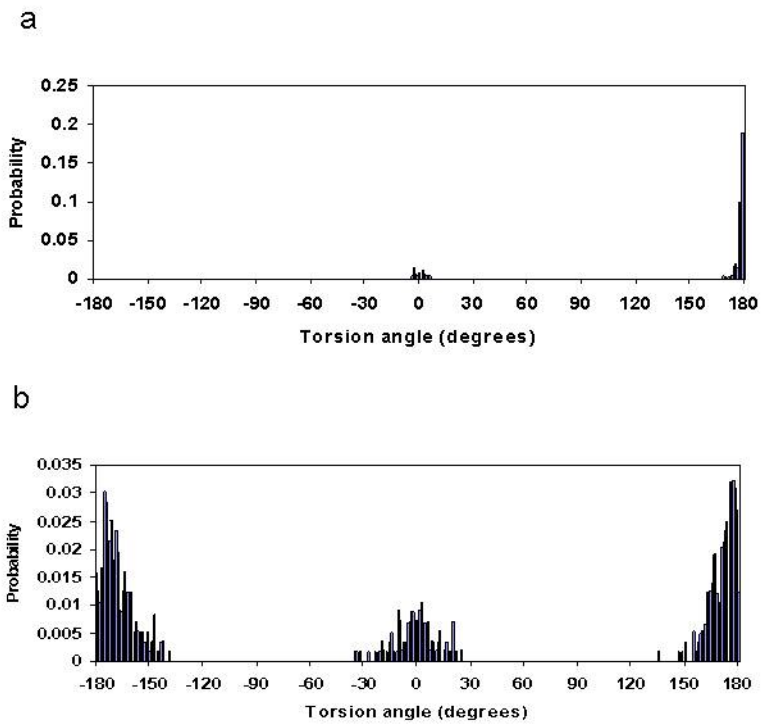

Figure 3.5: Boltzman distributions for torsion 2 a. unsolvated, b. solvated

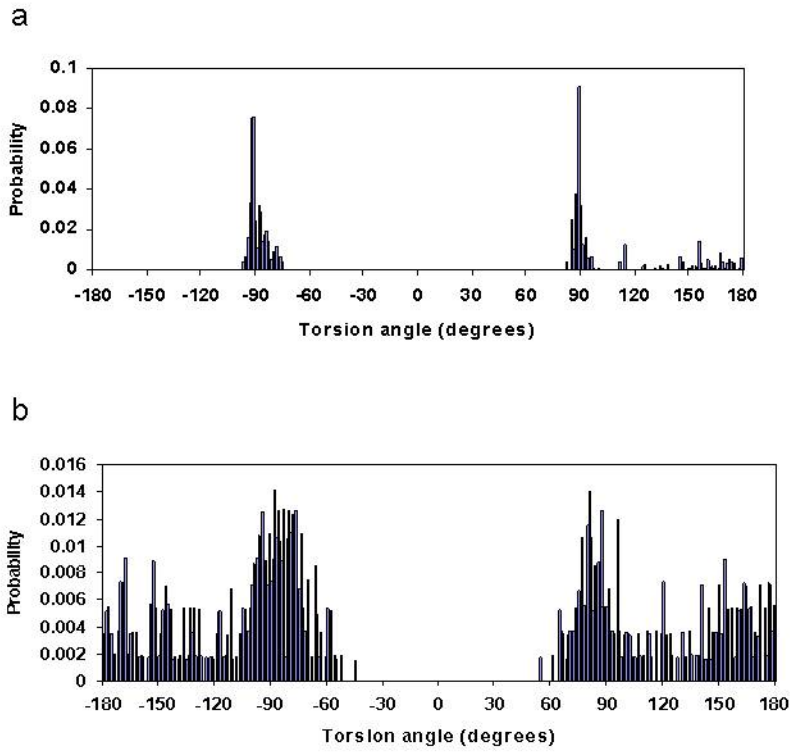

Figure 3.6: Boltzman distributions for torsion 3 a. unsolvated, b. solvated

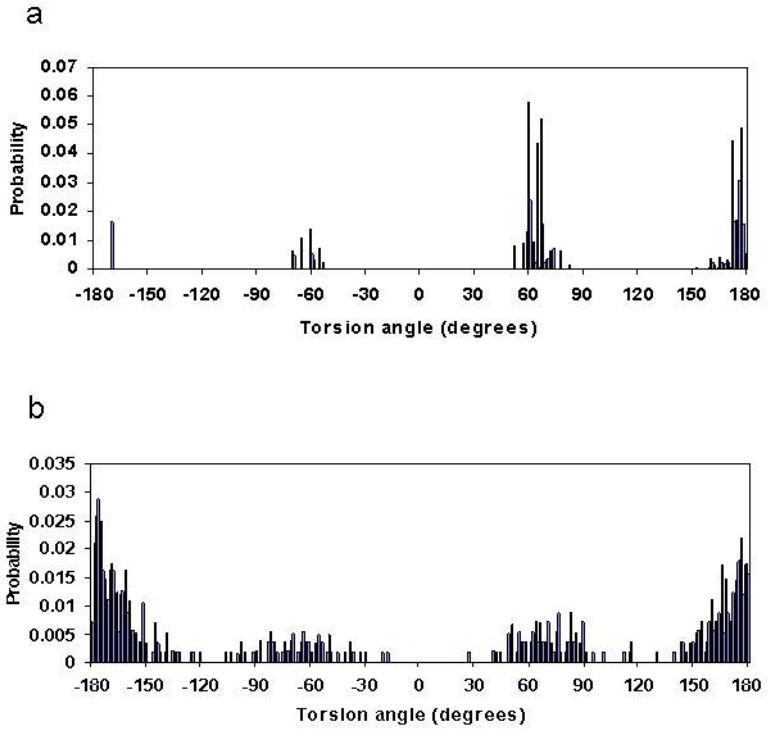

Figure 3.7: Boltzman distributions for torsion 4 a. unsolvated, b. solvated

These distributions based on conformational searches of the model compound identify the torsion angles that are energetically favorable for PEOX structures and were used as the basis angles for constructing larger molecular representations.

3.3.3 Helical Conformations

The plausible helices which could result from combinations of the backbone torsion angles 1, 4 and 5 were constructed with 10 repeat units and equilibrated.
Torsion angles 2,6,3 and 7 are side chain angles and were assigned values as follows:

- Torsion angles 2 and 6 determine the direction of the carbonyl group and were equally likely to be 0 or 180°. They were therefore assumed to be present in equal proportion by alternating between the two states along the polymer

chain. This alternating of the carbonyl direction is also the conformation which would best facilitate bridging between neighboring carbonyl groups by water molecules.

- Torsion angles 3 and 7 determine the orientation of the ethyl group on the side chain and were left in the minimized state on the monomer from which the polymer chain was constructed.

Torsion angles 1, 4 and 5 represent the backbone torsions which must repeat to result in a helical conformation. The 12 plausible 10mer helices which could be built from the possible combinations of the 3 angles were equilibrated with molecular dynamics and their angles assessed to determine if any of these helices were stable. A stable helix, with approximately 5 residues per turn, was found with average values of torsions 1,4 and 5 equal to 170, -88 and -85 degrees respectively. Figure 3.8 shows the comparison of the starting point estimation to the equilibrated 10mer helix which was obtained and Figure 3.9 shows the regularity of the angles on the equilibrated 10 repeat unit helix.

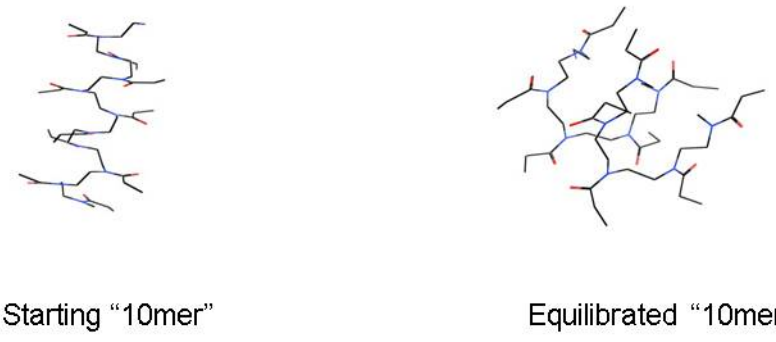

Figure 3.8: Ten repeat unit helix before and after equilibration.

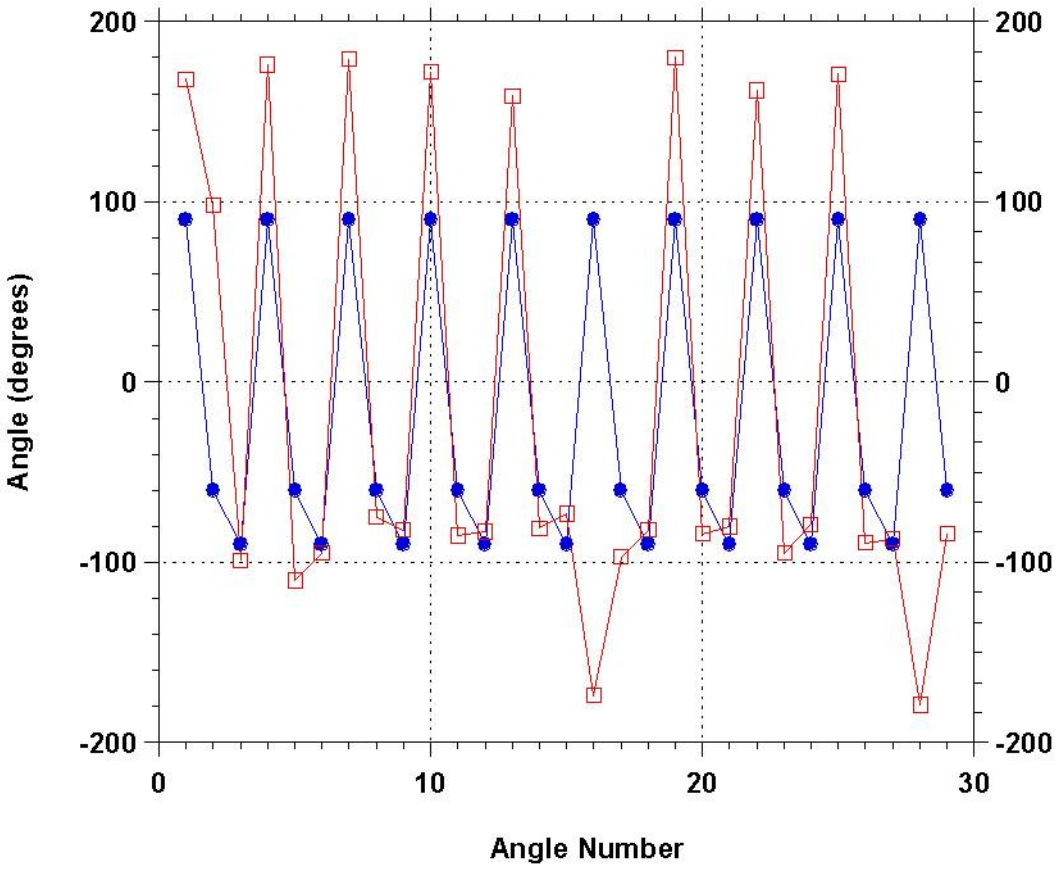

Figure 3.9: Starting point(closed circles) and equilibration(open squares) angles for 10mer helix.

Helices varying in size from 20 to 600 repeat units were built using the aforementioned repeating backbone torsion angles. The natural logarithm of the radius of gyration of the modeled helices is plotted in Figure 3.12 against the logarithm of the molecular weight. This slope of this line for the simulated helices before equilibration is 0.95, which is close to the rigid rod limit of 1. The slope is predicted as 0.5 for a random coil by extensive polymer theory and experiment and approaches 0.6 for a solvent system at the theta condition [18]. After molecular dynamics simulation of these helices in vacuum, the helices form secondary folded structures and have a

slope of 0.46, which is indicative of a random coil and not a rigid rod. These helices, shown in Figure 3.10, display a coiling behavior which could explain the Gaussian globule characterization suggested by Sung and Lee [24] in their light scattering study of PEOX in THF.

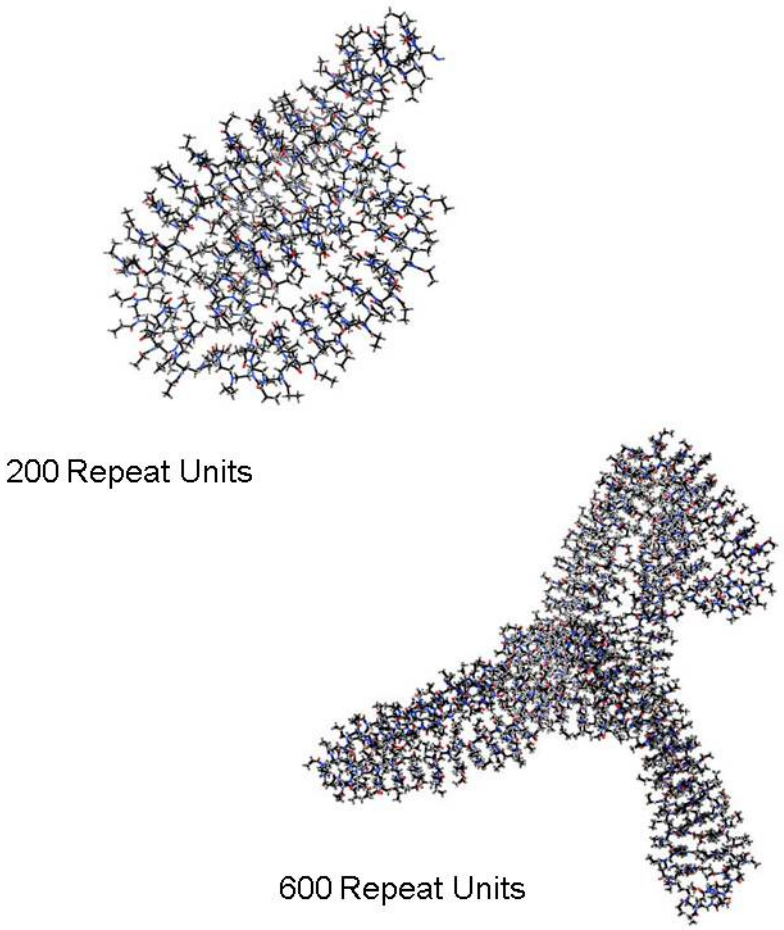

Figure 3.10: Poly(2-ethyl-2-oxazoline) coiled helices after equilibration in vacuum.

3.3.4 Random Coil Conformations

The condensing of these helices, suggests that PEOX may form a random coil in vacuum and therefore random coils of corresponding lengths were built for the same

range of polymer lengths as the helices and equilibrated relaxed using molecular dynamics for 1ns. The natural logarithm of the mean squared radius of gyration of these random coils is plotted against the natural logarithm of the molecular weight and the slope is 0.35. The coils show a significant contraction as well. Figure 3.11 shows examples of these equilibrated random coils. The potential energies of the helices were compared to those of the random coils to ascertain the more likely configuration.

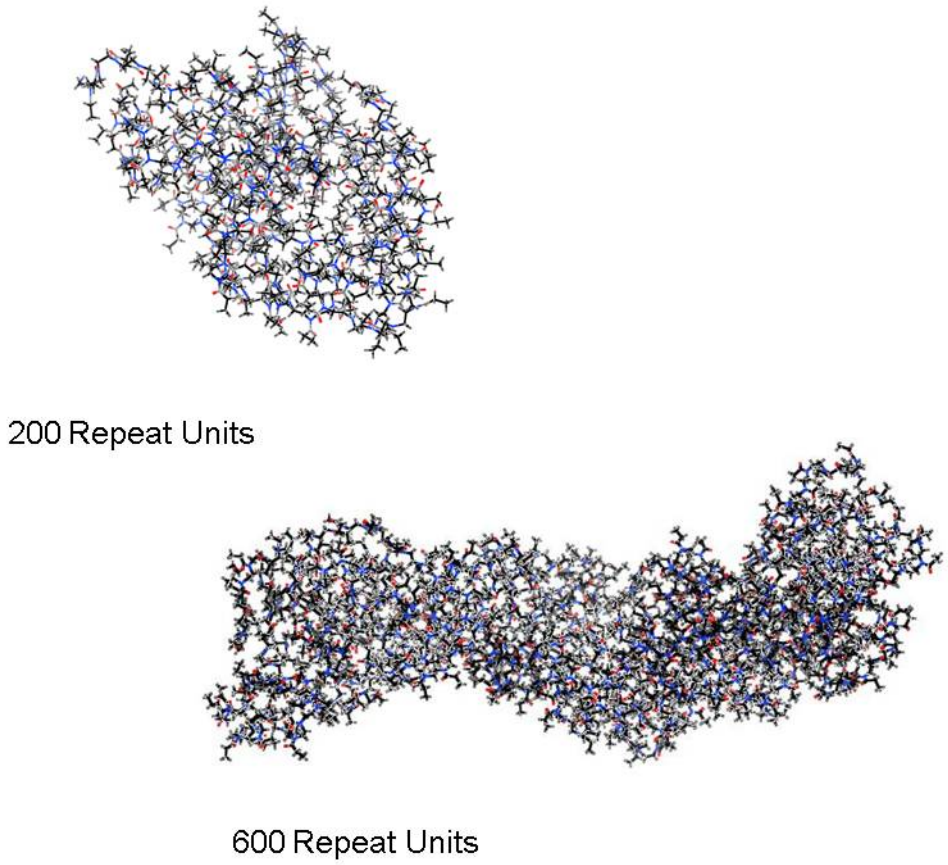

Figure 3.11: Poly(2-ethyl-2-oxazoline random coils after equilibration in vacuum.

The reported radii of PEOX in water and THF [24] are compared with simulated random coils and helices in Figure 3.12. The radii of gyration of simulated helices and random coils extrapolate well to the radii calculated from the intrinsic viscosities. The viscomectric radius is calculated from [7]:

$$R_v = \left[\frac{3[\eta]M}{10\pi N_A}\right]^{1/3} \tag{3.2}$$

Where $[\eta]$ is the intrinsic viscosity (reported in Chapter 2 for PEOX in water), M is the molecular weight and N_A is Avogadro's number.

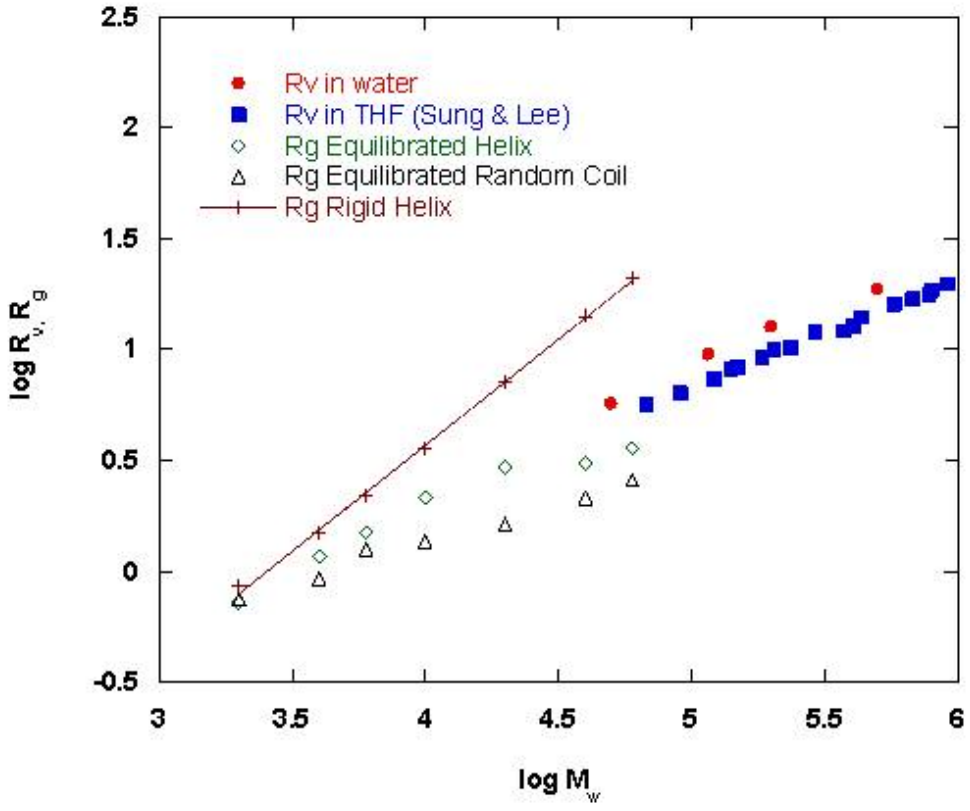

Figure 3.12: Logarithm of the radius of gyration as a function of the logarithm of the molecular weight from molecular simulation after equilibration of helices and random coils compared with experimental data for PEOX in THF by Sung and Lee.

The potential energy values after MD simulation shown in Figure 3.13, are not vastly different so do not conclusively rule out either conformation however the energy values for the helical conformation are lower for all but sizes except the "100mer". As shown in Figure 3.14, upon minimization the random coils obtain a lower energy state than the coiled helices suggesting that this is a preferred state.

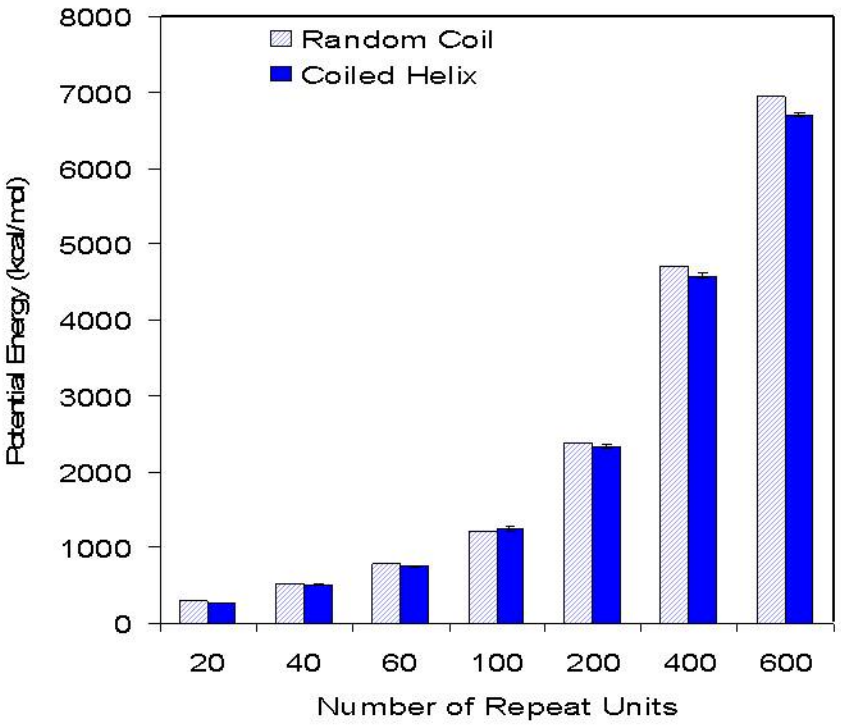

Figure 3.13: Potential energies of simulated helices compared to random coils for PEOX after MD only in vacuum. Error bars represent the 95% confidence interval.

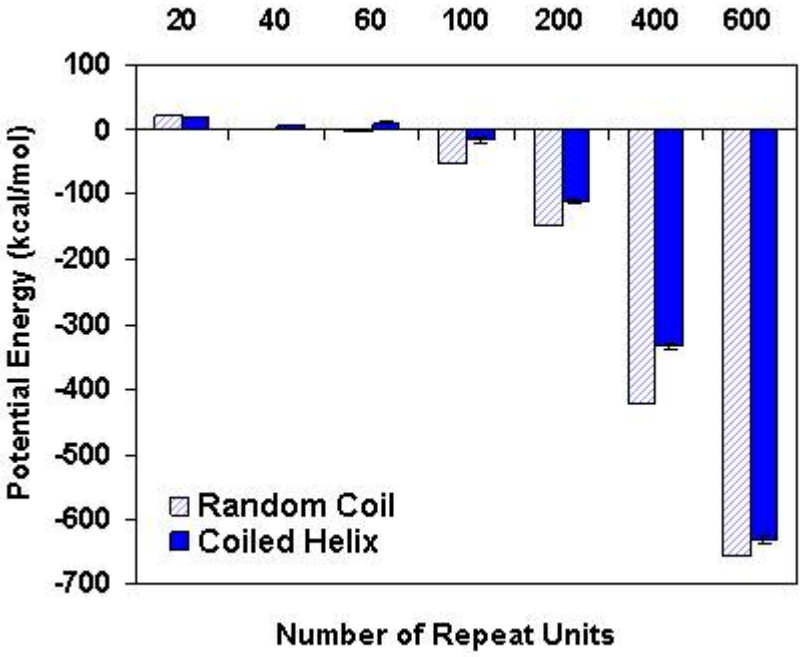

Figure 3.14: Potential energies of simulated helices compared to random coils for PEOX after MD and MM in vacuum. Error bars represent the 95% confidence interval.

Figure 3.15 shows the non-bonded energy terms for coils verses helices and Figure 3.16 shows the bonded energy terms. The potential energy of the random coils is lower due to the non-bonded energy terms, which include the Van der Waals and electrostatic interaction terms.

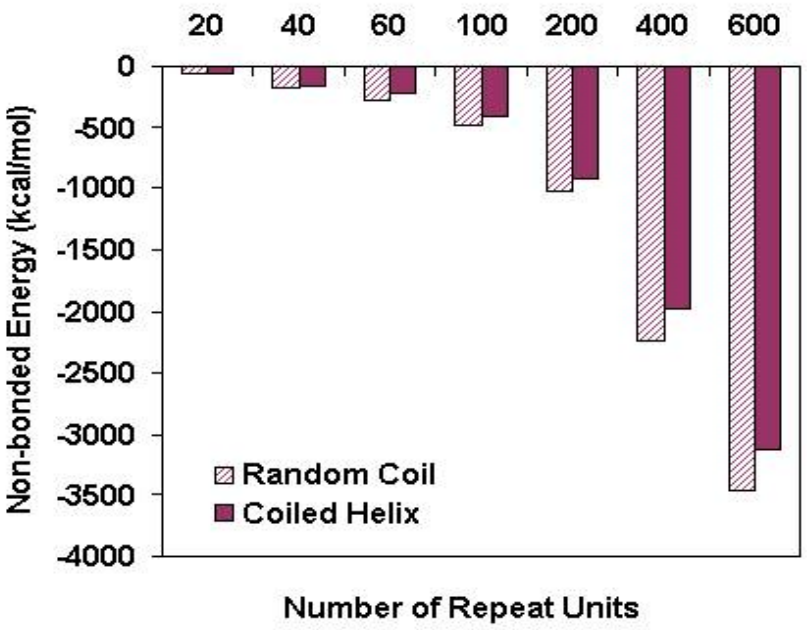

Figure 3.15: Non-bonded potential energy term of simulated helices compared to random coils for PEOX after MD and Energy Minimization. Error bars represent the 95% confidence interval.

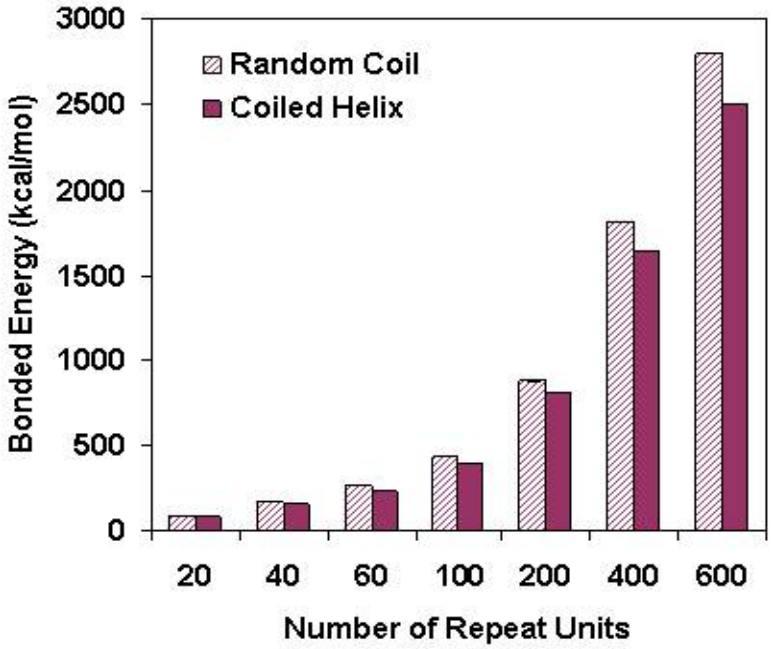

Figure 3.16: Bonded potential energy term of simulated helices compared to random coils for PEOX after MD and Energy Minimization. Error bars represent the 95% confidence interval.

The bonded energy terms are lower for the helices so the coils are clearly lower in potential energy because of minimized non-bonded interactions.

More specifically, the electrostatic contribution is much lower for the random coils than for the coiled helices. Figures 3.17 and 3.18 compare E_{ele} and $E_{vdw}$for the coils and helices. E_{ele} is much lower for random coils than helices, whereas E_{vdw} is similar to that of the helices

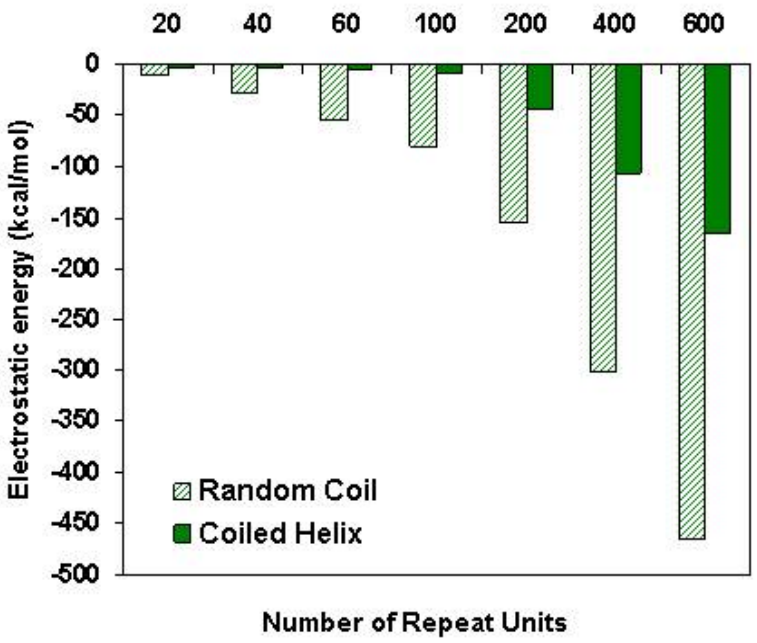

Figure 3.17: Electrostatic potential energy term of simulated helices compared to random coils for PEOX after MD and Energy Minimization. Error bars represent the 95% confidence interval.

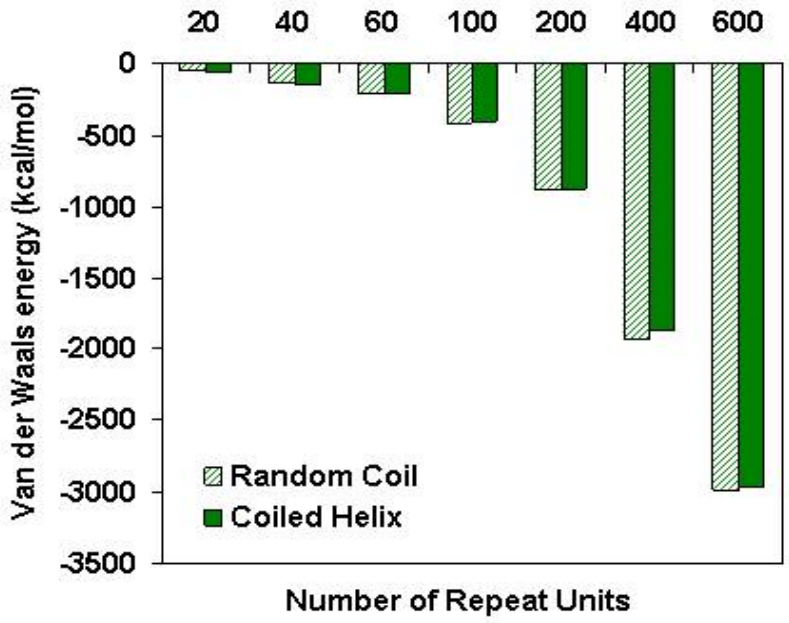

Figure 3.18: Van der Waals potential energy term of simulated helices compared to random coils for PEOX after MD and Energy Minimization. Error bars represent the 95% confidence interval.

It is not surprising that the electrostatic energy is much lower for the random coils since the more random conformation will allow for greater freedom to maximize the benefits of the electrostatic interactions.

3.3.5 Folded Helices

The collapse of the PEOX helical structures into folded conformations while maintaining secondary helical structure is shown in Figure 3.19 for the 60 repeat unit helix.

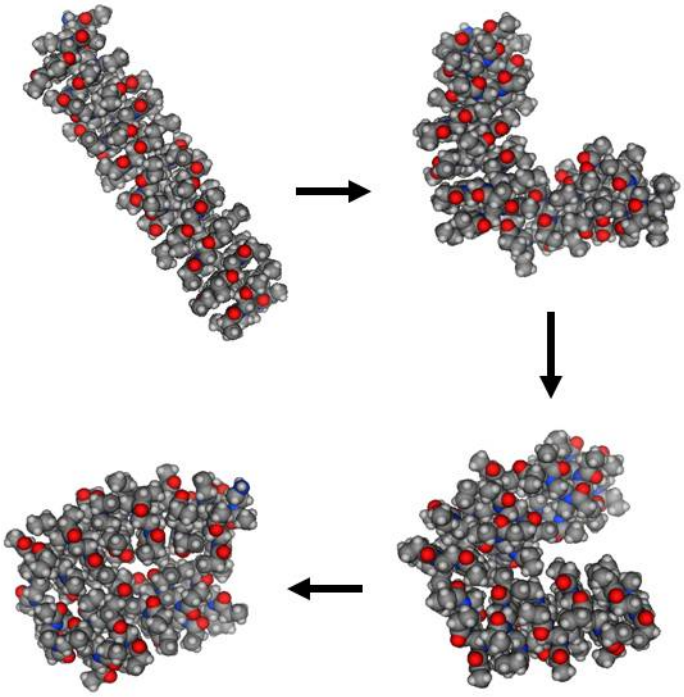

Figure 3.19: Folding of PEOX 60 repeat unit hairpin

The progression of the non-bonded potential energy contribution of electrostatic and Van der Waals interactions between the adjacent arms of this hairpin-like structure during the first 50ps of MD is plotted in Figure 3.20. Within the first 50ps of MD, the structure goes from linear to folded.

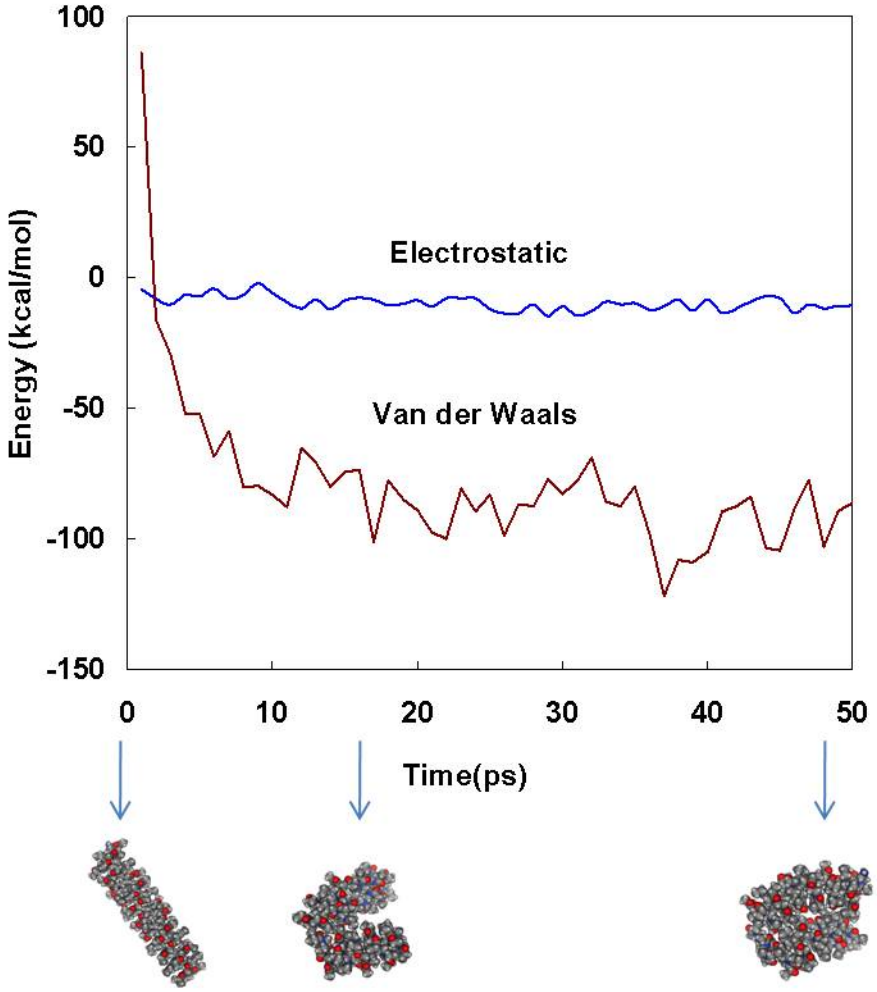

Figure 3.20: Van der Waals and electrostatic interactions between the adjacent arms of 60 repeat unit PEOX hairpin during the first 50ps of MD 60 repeat unit hairpin.

The folding of PEOX helices is due to the Van der Waals interactions that are made possible as the helix segments approach each other. The Van der Waals contribution to the potential energy decreases as the folding occurs while the electrostatic energy remains largely constant.

3.3.6 Wide Angle X-ray Diffraction

The WAXD patterns obtained for PEOX crystal structures for temperatures up to 700K are shown in Figures 3.21 and 3.22. The patterns feature 2 major peaks the first at about 9 degrees and the second close to 19 degrees. This corresponds to the two peak nature of curves for branched homopolymers in which the first peak represents the level of intermolecular order and the second peak the level of intramolecular order. The WAXD patterns are compared with the experimental pattern obtained by Choi and co-workers[5].

Figures 21(a) shows the resulting pattern for the crystal composed of helices at a density of 1.14 g cm^{-3} .Figure 21(b) shows the change in the WAXD pattern resulting from increasing the density by decreasing the cell size to achieve a density of 1.35 g cm^{-3}. Figures 22(a) and 22(b) show the same configurations for the crystal composed of random coils.

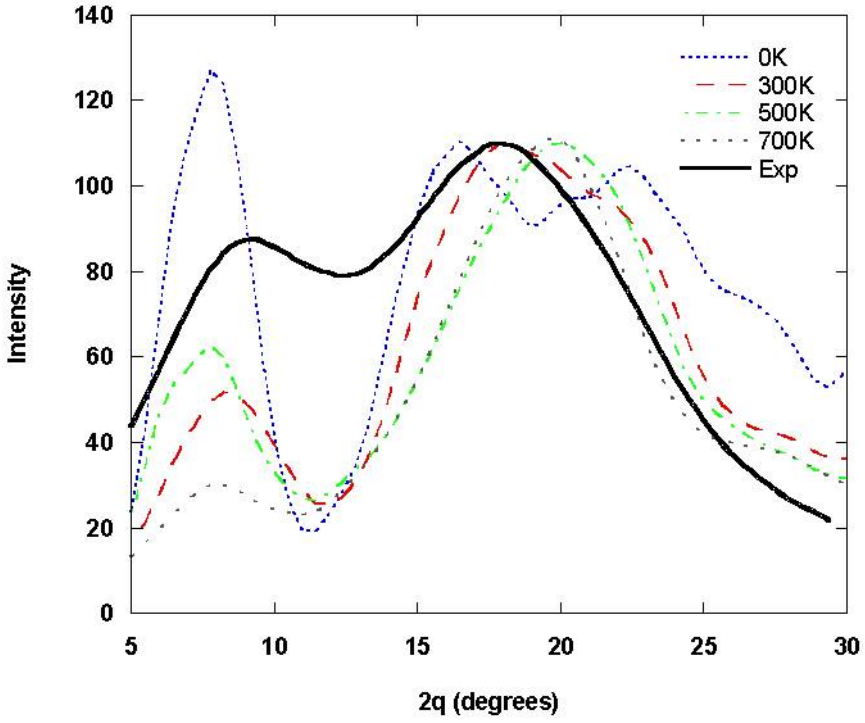

(a) Density = 1.14

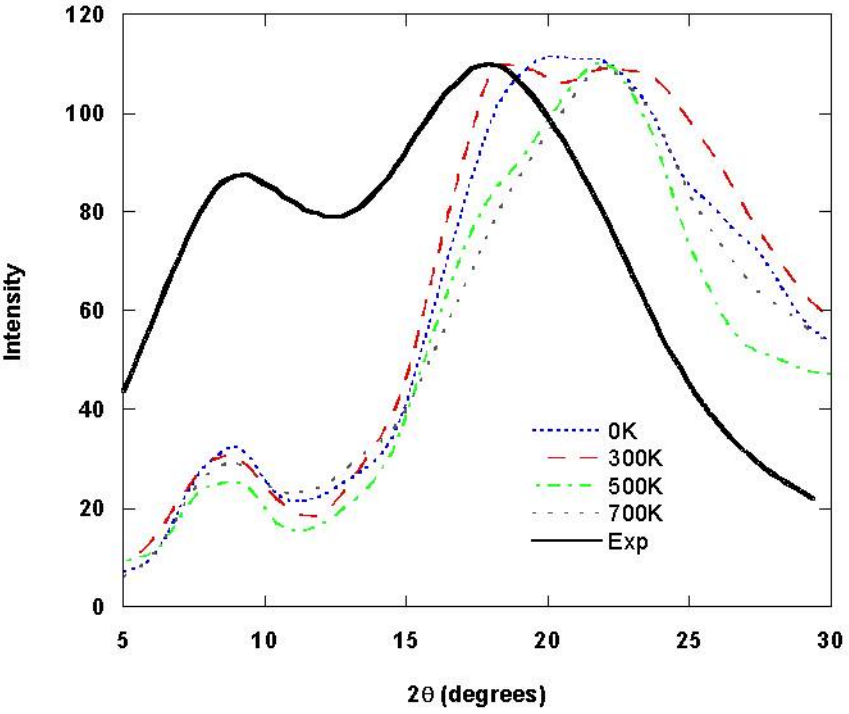

(b) Density = 1.35

Figure 3.21: WAXD patterns for PEOX helix

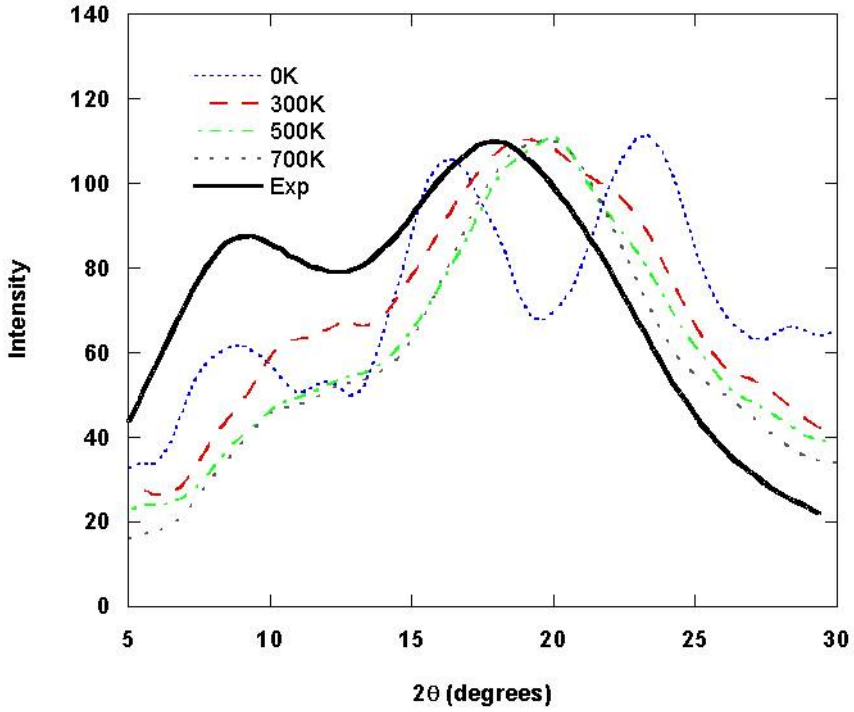

(a) Density = 1.14

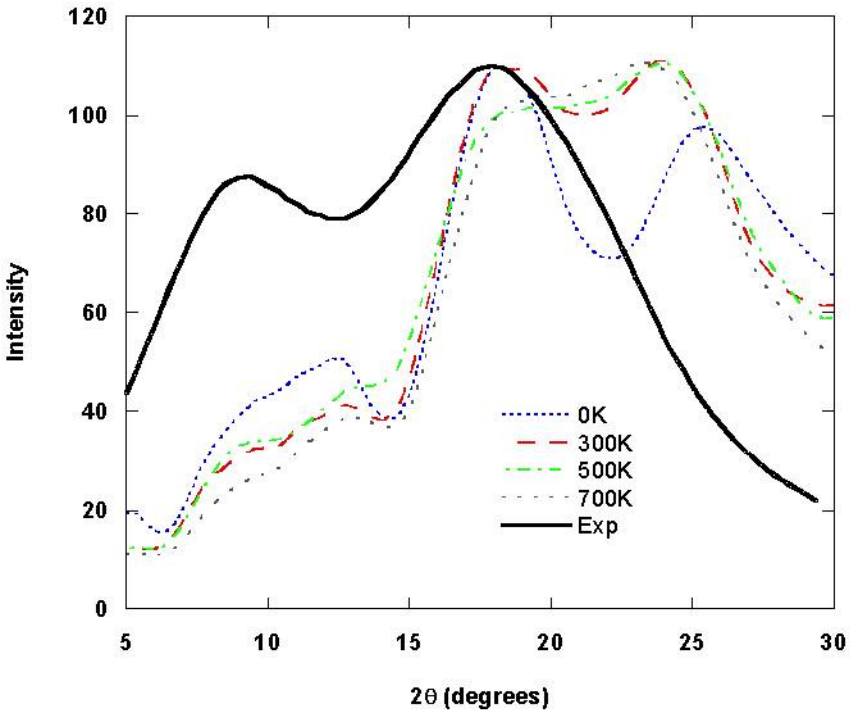

(b) Density = 1.35

Figure 3.22: WAXD patterns for PEOX random coil

The helix in crystal form before any MD is shown in Figure 24(a). This rigid regular structure becomes disordered with MD at elevated temperatures. Although the WAXD diffraction patterns shown for the helix and random coils in Figures 3.21 and 3.22 display peaks similar to the experimental peaks, the helix displays more pronounced peaks and the random coil conformation better reflects the relative heights of the two peaks more pronounced second peaks than the more organized structures.

As shown in Figure 3.23 for structures relaxed at 300K, increasing the density causes the peaks of both the helical and random coil structures to shift to a higher value of 2θ as would be expected particularly the second (intramolecular) peak which broadens and looses definition at a higher density.

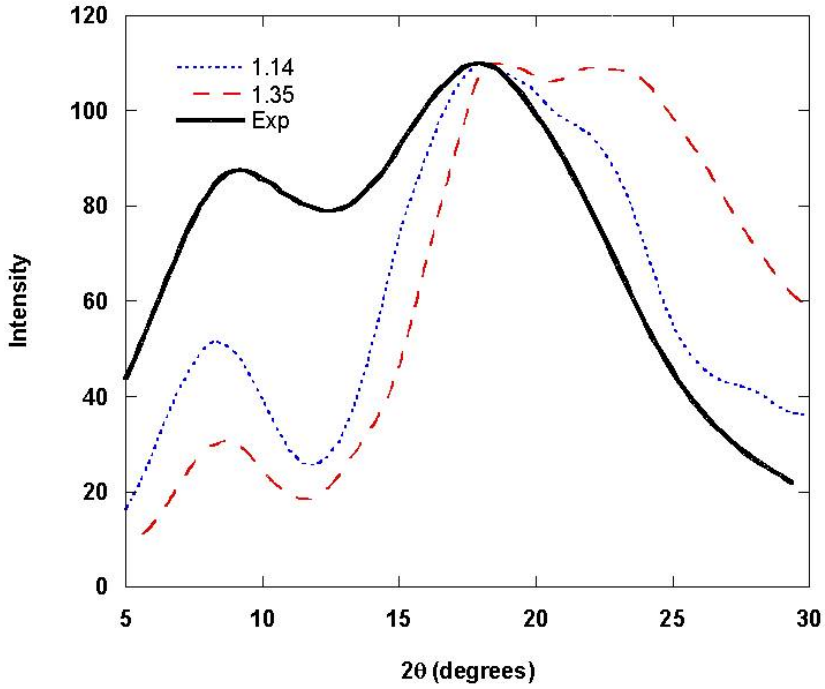

(a) Helix

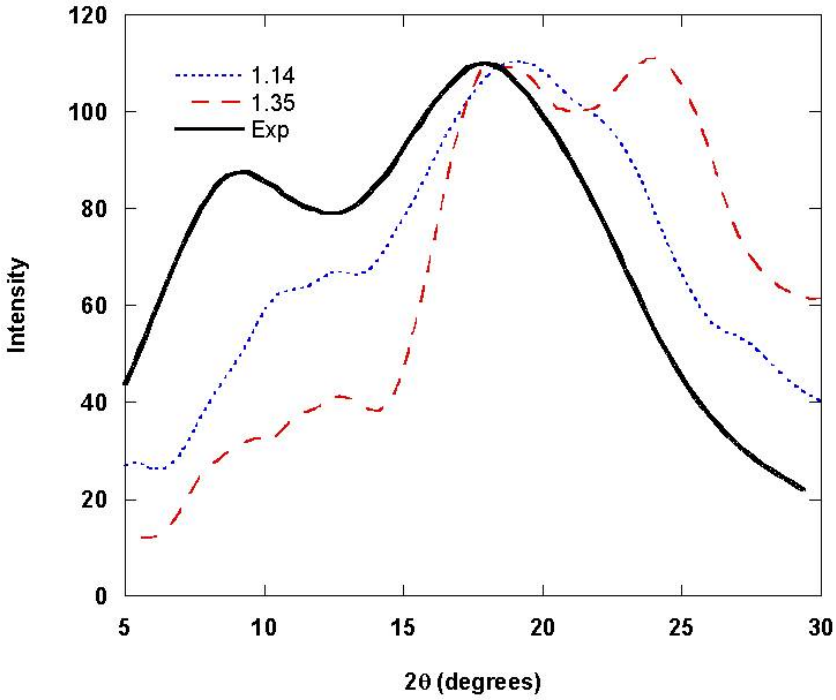

(b) Random Coil

Figure 3.23: Comparison of WAXD patterns of PEOX helix and random coil at densities of 1.14 and 1.35

With increasing temperature the helical conformation shown in its starting structure in Figure 24(a) becomes more disordered and as shown in Figure 24(b). This more disordered structure better reflects the relative prominence of the second (intramolecular) peak.

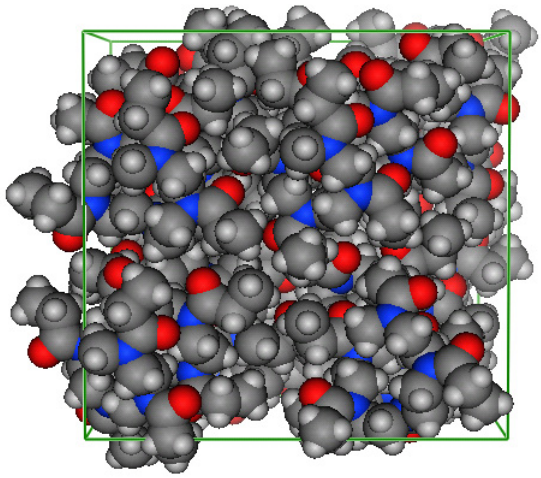

(a) Perfectly Aligned

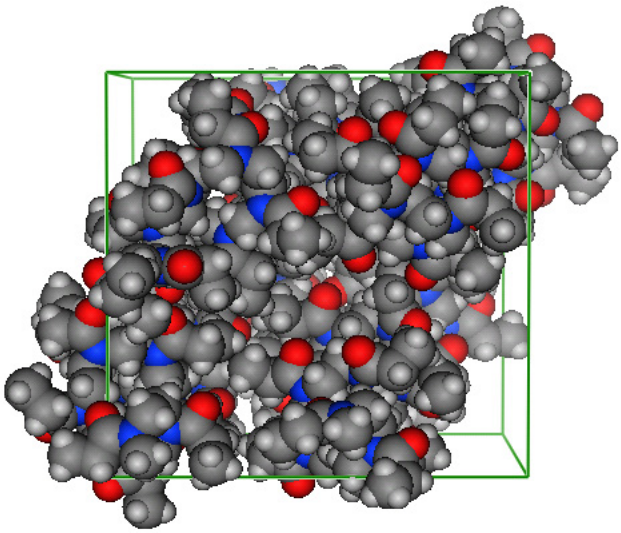

(b) After 700K MD

Figure 3.24: PEOX helical crystal structure before and after MD at 700K

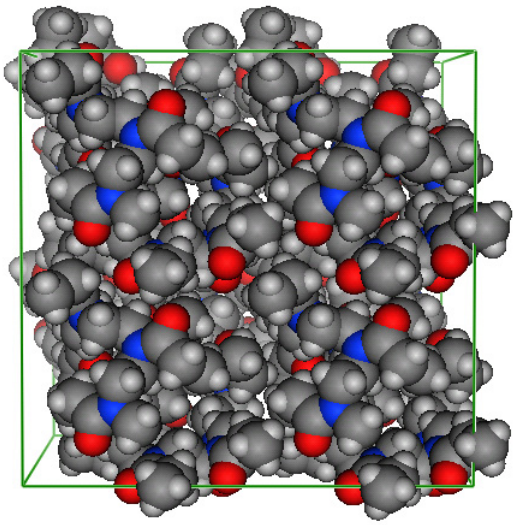

(a) Perfectly Aligned

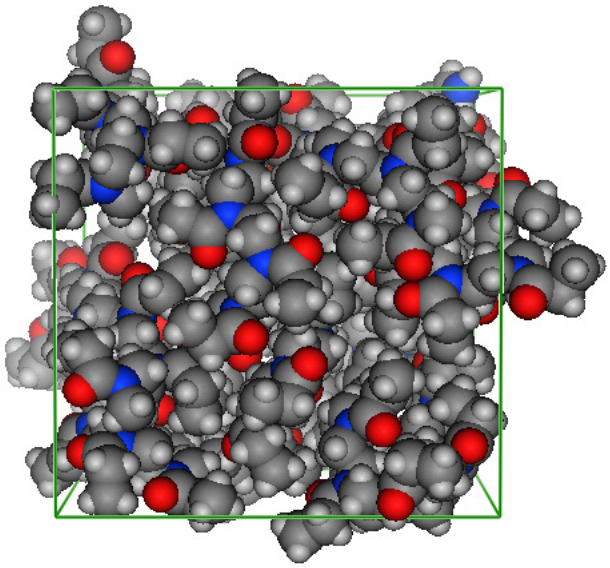

(b) After 700K MD

Figure 3.25: PEOX random coil structure before and after MD at 700K

The difference in angles at the starting helical crystal and the same structure after becoming more disordered during MD simulation at 700K is shown in Figure 3.26.

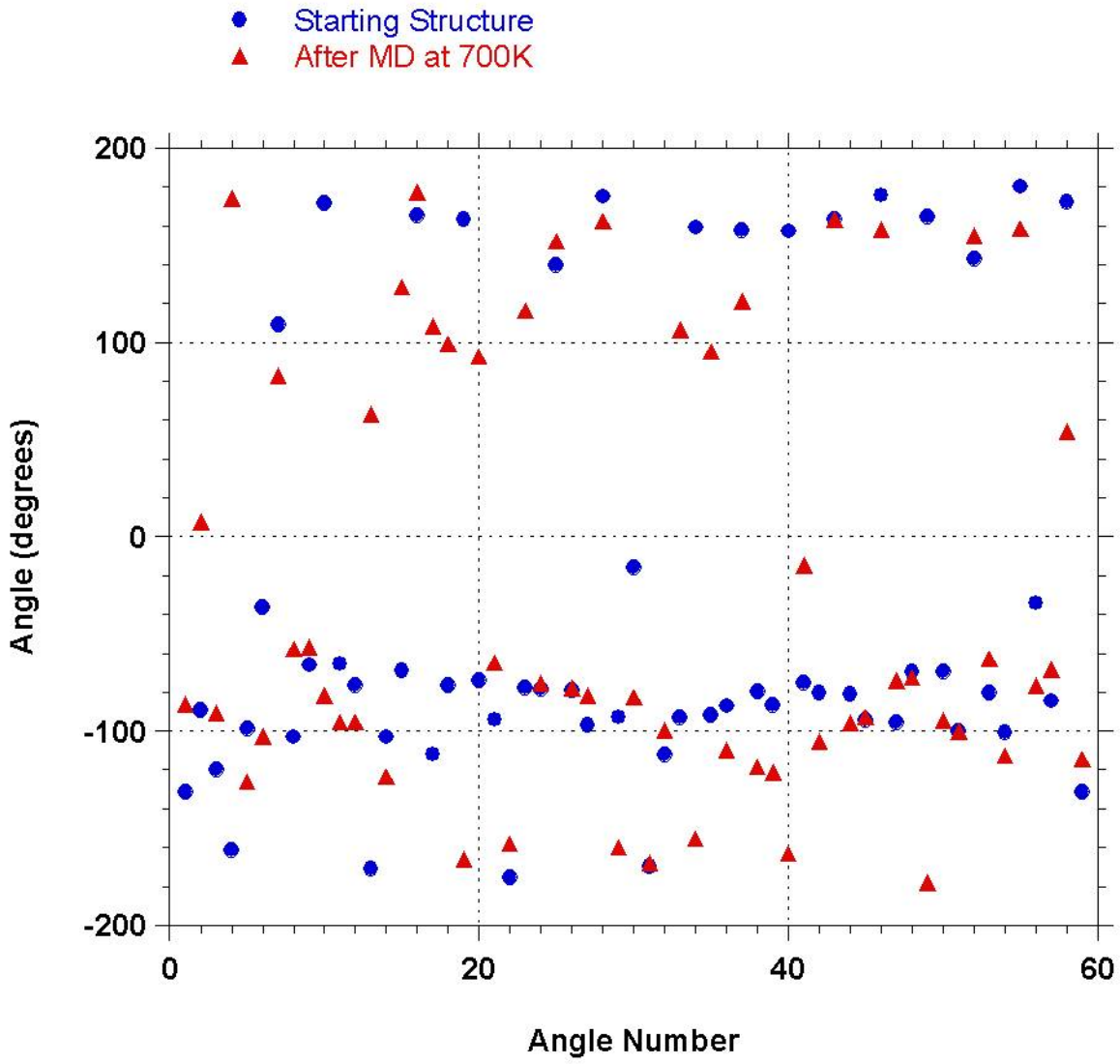

Figure 3.26: Starting point (open circles)and equilibration angles (closed squares)helical crystal after MD at 700K

3.4 Conclusions

PEOX does not form a rigid helical conformation as indicated by the experimental investigations in Chapter 2, however, simulations indicate that a folded helical formation could exist which corresponds to an experimental random coil scaling similar to a folded peptide or peptoid with secondary helical structure. This coiled helical structure may be present in both water and in organic solvents such as THF. These helices are a structural possibility, but random coils are more energetically favorable in vacuum. The effects of hydrogen bonding contributed in aqueous solution will be the subject of the following Chapter. In addition to comparing the potential energy function for both a random coil and folded helix, the effect of each on water structure will be examined since more highly ordered water molecules. The low entropy of water molecules around a conformation while contributing to an increase in free energy of mixing could help to explain the negative entropy of mixing which has been experimentally observed.

3.5 References

[1] Baldauf, C., Günther, R., and Hofmann, H.-J., "Helices in peptoids of alpha and beta peptides," *Physical Biology*, vol. 3, no. 1, p. S1, 2006. 1478-3975.

[2] Bond, Stephen, D., Leimkuhler, Benedict, J., and Laird, Brian, B., "The nosé-poincaré method for constant temperature molecular dynamics," *J. Comput. Phys.*, vol. 151, no. 1, pp. 114–134, 1999. 316646.

[3] Chen, C. H., Wilson, J. E., Davis, R. M., Chen, W., and Riffle, J. S., "Measurement of the segmental adsorption energy of poly(2-ethyl-2-oxazoline) on silica in water and ethanol," *Macromolecules*, vol. 27, no. 22, pp. 6376–6382, 1994.

[4] Chiu, T. T., Thill, B. P., and Fairchok, W. J., "Poly (2-ethyl-2-oxazoline): A new water-and organic soluble adhesive," *by JE Glass, ACS*, p. 425, 1986.

[5] Choi, S., Kim, J. H., and Kang, Y. S., "Wide-angle x-ray scattering studies on the structural properties of polymer electrolytes containing silver ions," *Macromolecules*, vol. 34, no. 26, pp. 9087–9092, 2001.

[6] Cornell, W. D., Cieplak, P., Bayly, C. I., Gould, I. R., Merz, K. M., Ferguson, D. M., Spellmeyer, D. C., Fox, T., Caldwell, J. W., and Kollman, P. A., "A second generation force field for the simulation of proteins, nucleic acids, and organic molecules," *Journal of the American Chemical Society*, vol. 117, no. 19, pp. 5179–5197, 1995.

[7] Douglas, J. F., Roovers, J., and Freed, K. F., "Characterization of branching architecture through "universal" ratios of polymer solution properties," *Macromolecules*, vol. 23, no. 18, pp. 4168–4180, 1990.

[8] Halgren, T. A., "Merck molecular force field. i. basis, form, scope, parameterization, and performance of mmff 94," *Journal of Computational Chemistry*, vol. 17, no. 5-6, pp. 490–519, 1996.

[9] Halgren, T. A., "Merck molecular force field. ii. mmff94 van der waals and electrostatic parameters for intermolecular. interactions," *Journal of Computational Chemistry*, vol. 17, no. 5-6, pp. 520–552, 1996.

[10] Halgren, T. A., "Merck molecular force field. iii. molecular geometries and vibrational frequencies for mmff 94," *Journal of computational chemistry*, vol. 17, no. 5-6, pp. 553–586, 1996.

[11] Halgren, T. A., "Merck molecular force field. v. extension of mmff 94 using experimental data, additional computational data, and empirical rules," *Journal of Computational Chemistry*, vol. 17, no. 5-6, pp. 616–641, 1996.

[12] Halgren, T. A., "Mmff vi. mmff94s option for energy minimization studies," *Journal of Computational Chemistry*, vol. 20, no. 7, pp. 720–729, 1999.

[13] Halgren, T. A., "Mmff vii. characterization of mmff 94, mmff 94 s, and other widely available force fields for conformational energies and for intermolecular-interaction energies and geometries," *Journal of Computational Chemistry*, vol. 20, no. 7, pp. 730–748, 1999.

[14] Halgren, T. A. and Nachbar, R. B., "Merck molecular force field. iv. conformational energies and geometries for mmff 94," *Journal of Computational Chemistry*, vol. 17, no. 5-6, pp. 587–615, 1996.

[15] Huang, K., Wu, C. W., Sanborn, T. J., Patch, J. A., Kirshenbaum, K., Zuckermann, R. N., Barron, A. E., and Radhakrishnan, I., "A threaded loop conformation adopted by a family of peptoid nonamers," *J. Am. Chem. Soc.*, vol. 128, no. 5, pp. 1733–1738, 2006.

[16] Lee, B. C., Zuckermann, R. N., and Dill, K. A., "Folding a nonbiological polymer into a compact multihelical structure," *J. Am. Chem. Soc.*, vol. 127, no. 31, pp. 10999–11009, 2005.

[17] Lucas, A., Huang, L., Joshi, A., and Dill, K. A., "Statistical mechanics of helix bundles using a dynamic programming approach," *J. Am. Chem. Soc.*, vol. 129, no. 14, pp. 4272–4281, 2007.

[18] Mattice, W. L. and Suter, U., "Conformational theory of large molecules : the rotational isomeric state model in macromolecular systems," 1994.

[19] Pauling, L., Corey, R. B., and Branson, H. R., "The structure of proteins - 2 hydrogen-bonded helical configurations of the polypeptide chain," *Proceedings Of The National Academy Of Sciences Of The United States Of America*, vol. 37, no. 4, pp. 205–211, 1951.

[20] Rice, S. A. and Nagasawa, M., *Polyelectrolyte solutions, a theoretical introduction*. London, New York,: Academic Press, 1961.

[21] Schild, H. G., "Poly(n-isopropylacrylamide): experiment, theory and application," *Progress in Polymer Science*, vol. 17, no. 2, p. 163, 1992.

[22] Spevacek, J., Brus, J., Dybal, J., and Kang, Y. S., "Solid-state ^{13}c nmr and dft quantum-chemical study of polymer electrolyte poly(2-ethyl-2-oxazoline)/agcf$_3$so$_3$," *Macromolecules*, vol. 38, no. 12, pp. 5083–5087, 2005.

[23] Sturgeon, J. B. and Laird, B. B., "Symplectic algorithm for constant-pressure molecular dynamics using a nosé-poincaré thermostat," *Journal of Chemical Physics*, vol. 112, no. 8, pp. 3474–3482, 2000.

[24] Sung, J. and Lee, D., "Molecular shape of poly(2-ethyl-2-oxazoline) chains in thf," *Polymer*, vol. 42, pp. 5771–5779, 2001.

CHAPTER IV

MOLECULAR SIMULATION OF PEOX IN WATER

4.1 Introduction

In the previous chapter we studied the conformation of PEOX and compared helical and random coil conformations in isolation. This analysis was conducted in vacuum but our true interests lie in the aqueous conformation. The experimental investigation of PEOX aqueous structure in Chapter 2 indicates that it does not form a rigid helix. In Chapter 3 we examined two major conformations, the first conformation is one with secondary helical structure but a folded tertiary structure and the second a random coil. Both of these configurations could potentially explain the experimentally determined random coil scaling of Chapter 2. Representative structures of these conformations were therefore solvated to find which conformations are favored by aqueous solutions and why.

The aqueous solution behavior of PEOX has been attributed to hydrogen bonding between the PEOX carbonyl group and water molecules [5, 4]. Comparison of the helical and random conformations will reveal which conformation best explains the PEOX-water interactions which have been experimentally observed.This study explores the possible existence of a rigid structure of PEOX, which accompanied by a network of hydrogen bonded water molecules, could explain the net decrease in entropy when PEOX is dissolved in water similar to a globular protein.

Similar to an N-substituted glycine (peptoid) polymer, PEOX cannot hydrogen bond with its own chain segments because of the lack of a proton donating group but has a backbone similar to a peptide. PEOX also has its carbonyl group located on its side chain as opposed to the backbone, limiting the ability of water molecules to

stabilize helical structures.

Peptides and peptoids often exist in the form of helical bundles [10, 17, 9, 3, 12] held together by hydrophobic interactions. In peptides, helical structures are also stabilized by networks of water molecules, however in peptoids the structures are considered to be stabilized by steric factors and more independent of solvent effects [3, 17].

The hydration structures of are important in understanding protein folding. Studying the crystal structure of water molecules around theses structures provides evidence as to the contributions of the water molecules to the stability of the structure [13].

The comparison of coiled helices and random coil conformations in explicit water simulation looks into which conformation will best explain the presence of ordered water around the polymer.

In Chapter 2 we also learned about the effect of sodium chloride(NaCl)on aqueous PEOX solutions. PEOX salts out of solution [11] as does poly(2-isopropyl-2-oxazoline)[7]. This is caused by the reduced availability of water molecules which increases hydrophobic interactions causing precipitation. Salting out is generally associated with globular proteins[2, 6] which again lends credence to the comparison of PEOX to peptides and the possible existence of folded helices in poly(oxazolines).

Other water soluble polymers also salt out such as poly(vinyl pyrrolidone) (PVPD) which in aqueous solution is surrounded by regularly arranged water molecules in a hydrogen bond network. These interactions account for decreases in the heat of mixing of aqueous PVPD solutions when salt is added [15]. PNIPAM also salts out and its LCST decreases the addition of salt [18]. The effect of an electrolyte reducing the availability of water molecules to hydrogen bond with the PEOX molecule was also investigated.

4.2 Methodology

PEOX structures were solvated using an explicit solvation scheme similar to the scheme described in Chapter 3 for the solvated conformational search.

4.2.1 Folded Helices verses Random Coils

A folded helical conformation of PEOX simulated in Chapter 3 was examined to test the viability of such a structure. The structure chosen was a 60 repeat unit folded helix. The 60mer was chosen because it was the smallest of the 20 - 600 repeat unit structures to demonstrate folding. The helix was solvated at various stages of the folding process to compare the possible advantages of folding in water.

Hairpin 60mers folded to angles of 90, 30 and 0 degrees were placed in identical cubic periodic cells of length 40Åto which water molecules were added randomly to achieve a density of 1 g cm^{-3}. The hairpin was fixed and the water was allowed to equilibrate by employing molecular mechanics(MM) and molecular dynamics(MD) simulations at 300K. The PEOX was then unfixed and the entire system allowed to equilibrate using 2ns of molecular dynamics. The resulting structures were compared to determine the advantages of helices folding in water as well as comparison to random coil verses folded helical conformations in water.

4.2.2 Effect of Salt on PEOX Random Coils

As previously determined by viscometry results in Chapter 2, the addition of salt to the solution has the effect of collapsing the polymer chain so investigations into whether this effect could be demonstrated by simulation were conducted. Random coils of 40 repeat units were solvated in a periodic cell by methods similar to those previously described. In order to simulate the effect of sodium chloride on the solvent properties of the water the dielectric constant (ε) of the solvent was adjusted to reflect a salt solution and compared with simulations using the dielectric constant of pure water. After 1ns of initial MD, the dielectric constant was set to the desired value

and 150ps of MD simulation was performed. Dielectric constants ranging from 80 to 68 were used to represent various NaCl salt concentrations (c) according to the equation [14]:

$$\varepsilon = 78.5 - 11c \tag{4.1}$$

Random coils of the same number of repeat units but differing radii of gyration were compared to test the effect of the simulated salt solution on expanded verses collapsed chains. The random coils generated for the isolated simulations in Chapter 3 were solvated began as fairly expanded structures after initial minimization but after relaxation with MD formed considerably more compact structures. Two 40 repeat unit structures with radii of gyration (R_g) 9 and 14$\mathring{A}$ respectively were compared with the smaller R_g representing a more compact conformation. After 150ps of MD at 300K the potential energy was compared for these expanded and collapsed coils in water and salt solution.

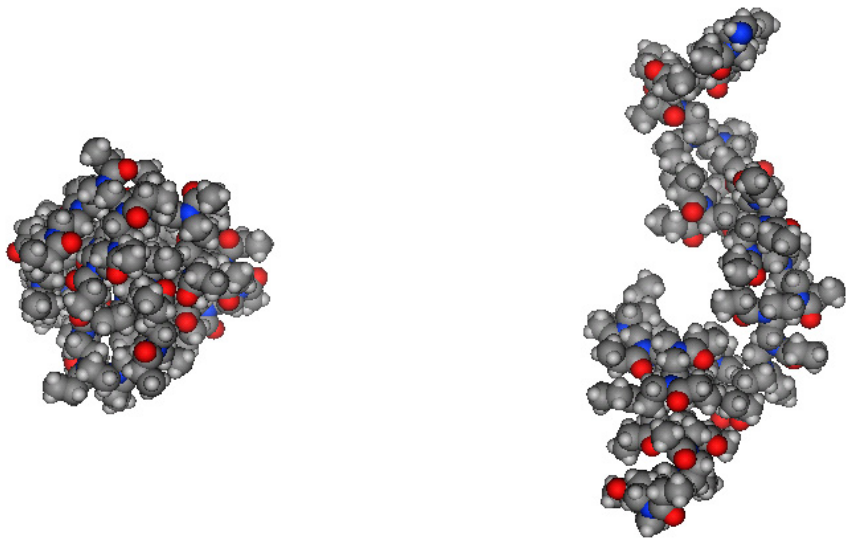

(a) Collapsed (b) Expanded

Figure 4.1: Collapsed and expanded PEOX random coils.

4.3 Results and Discussion

4.3.1 Folded Helices verses Random Coils

The folding of PEOX helices, as discussed in Chapter 3, is due to the hydrophobic interactions between the helix segments as they approach each other. Figure 3.20 shows the change in the non-bonded potential energy terms as the 60mer hairpin folds during MD.

Figures 4.2through 4.9show the potential energy and components thereof of the solvated random coil and hairpin helix folded to various extents.All error bars in the following figures indicate the 90% confidence interval. The potential energies of the hairpin structures and the random coil of comparable size are plotted in Figure 4.2.

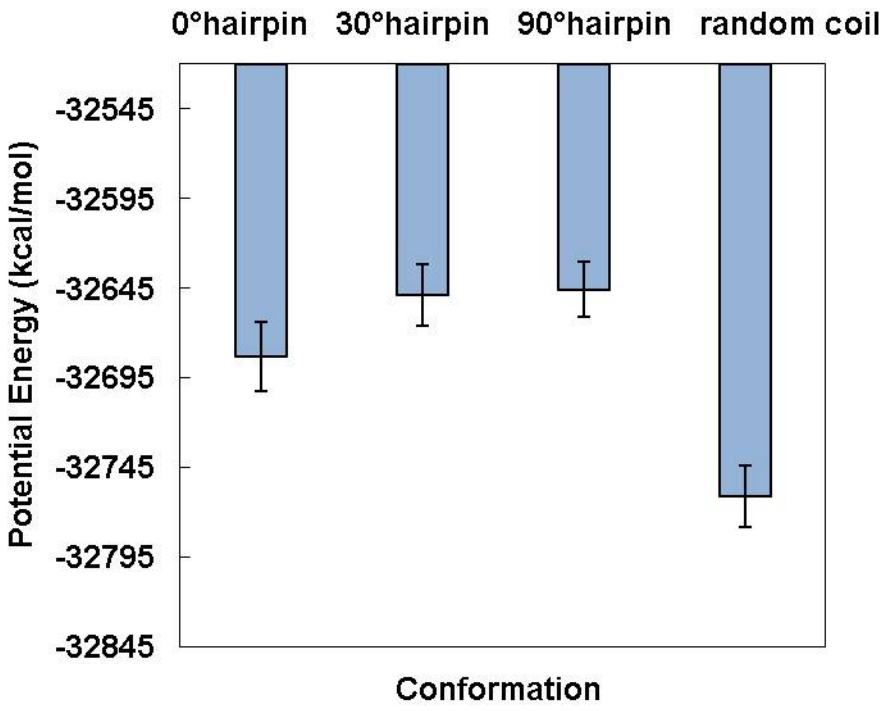

Figure 4.2: Total Potential Energy of PEOX 60mer structures in water.

The completely folded or 0° hairpin in water system has a lower potential energy than the open hairpin structures (30° and 90°) and the random coil has a lower potential energy than any other conformation. These differences in potential energy are largely due to non-bonded interactions graphed in Figure 4.3 which follow the same trends as the total potential energy.

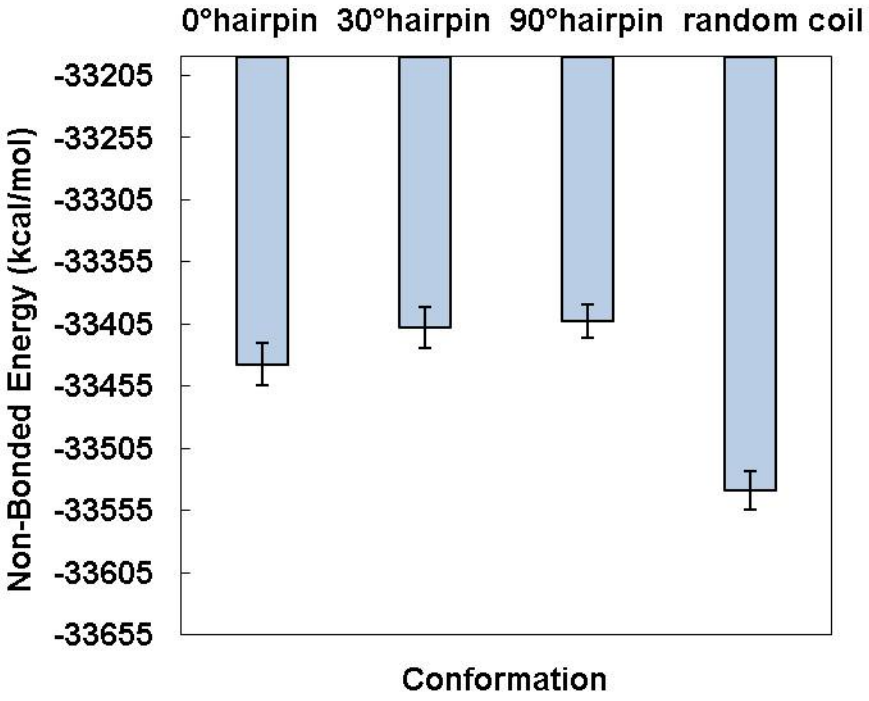

Figure 4.3: Non-Bonded Energy of PEOX 60mer structures in water.

The bonded energy, plotted in Figure 4.4, is comparable for the helices but somewhat higher for the random coil. The non-bonded potential energy is composed of the Van der Waals and the electrostatic energies.

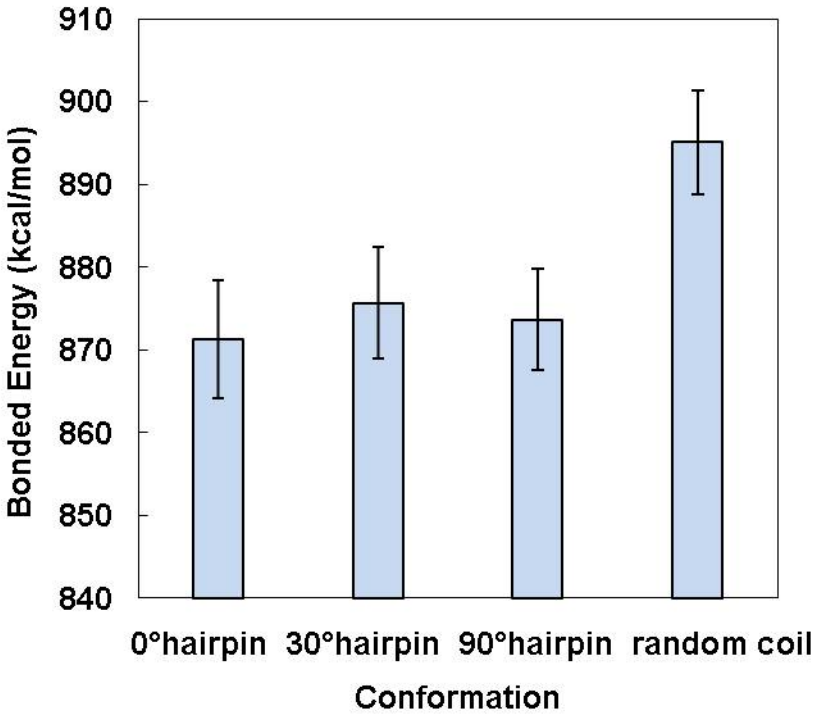

Figure 4.4: Bonded Energy of PEOX 60mer structures in water.

The Van der Waals energy, plotted in Figure 4.5, is lowest for the closed hairpin which has optimized these hydrophobic Van der Waals interactions through folding.

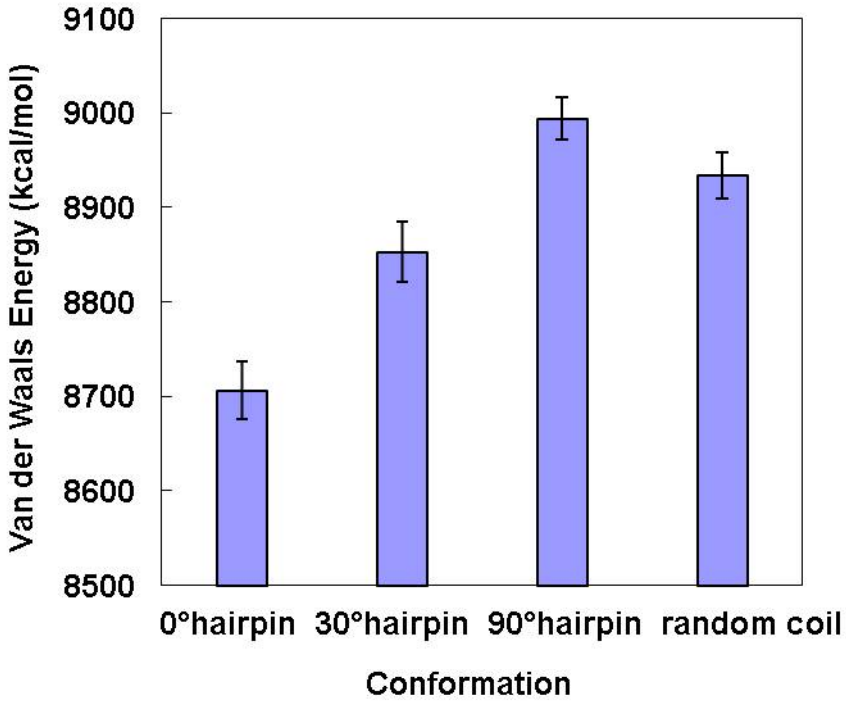

Figure 4.5: Van der Waals Energy of PEOX 60mer structures in water.

The electrostatic energy includes permanent dipole interactions and, for the purpose of this model, includes hydrogen bonds between water molecules and between water molecules and the polymer chain. This term is lowest for the random coil, as shown in Figure 4.6, and increases as the hairpin closes.

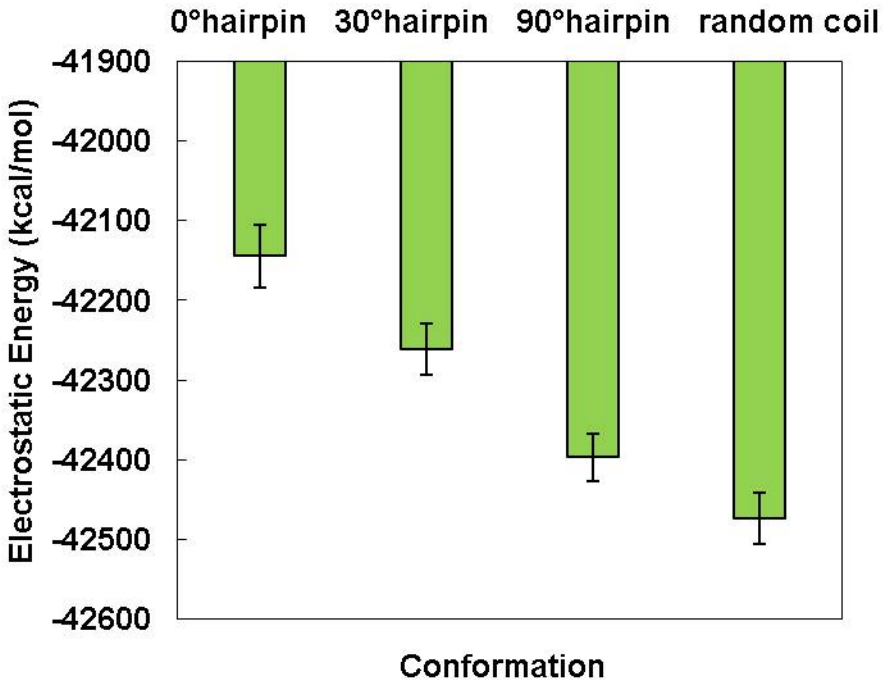

Figure 4.6: Electrostatic Energy of PEOX 60mer structures in water.

The electrostatic energy is minimized for the random coil because of the favorable interactions within the PEOX molecule as demonstrated in Figure 4.7 and because the water molecules surrounding the polymer have greater electrostatic interactions among themselves as demonstrated in Figure 4.8.

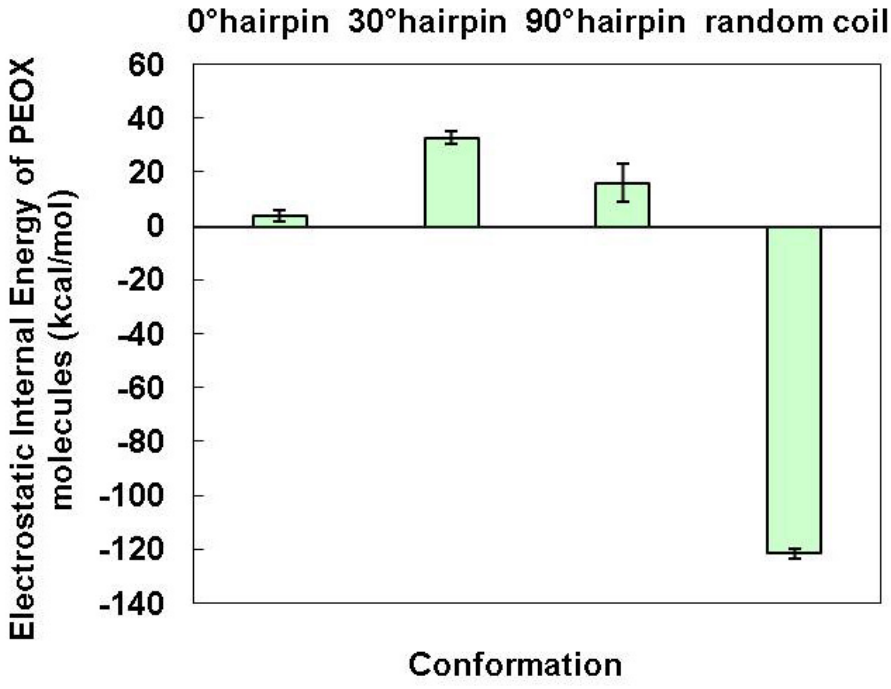

Figure 4.7: Internal Polymer Electrostatic Energy of PEOX 60mer structures in water.

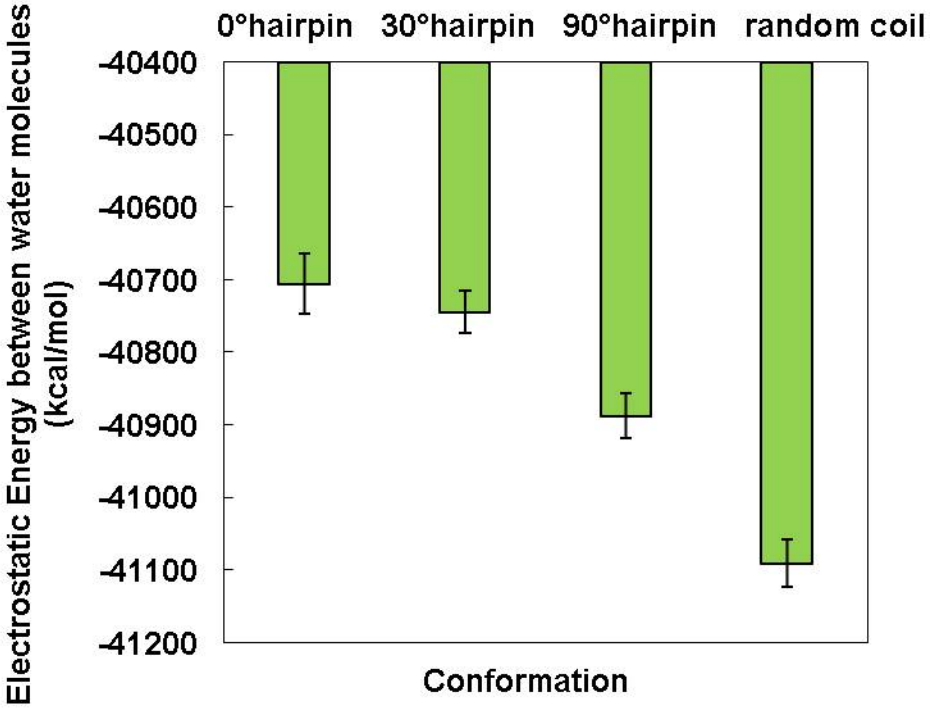

Figure 4.8: Internal Electrostatic Energy between water molecules around of PEOX 60mer structures.

Examination of the electrostatic interactions between the polymer and the water molecules in Figure 4.9 reveals that there are greater interactions between the folded helices and water than between the random coil and water.This is evidenced by not only the better electrostatic interaction energy between the polymer and water molecules but by the examination of the number of hydrogen bonds, listed in Table 4.1, formed between the polymer and the water molecules.

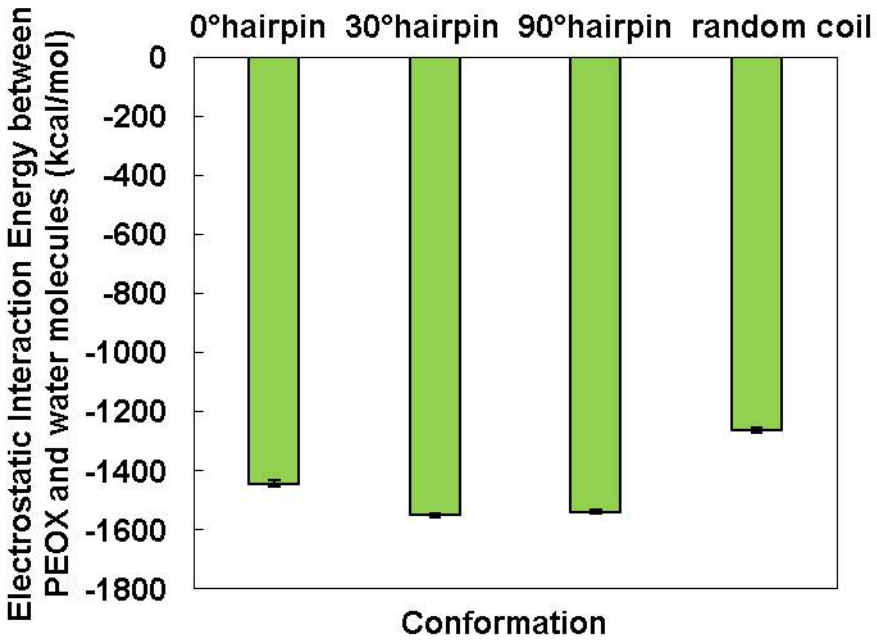

Figure 4.9: Internal Electrostatic Interaction Energy between water molecules and PEOX 60mer structures.

In order to verify that the lower potential energy of the random coil was not an artifact of the simulation the simulation was repeated but without the use of periodic boundary conditions [20] to eliminate the effect of the periodic box on the energy of the bulk water molecules. For this simulation the random coil is still the structure with the lowers potential energy as shown in Figure 4.10.

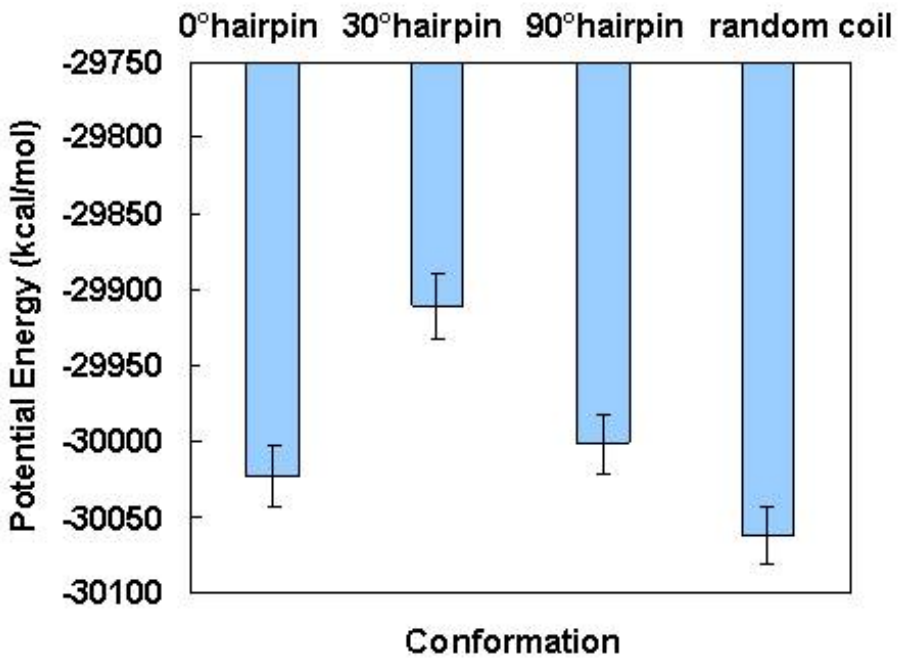

Figure 4.10: Total Potential Energy of PEOX 60mer structures in water and non-periodic boundary conditions.

The hydrogen bonding between water molecules is greater around the random coil than around the folded helical conformation.

The arrangement of water molecules around both the helical and random structures was examined but counting the number of hydrogen bonds between water molecules and PEOX carbonyl oxygens and by examination of the hydrogen bond network surrounding the polymer molecule.

Water molecules have the ability to hydrogen bond with the carbonyl and then with each other or a second carbonyl. This facilitates the formation of water bridges

Table 4.1: Number of hydrogen bonds between water molecules and PEOX 60mer structures

Structure	Number of hydrogen bond sites between water and PEOX
0°hairpin	82
30°hairpin	83
90°hairpin	84
random coil	73

or networks which connect polymer atoms. In peptides, these bridges connect backbone atoms and therefore have a profound impact on backbone structure [19]. Understanding these hydration structures is seen as integral to understanding protein folding mechanisms[16].

The solvated PEOX hairpin and random coil structures are shown in Figure 4.11. The greater number of hydrogen bonds between water molecules and the helical PEOX structures, shown in Table 4.1, indicates that the helical structures provide greater accessability to the carbonyl on the side chain.

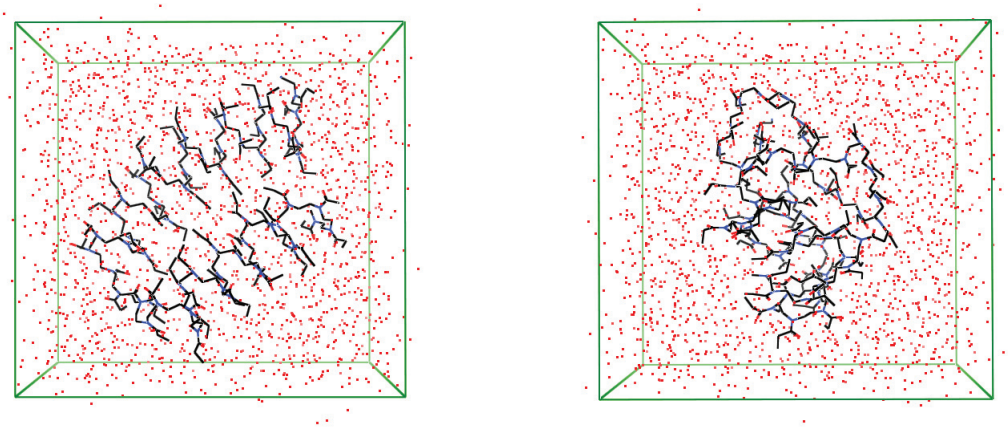

(a) 0 degree hairpin

(b) random coil

Figure 4.11: Solvated PEOX hairpin and random coil

Radial distribution functions from molecular simulations can be valuable in determining water structure [8]. The general distribution of water molecules is not vastly different between the two major structures (random coil and closed helix hairpin)as shown in Figure 4.12.

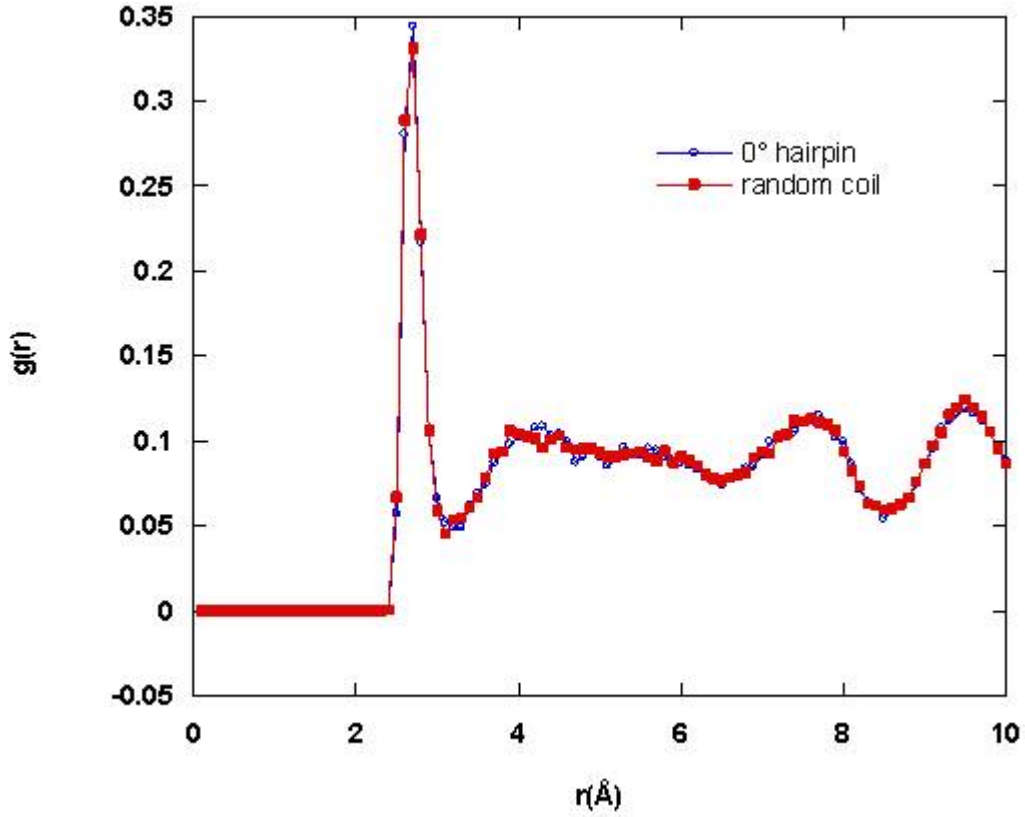

Figure 4.12: Radial pair distribution function of water molecules averaged over 600ps of MD.

The hydration networks were therefore examined to infer the influence of each conformation on water structure. The water networks around the 0 degree hairpin helical structure and the random coil conformation were compared. The results are

shown in Table 4.2. If the number of hydrogen bonds between carbonyl groups and water molecules are compared the hairpin has a higher number of these interactions. This would help to account for the better electrostatic interaction energy between the helix and the water molecules than between the random coil and the water molecules.

Table 4.2: Number of hydrogen bonds between water molecules and PEOX 60mer structures. Level 1 waters are directly H-bonded to a carbonyl group and Extended Level waters are directly H-bonded or connected by a bridge of 1 or 2 waters

Structure	Level 1 waters	Extended Level waters	R_g (Å)
0°hairpin	68	156	11.7
random coil	66	171	10.7

Upon closer examination, water molecules may be hydrogen bonded to more than one carbonyl group or connect carbonyl groups through a series of hydrogen bonded water molecules. Examples of the water bridge networks around PEOX are shown in Figure 4.13. For peptides, structurally important bridges are assumed to involve 1 to 3 water molecules [19] so the same was assumed in this study.

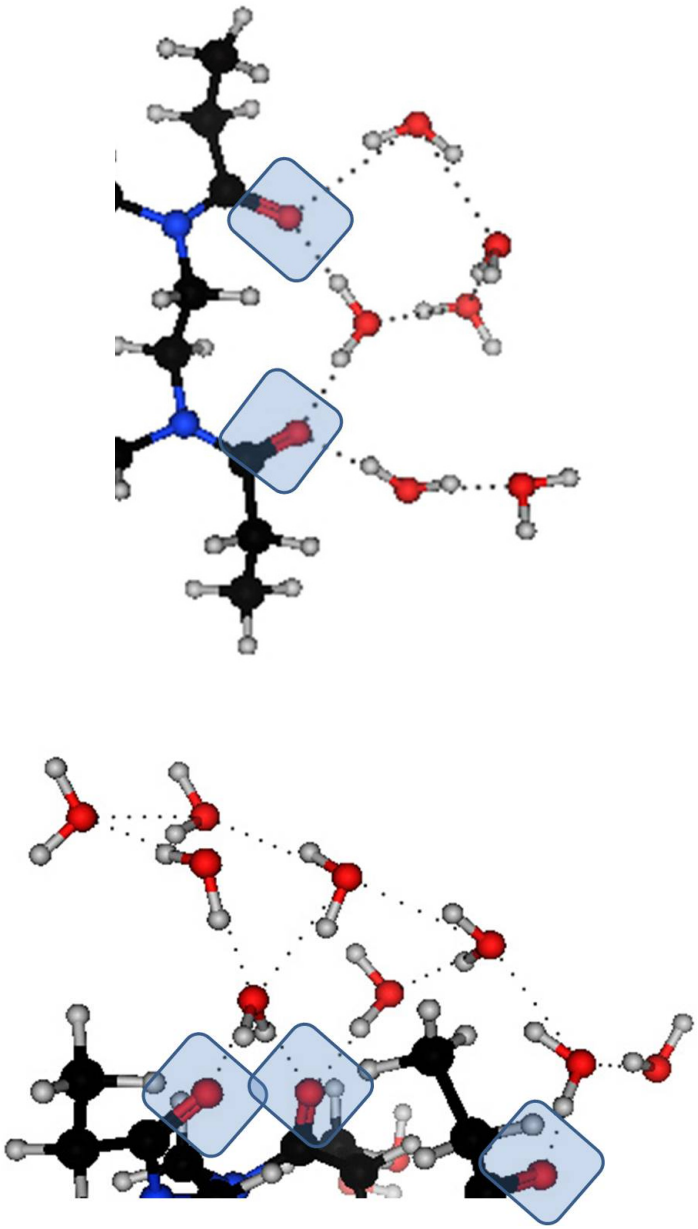

Figure 4.13: Examples of water bridge networks. Dashed lines represent hydrogen bonds and participating carbonyl oxygens are highlighted.

If we consider how many water molecules are directly attracted to a carbonyl group by a hydrogen bond (denoted as Layer 1 waters in Table 4.2) there are only two more water molecules for the helix hairpin than the random coil which is a 3% difference

and is less striking than the 12% difference in total water-carbonyl interactions. This difference may be accounted for by examination of the networks of water formed around the structure. For the random coil, the largest network detected involves 2 carbonyl groups, whereas for the hairpin helix as many as 5 carbonyls are connected by bridges of 1 to 3 water molecules.

We have found that although the electrostatic interaction energy is better for the hairpin helix, the internal electrostatic energy of the water around the random coil is more favorable. To investigate the possible explantation for this effect, the extended network of water molecules was examined. If we count the number of water molecules hydrogen bonded to a carbonyl, either directly or by 1 or 2 bridging water molecules we find that more water molecules are associated with the random coil than with the hairpin helix. This value is denoted as Extended Layer waters in Table 4.2.

In protein hydration, water molecules further and 4Åfrom the protein surface are not considered participants in the hydration and do not have a controlling effect on the structure [13]. Similarly this extended network for PEOX is not stabilizing the PEOX conformation.

The random coil has a greater networking effect overall on the surrounding water molecules and influences a larger network of water molecules although fewer carbonyl groups are accessible to water molecules than is the case with the hairpin helix. This may, at least partially, be accounted for by the smaller radius of gyration of the random coil. Although the helix is a more regular structure and facilitates more complex networks, the random coil is a more compact structure and stabilizes more water molecules around it.

The larger extended network of water molecules around the random coil conformation also better accounts for the reduced entropy upon dissolution in water than does the smaller network around the hairpin helix.

The mean squared displacement of water molecules around the folded helix and

random coil are over the last 600ps of MD simulation are shown in Figure 4.14. The slope, which represents the diffusivity, for the helix taken over the last 400ps is $2.2 \pm 0.5 \times 10^{-4} \mathring{A}^2 ps^{-1}$which is higher than that of the random coil ($1.7 \pm 0.3 \times 10^{-4} \mathring{A}^2 ps^{-1}$)indicating that the diffusivity may be higher for water molecules around the helix.

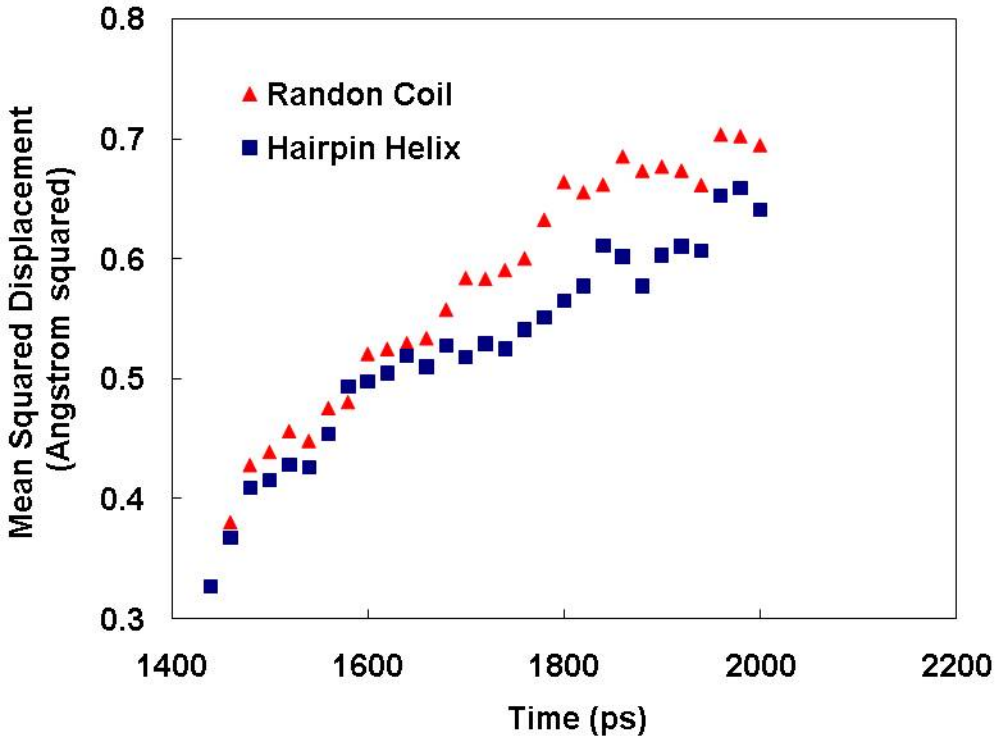

Figure 4.14: Mean squared displacement of water molecules over last 600ps of MD.

4.3.2 Effect of Salt on PEOX Random Coils

The potential energy averaged over the last 50ps of a 150ps MD simulation are shown in Figure 4.15 for random coils of R_g=9 and 14 $\mathring{A}$. Error bars for Figures 4.15 through

4.22 represent the 95% confidence interval averaged over 50 values. In general the more expanded coil has a lower potential energy at most values of ε whereas the reverse is true in vacuum. This suggests that in water the conformation of PEOX is more expanded than it would be in a non hydrogen bonding solvent. Additionally it should be observed that at a very low ε=68 (high salt concentration) the potential energy becomes much lower for the more collapsed coil which corresponds with the experimental observation in Chapter 2 of a more collapsed conformation at high salt concentration.

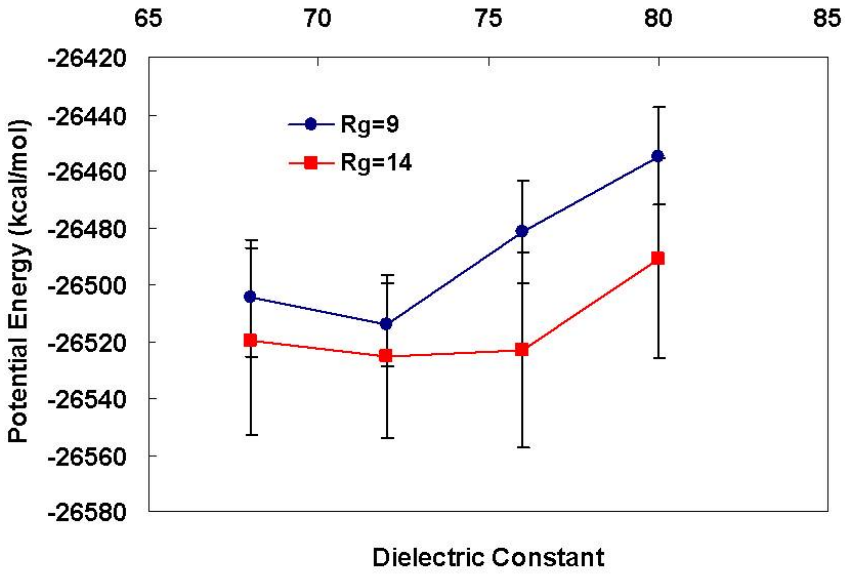

Figure 4.15: Potential energy verses dielectric constant for random coils of differing radii.

The overall bonded energy shown in Figure 4.16 is lower for the more collapsed coil. The non-bonded energy shown in Figure 4.17 dominates the general trend of the potential energy verses dielectric constant. When split into its components of electrostatic (Figure 4.18) and Van der Waals (Figure 4.19)energy we see that the electrostatic energy accounts for the trend in non bonded energy.

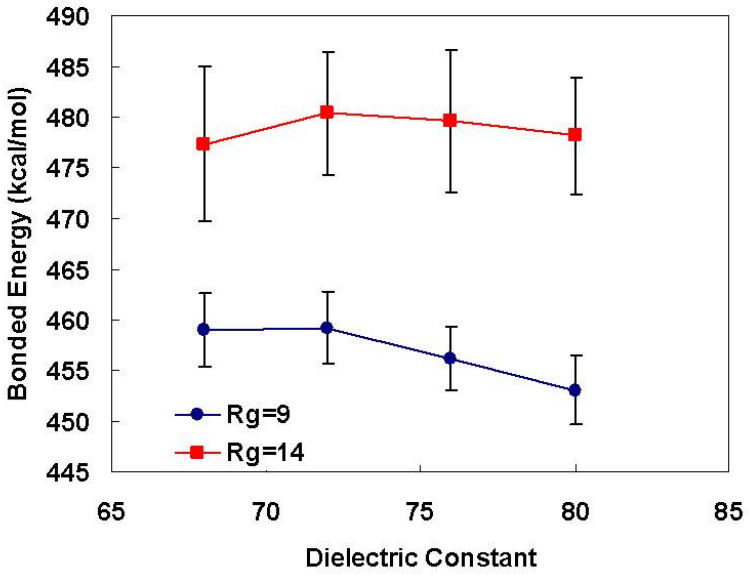

Figure 4.16: Bonded Energy verses dielectric constant for random coils of differing radii.

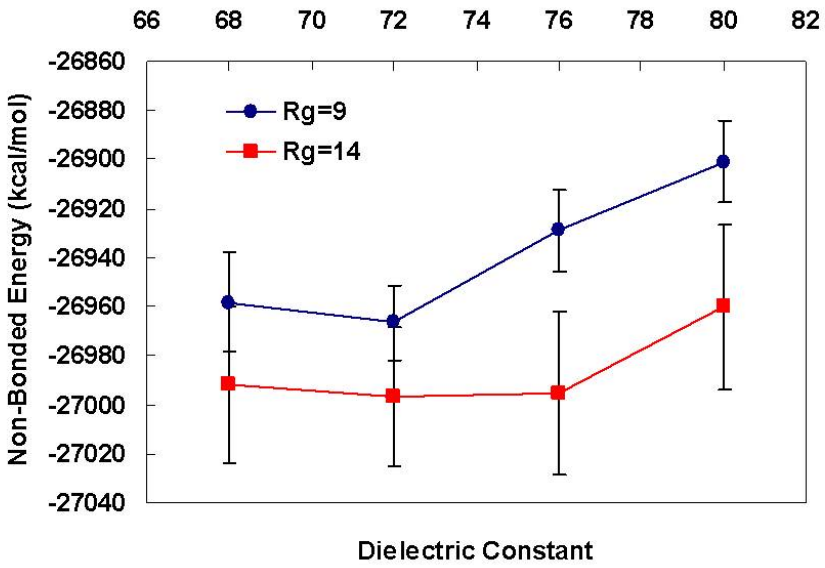

Figure 4.17: Non-bonded Energy verses dielectric constant for random coils of differing radii.

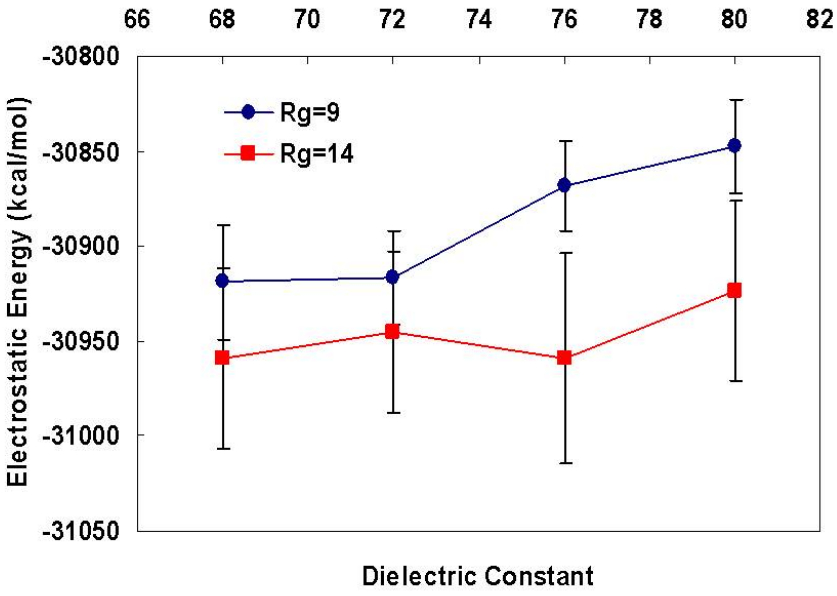

Figure 4.18: Electrostatic Energy between verses dielectric constant for random coils of differing radii.

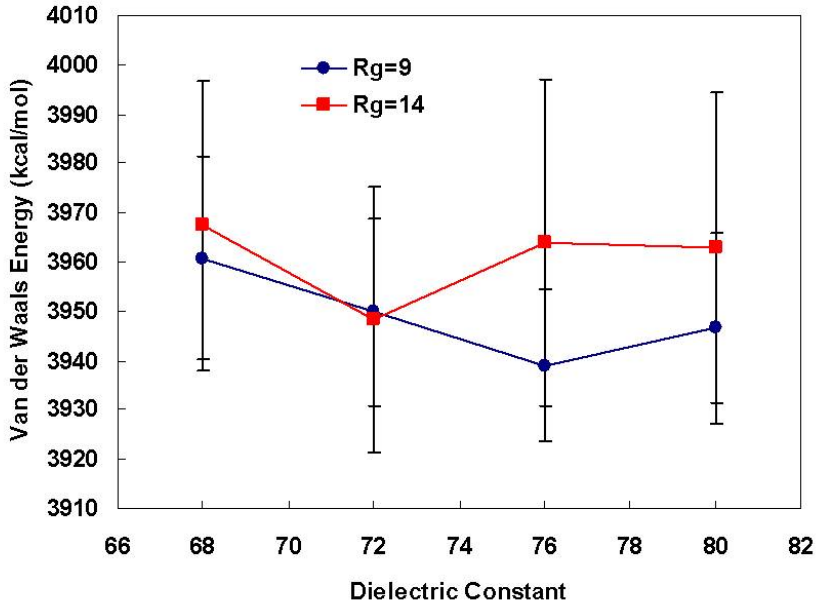

Figure 4.19: Van der Waals Energy between PEOX and water molecules verses dielectric constant for random coils of differing radii.

Examination of the components of the electrostatic energy plotted in Figures 4.20 through 4.22 demonstrates that salting out at high concentration (dielectric constant =68) is due to the effect of the ions on the electrostatic interactions between the water molecules. In proteins a similar effect is observed where increased salt concentration causes increased surface tension of water reflecting greater solvent-solvent interactions and therefore salting out [1].

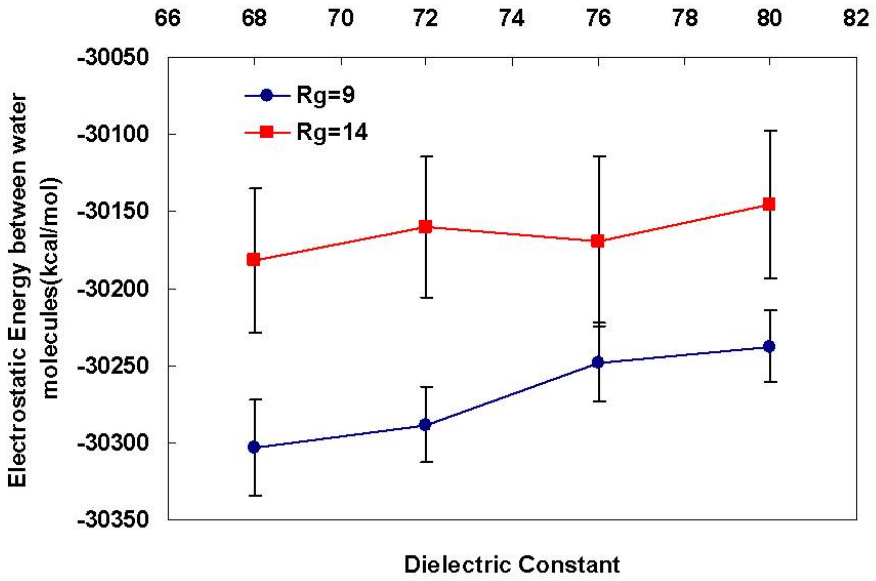

Figure 4.20: Electrostatic Energy between water molecules verses dielectric constant for random coils of differing radii.

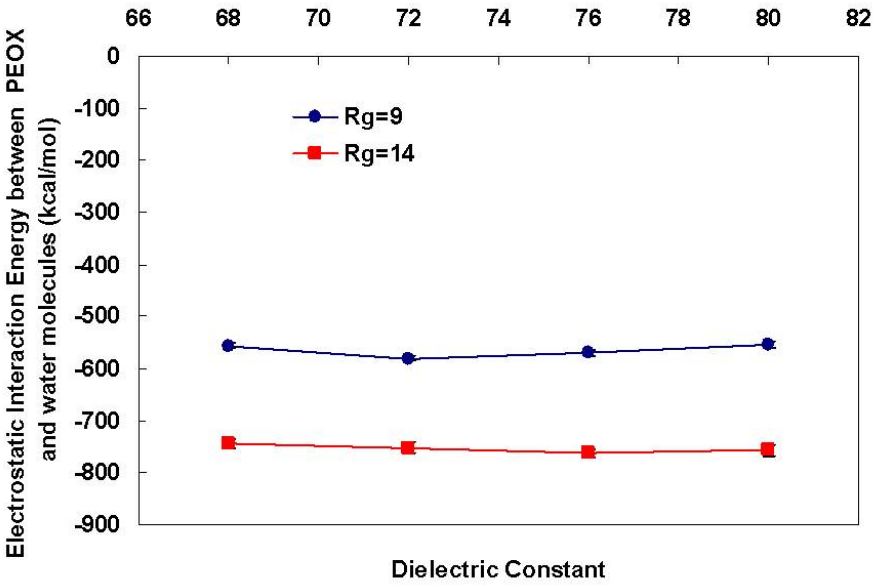

Figure 4.21: Electrostatic Energy between PEOX and water molecules verses dielectric constant for random coils of differing radii.

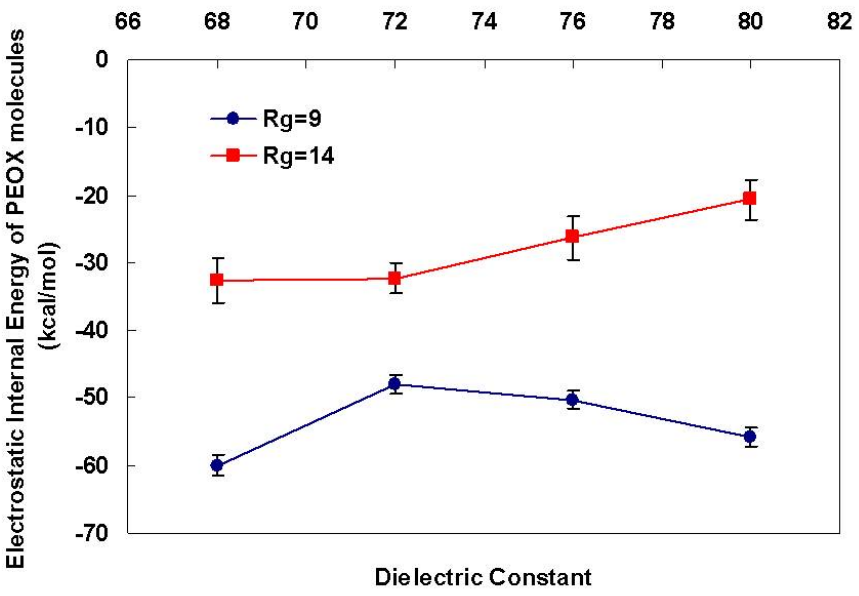

Figure 4.22: Internal Polymer Electrostatic Energy of PEOX verses dielectric constant for random coils of differing radii.

4.4 Conclusions

PEOX does not form a rigid helical conformation, but simulations indicate that a helical formation could exist which scales similar to a random coil. This coiled helical structure may be present in both water and in organic solvents such as THF. Solvated simulations have revealed that a random coil system has a lower potential energy that a folded helix and may have a greater networking effect overall on the surrounding water molecules explaining the reduced entropy of mixing and random coil scaling without the presence of helical structure. The random coil conformation seems to be the energetically preferred conformation in water and is consistent with observed salting out behavior.

A more expanded random coil has a lower potential energy at most values of

ε whereas in vacuum chains collapse to a compact configuration during molecular dynamics. This suggests that in water the conformation of PEOX is more expanded than it would be in a non hydrogen bonding solvent. At a high salt concentration the potential energy becomes much lower for a more collapsed coil which corresponds with the experimental observation that PEOX is more collapsed at high salt concentration.

4.5 References

[1] Arakawa, T., Bhat, R., and Timasheff, S. N., "Preferential interactions determine protein solubility in three-component solutions: the magnesium chloride system," *Biochemistry*, vol. 29, no. 7, pp. 1914–1923, 1990.

[2] Arakawa, T. and Timasheff, S. N., "Mechanism of protein salting in and salting out by divalent cation salts: balance between hydration and salt binding," *Biochemistry*, vol. 23, no. 25, pp. 5912–5923, 1984.

[3] Baldauf, C., Günther, R., and Hofmann, H.-J., "Helices in peptoids of alpha and beta peptides," *Physical Biology*, vol. 3, no. 1, p. S1, 2006. 1478-3975.

[4] Chen, C. H., Wilson, J. E., Davis, R. M., Chen, W., and Riffle, J. S., "Measurement of the segmental adsorption energy of poly(2-ethyl-2-oxazoline) on silica in water and ethanol," *Macromolecules*, vol. 27, no. 22, pp. 6376–6382, 1994.

[5] Chen, F., Ames, A., and Taylor, L., "Aqueous solutions of poly(ethyloxazo1ine) and its lower consolute phase transition," *Macromolecules*, vol. 23, no. 21, pp. 4688–4695, 1990.

[6] Chi, E. Y., Krishnan, S., Randolph, T. W., and Carpenter, J. F., "Physical stability of proteins in aqueous solution: Mechanism and driving forces in nonnative protein aggregation.," *Pharmaceutical Research*, vol. 20, no. 9, pp. 1325–36, 2003.

[7] Diab, C., Akiyama, Y., Kataoka, K., and Winnik, F. M., "Microcalorimetric study of the temperature-induced phase separation in aqueous solutions of poly(2-isopropyl-2-oxazolines)," *Macromolecules*, vol. 37, no. 7, pp. 2556–2562, 2004.

[8] Fois, E., Gamba, A., Morosi, G., Ponti, A., Demontis, P., and Suffritti, G., "The structure of liquid water: simulations vs. experiments," *Gazzetta Chimica Italiana*, vol. 120, pp. 591–597, 1990.

[9] Huang, K., Wu, C. W., Sanborn, T. J., Patch, J. A., Kirshenbaum, K., Zuckermann, R. N., Barron, A. E., and Radhakrishnan, I., "A threaded loop conformation adopted by a family of peptoid nonamers," *J. Am. Chem. Soc.*, vol. 128, no. 5, pp. 1733–1738, 2006.

[10] Lee, B. C., Zuckermann, R. N., and Dill, K. A., "Folding a nonbiological polymer into a compact multihelical structure," *J. Am. Chem. Soc.*, vol. 127, no. 31, pp. 10999–11009, 2005.

[11] Lin, L.-N., Brandts, J. F., Brandts, J. M., and Plotnikov, V., "Determination of the volumetric properties of proteins and other solutes using pressure perturbation calorimetry," *Analytical Biochemistry*, vol. 302, no. 1, p. 144, 2002.

[12] Lucas, A., Huang, L., Joshi, A., and Dill, K. A., "Statistical mechanics of helix bundles using a dynamic programming approach," *J. Am. Chem. Soc.*, vol. 129, no. 14, pp. 4272–4281, 2007.

[13] Nakasako, M., "Water-protein interactions from high-resolution protein crystallography," *Philosophical Transactions of the Royal Society B: Biological Sciences*, vol. 359, no. 1448, pp. 1191–1206, 2004.

[14] Parsons, R., *Handbook of electrochemical constants*. New York: Academic Press, 1960.

[15] Rice, S. A. and Nagasawa, M., *Polyelectrolyte solutions, a theoretical introduction*. London, New York,: Academic Press, 1961.

[16] Rupley, J. A. and Careri, G., "Protein hydration and function," *Adv Protein Chem*, vol. 41, pp. 37–172, 1991.

[17] Sanborn, T. J., Wu, C. W., Zuckermann, R. N., and Barron, A. E., "Extreme stability of helices formed by water-soluble poly-n-substituted glycines (polypeptoids) with," *Biopolymers*, vol. 63, no. 1, pp. 12–20, 2002.

[18] Schild, H. G., "Poly(n-isopropylacrylamide): experiment, theory and application," *Progress in Polymer Science*, vol. 17, no. 2, p. 163, 1992.

[19] Sreerama, N. and Woody, R. W., "Molecular dynamics simulations of polypeptide conformations in water: A comparison of alpha, beta, and poly(pro)ii conformations," *Proteins: Structure, Function, and Genetics*, vol. 36, no. 4, pp. 400–406, 1999.

[20] Weis, A., Katebzadeh, K., Soderhjelm, P., Nilsson, I., and Ryde, U., "Ligand affinities predicted with the mm/pbsa method: Dependence on the simulation method and the force field," *J. Med. Chem.*, vol. 49, no. 22, pp. 6596–6606, 2006.

CHAPTER V

ADSORPTION OF POLY(2-ETHYL-2-OXAZOLINE) ON CELLULOSE

5.1 Introduction

Adsorption on cellulose is a prerequisite property of water soluble polymers which are used in the wet end of paper processing. High molecular weight polymer additives are used as flocculants or retention aids. Polymers such as polydimethyldiallylammonium chloride (poly(DADMAC)), and cationic polyacryamides (C-PAM) [13, 7] are adsorbed because of an ion-exchange process or an electrostatic attraction between the polymer and the negatively charged cellulose fibers, fines and fillers [14, 15].

So many charged polymer additives, both anionic and cationic, are used in paper making for various purposes, that there is charge interference affecting their adsorption. The adsorption of cationic polyelectrolytes on cellulose is seen as following a matching of charges between the cationic polyelectrolytes and negatively charged sites on the cellulose. These cationic polymers compete for adsorption sites on the cellulose fibers and re-conform on the cellulose surface [14]. Cationic polymers are able to flocculate fine cellulose particles which enables them to be used as retention aids [8]. Non-ionic polymers are less susceptible to these charge interactions and non-ionic additives such as poly(ethylene oxide) (PEO) are often used along with a cofactor which aids their adsorption [12].

The free energy of adsorption of a polymer on a surface must be negative for adsorption to occur and this is achieved by decreases in enthalpy which offset the accompanying decrease in entropy. As demonstrated in Figure 5.1, when a polymer is adsorbed on a surface the interaction between the two releases energy and therefore

results in a negative change in the enthalpy. The entropic contribution to the free energy is dependant on the polymer conformation. The adsorption of a typical random coil will result in a decrease in entropy due to the polymer being more constrained on the surface. A more rigid conformation such as a helix will result in a smaller decrease in entropy and if that rigid conformation is stabilized by constrained water molecules, the release of these water molecules upon adsorption will contribute to an increase in entropy. In addition to entropic effects, hydrogen bonding bridges between PEOX and cellulose may also contribute to its adsorption.

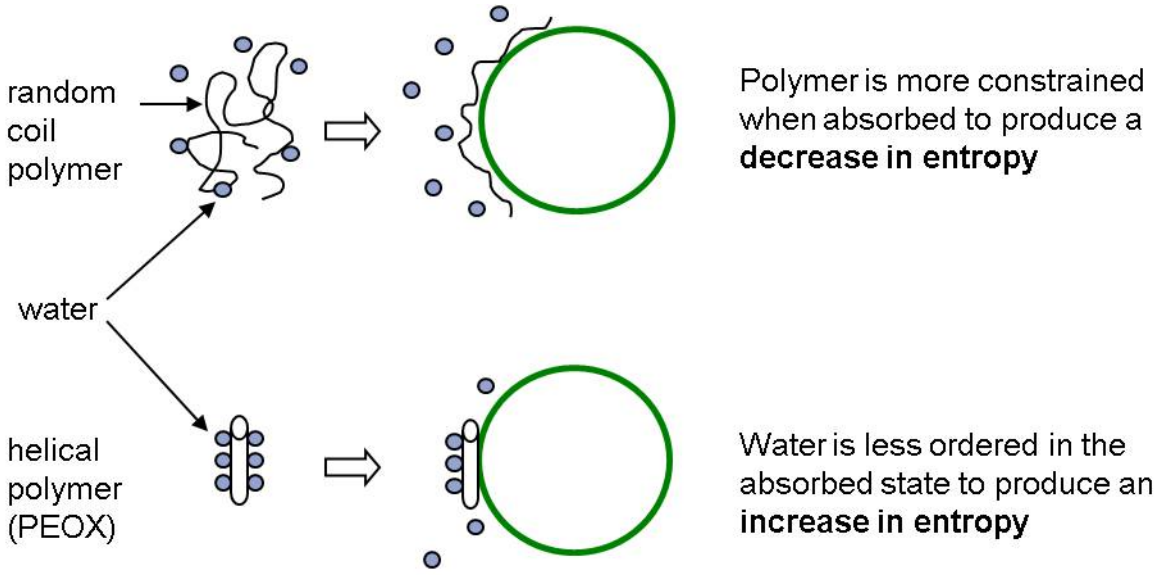

Figure 5.1: Schematic of Adsorption of Non-ionic Polymers

In this Chapter we investigate the effect of electrolyte concentration on the adsorption of PEOX, since as shown in Chapter 2, electrolyte concentration has a significant

effect on polymer conformation which may in turn affect adsorption. Electrolyte concentration also affects aggregation of cellulose particles by decreasing the electronic double layer.

Starch has been used as an adhesive for many years in wet end paper processing in order to improve the dry strength of paper. The addition of NaCl decreases the adsorption of cationic and nonionic starch on cellulose [9]. Hydroxylethyl ether starches, which are nonionic polymers, adsorb mainly through hydrogen bonding onto cellulose [5]. This adsorption is less than that of cationic starch [9] which adsorbs primarily by electrostatic interaction. With the addition of salt these electrostatic interactions are screened and adsorption of cationic starch decreases. Hydroxylethyl starches are nonionic and therefore do not experience a change in adsorption for low salt concentrations since their size is not dependent on salt concentration.

The agglomeration of charged colloidal particles dissolved in an ionic solvent is controlled by Van der Waals attractions between the particles and electrostatic repulsive forces between the particles which are due to charged surface groups. Particles are more likely to interact if the electronic double layer formed by the repulsive forces is reduced in size by the addition of electrolytes to the solvent.

Electrolytes are considered to affect primarily the adsorption of polyelectrolytes but in the case of polymers such as PEOX, which salt out, increasing electrolyte concentration may improve adsorption by its effect on the polymer conformation. Due to the energetic relationships governing adsorption, temperature is also an important governing factor in the process.

5.2 Methodology

5.2.1 Specific Surface Area of Microcrystalline Cellulose

In order to determine the specific surface area of the microcrystalline cellulose (MCC) employed in the experiments, the system for determining fiber specific surface area

developed by Kaewprasit and co-workers using adsorption of methylene blue dye(MB) on the MCC in aqueous solution was employed [6]. This method finds the accessible surface area of the adsorption surface and has the advantage over traditional methods such as nitrogen or noble gas adsorption of being conducted in the liquid phase in order to more accurately account for the effect of particle swelling on the surface area. Microcrystalline cellulose was chosen because of its homogeneity relative to commercial pulps.

Methylene blue chloride was obtained from Fisher Scientific and dried at 110°C before use. Microcrystalline cellulose was attained from Sigma-Aldrich and used as received. PEOX of reported molecular weight 500 $kg\ mol^{-1}$ was obtained from Sigma-Aldrich and used as received. All water used in the experiments was deionized. Methylene blue experiments were conducted in plastic lab ware since the methylene blue was found to adsorb significantly on glass from aqueous solutions.

In general adsorption measurements were conducted by agitating the cellulose suspension with the added adsorbent at 200rpm and separation of the solution by centrifugation. UV-Visible spectroscopy was used to analyze the starting concentrations and supernatant concentrations.

Adsorption of methylene blue on MCC was determined by adding MCC to methylene blue solutions of measured concentration. All MB solution concentrations were determined based on a calibration curve developed by plotting visible light absorbance at 660nm verses concentration of solutions ranging from 0 to $5\times10^{-5}\ mol\ L^{-1}$. Absorbance, A, is directly proportional to the path length, b, and the concentration, c, of the absorbing species according to Beer's Law which states that:

$$A = \epsilon bc \tag{5.1}$$

where ϵ is the absorbtivity (proportionality constant). The kinetics of methylene blue adsorption was determined by measuring the concentration of methylene blue over

time in 1% MCC suspended in various starting concentrations of methylene blue. The adsorption time was estimated from these measurements.

The adsorption of methylene blue on MCC was measured at room temperature (˜24°C) for a range of concentrations from 0 to 0.5 $mg\ L^{-1}$ and the adsorbed amount plotted against the equilibrium concentration to form the adsorption isotherm for methylene blue on MCC. The specific surface area was them determined from the maximum adsorbed amount the following equation [3]:

$$S_{MB} = \frac{N_g a_{MB} N \times 10^{-20}}{M_{MB}} \tag{5.2}$$

where

S_{MB} is the specific surface area in $10^{-3} km^2 kg^{-1}$

N_g is amount of methylene blue adsorbed at the monolayer of fibers in $kg\ kg^{-1}$

a_{MB} is the surface area occupied by one molecule of methylene blue ($197.2 \mathring{A}^2$) [2]

N is Avogadro's number ($6.02 \times 10^{23} mol^{-1}$)

M_{MB} is the molecular weight of methylene blue ($373.9 g\ mol^{-1}$)

5.2.2 Adsorption of PEOX

Poly (2-ethyl-2-oxazoline) samples of molecular weight 500 $kg\ mol^{-1}$ were investigated in a similar manner to methylene blue for their adsorption on MCC. In addition the effect of salt concentration and temperature on adsorption were investigated by repeating the experiments in 0.1M NaCl and then at 50°C respectively. UV absorbance spectra were used to obtain the concentrations of PEOX solutions.

5.2.3 Flocculation of MCC by PEOX

In order to determine the flocculation capacity of PEOX a column settling study using a method similar to that of Biswal and Singh [1]was carried out in 10 wt% MCC suspensions. The test was done by placing the cellulose suspension into a

25mL graduated cylinder which was sealed and mixed by inverting 10 times. The cylinder was then placed upright and the height of the interface between the water and the settled portion was measured over time.

5.3 Results and Discussion

5.3.1 Specific Surface Area of Microcrystalline Cellulose

Methylene blue concentrations were determined by the visible absorbance spectrum of methylene blue in water. The maximum point of the absorbance peak was found to be at 660nm and all methylene blue absorbencies were measured at this wavelength. The resulting calibration curve is shown in Figure 5.2.

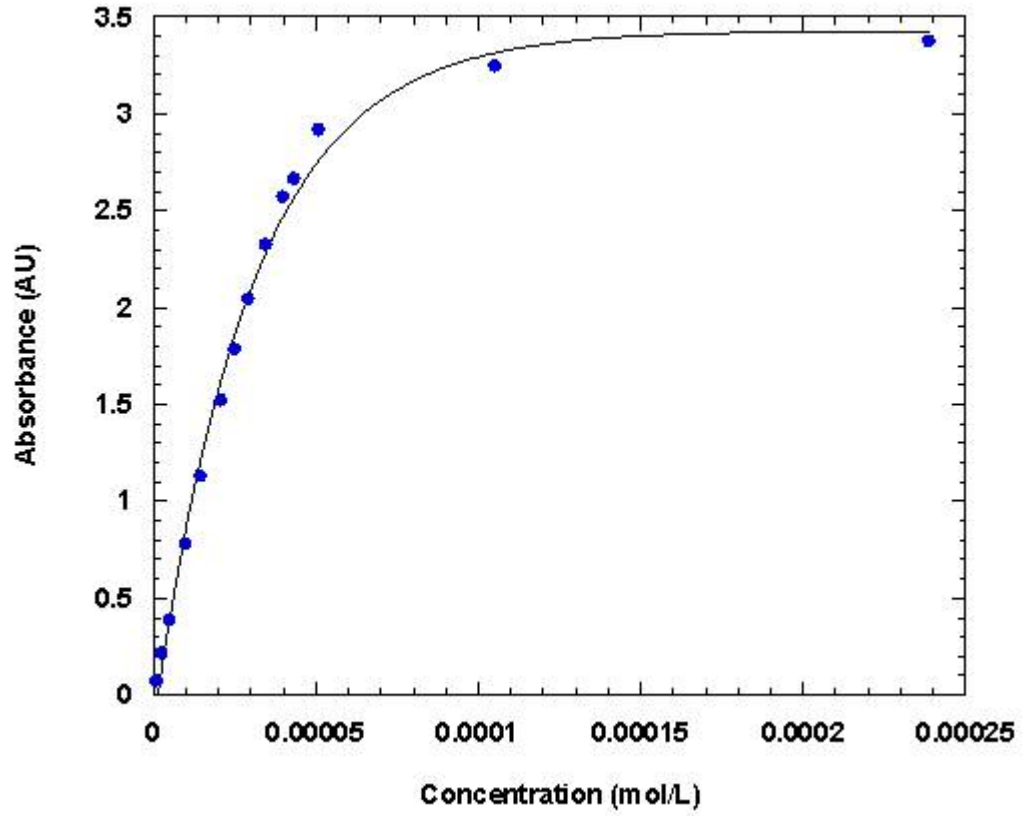

Figure 5.2: Calibration curve of absorbance verses methylene blue concentration

The linear portion of this curve, which corresponds to Beer's law for the relationship between absorbance and concentration, falls below a concentration of 3.5×10^{-5} $mol\ L^{-1}$ and is plotted in Figure 5.3. When fitted to a straight line through the origin a high determination coefficient (R^2) of 0.99 is obtained and the resulting equation relating visible absorbance to concentration is:

$$A = 6.69 \times 10^4 c \tag{5.3}$$

where the slope, $6.69\times10^4 AULmol^{-1}$, is the product of the path length and the absorbtivity which are both constant. The high R^2 value (0.99) allowed for precise determination of concentrations using the resulting equation.

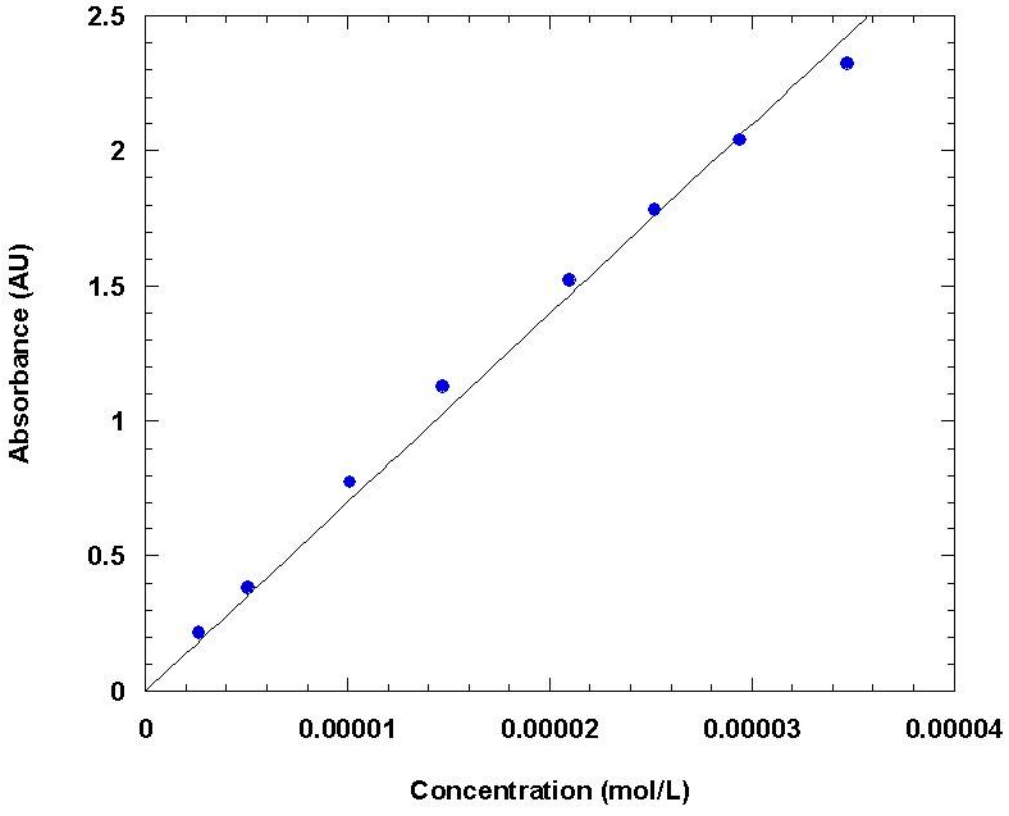

Figure 5.3: Linear calibration curve of absorbance verses methylene blue concentration

The adsorption kinetics of methylene blue on MCC is depicted in Figure 5.4. The adsorption amount is observed to plateau well before 6 hours into the experiment. Subsequent adsorption isotherms were prepared using a 6 hour total adsorption time.

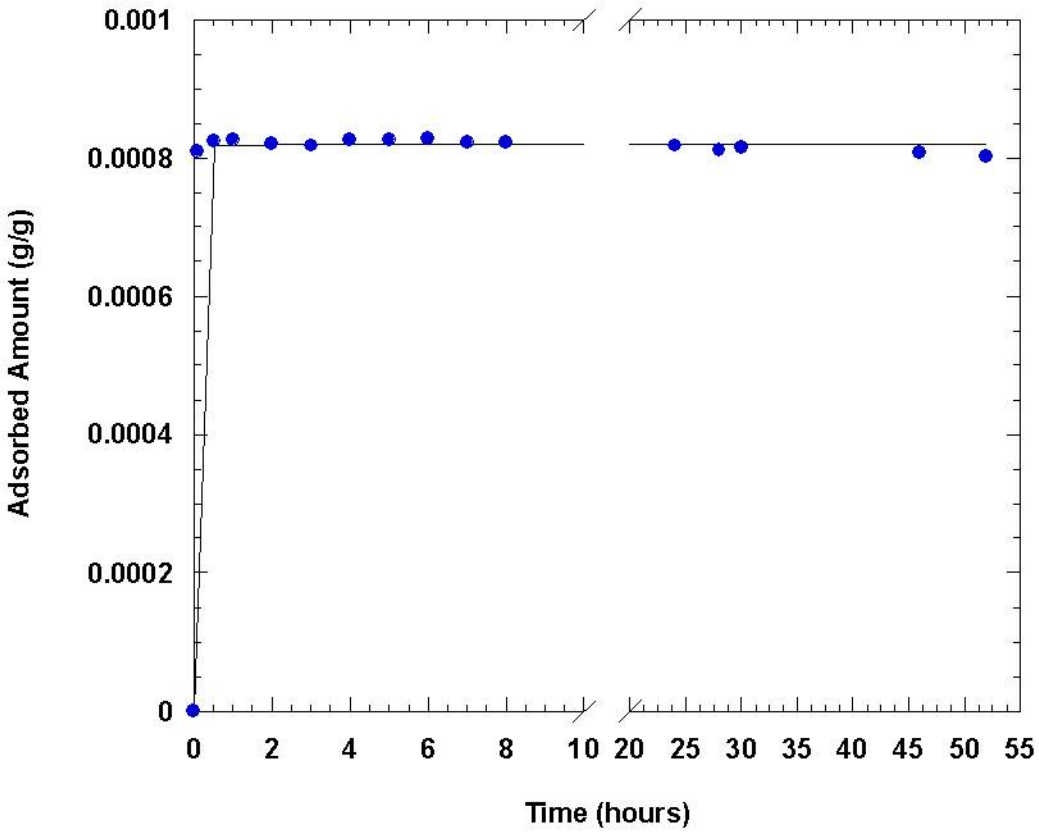

Figure 5.4: Kinetic curve of methylene blue adsorption at room temperature (24±1°C)

The adsorption isotherm for methylene blue on MCC is shown in Figure 5.5. This shape corresponds to Langmuir type adsorption behavior and when fitted to the Langmuir equation for the adsorbed amount N_g:

$$N_g = \frac{2.5C}{1 - 514C} \tag{5.4}$$

where C is the equilibrium concentration, results in a specific surface area of 15.3×10^{-3} $km^2\ kg^{-1}$. This value is compared with previous measurements in Table 5.1.

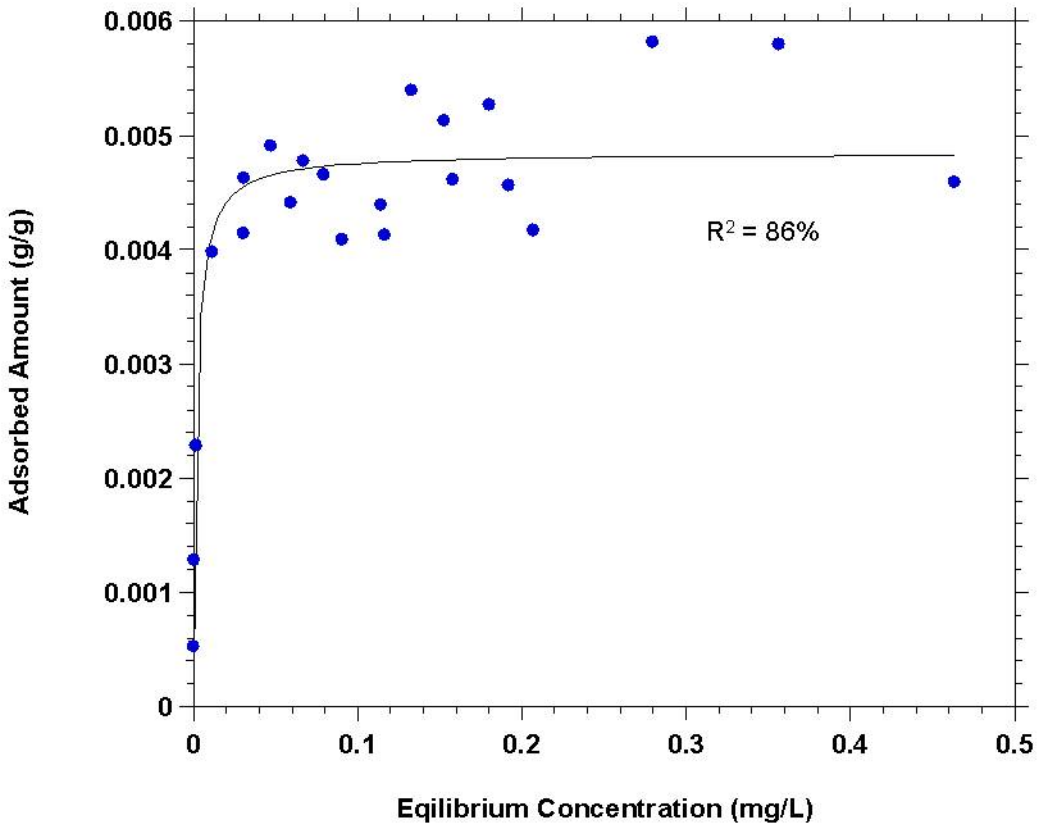

Figure 5.5: Adsorption isotherm of methylene blue at room temperature (24±1°C)

Reasonable agreement was found with the reported specific surface area of Kaewprasit et al. The specific surface areas determined by methylene blue adsorption are considerably higher than those determined by other methods such as BET adsorption [4]. This is attributed to the collapse of pores during the drying techniques used for BET adsorption measurements. Van de Steeg et al. also obtained a similar value through krypton adsorption [10] but through the use of a solvent exchange drying

method which reduced the collapse of pores.

Table 5.1: Specific surface area of microcrystalline cellulose

Source	MCC specific surface area ($10^{-3} km^2 kg^{-1}$)
Experiment	15.3
Van de Steeg et al [10]BET gas adsorption	17
Kaewprasit et al [6]Methylene Blue	13.4
Gustafsson et al [4]Blaine permeametry	0.42
Gustafsson et al [4]BET gas adsorption	1.36

5.3.2 Adsorption of PEOX

The calibration line for PEOX UV-Visible absorbance verses concentration is shown in Figure 5.6 for both the maximum absorbance peak, which was observed to be at 201nm, and for 220 nm.

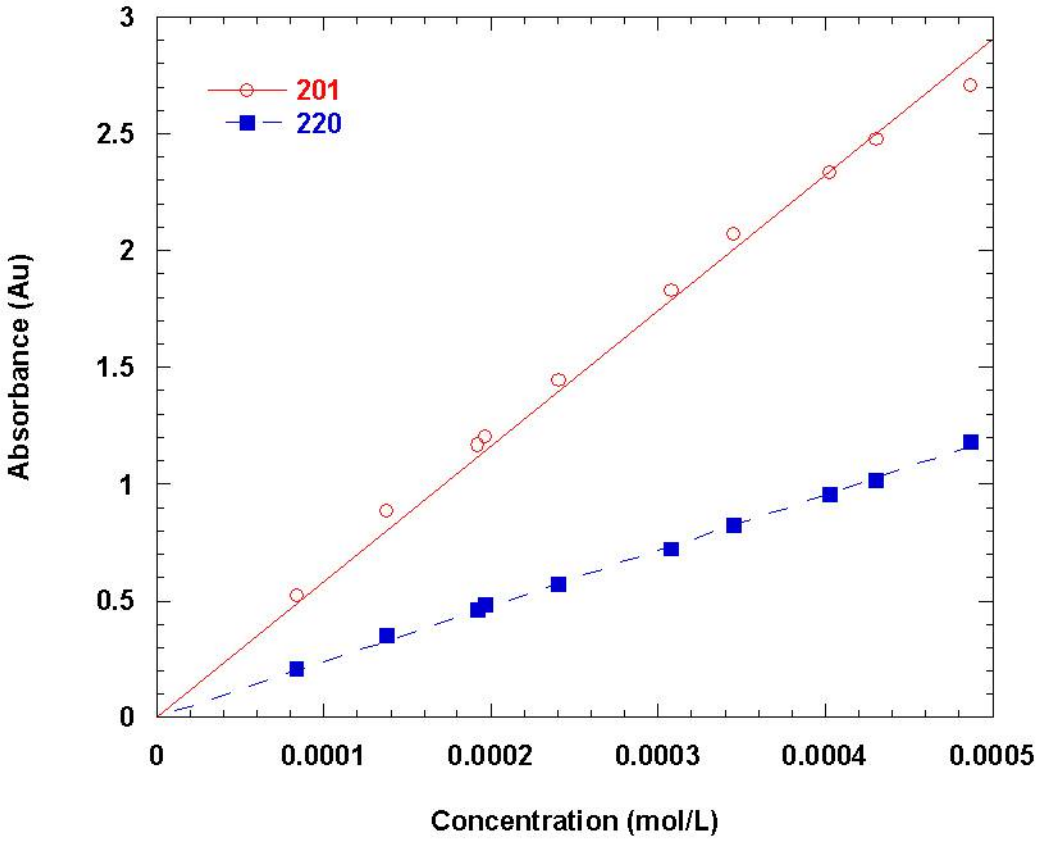

Figure 5.6: Linear calibration curve of absorbance verses PEOX concentration at 201 and 220 nm

The absorbance of NaCl, was found to overlap with the absorbance spectrum of PEOX, as shown in Figure 5.7, so to compensate for this fact the initial concentration before the addition of cellulose was measured after the addition of 0.1M NaCl and UV absorbance at 220nm was utilized for calculating solutions to which NaCl as added. Although 220nm was not a maximum wavelength it calibrated well with PEOX concentration as demonstrated in Figure 5.6.

The MCC was also found to have some residue of water soluble matter with UV absorbance spectrum which overlapped with the PEOX spectra. The absorbance of these residues was measured and subtracted from all UV absorbance spectra for

PEOX. Acid washing of cellulose and alternative pulps should be considered for future experiments.

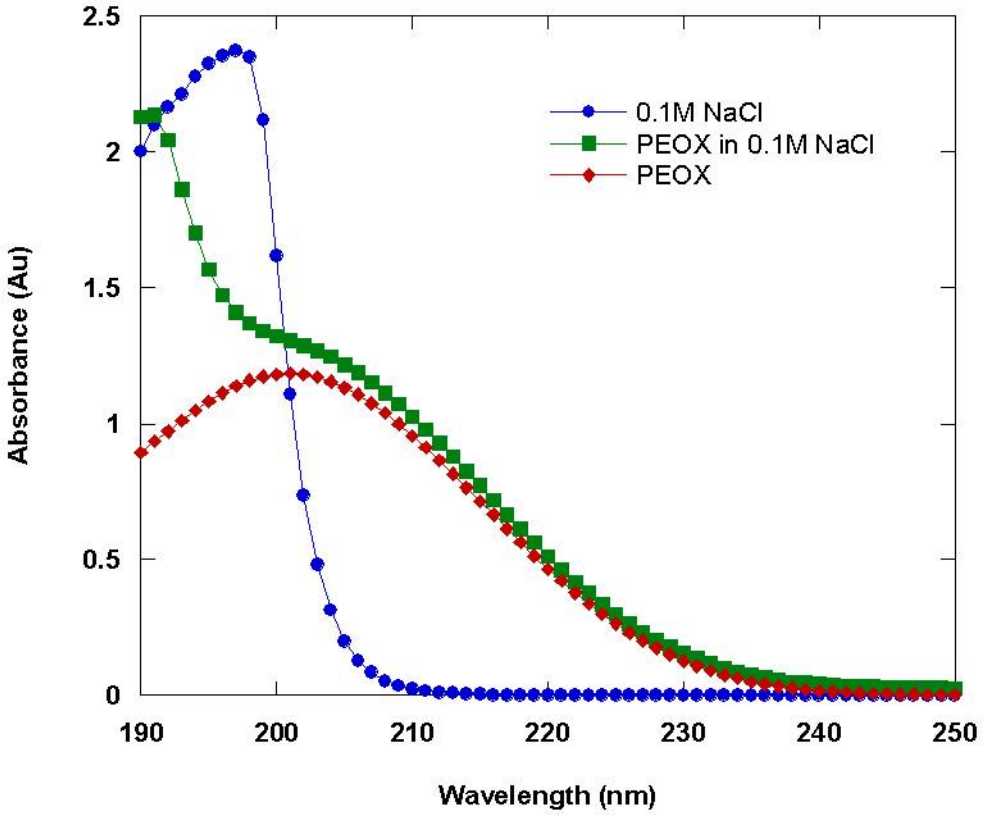

Figure 5.7: UV Absorbance Sectra of PEOX, NaCl and both in water

The adsorption kinetics of $500 kg\ mol^{-1}$ PEOX on MCC is depicted in Figure 5.8. The adsorption amount is observed to plateau by 6 hours into the experiment. Subsequent adsorption isotherms were prepared using a 6 hour adsorption total adsorption time.

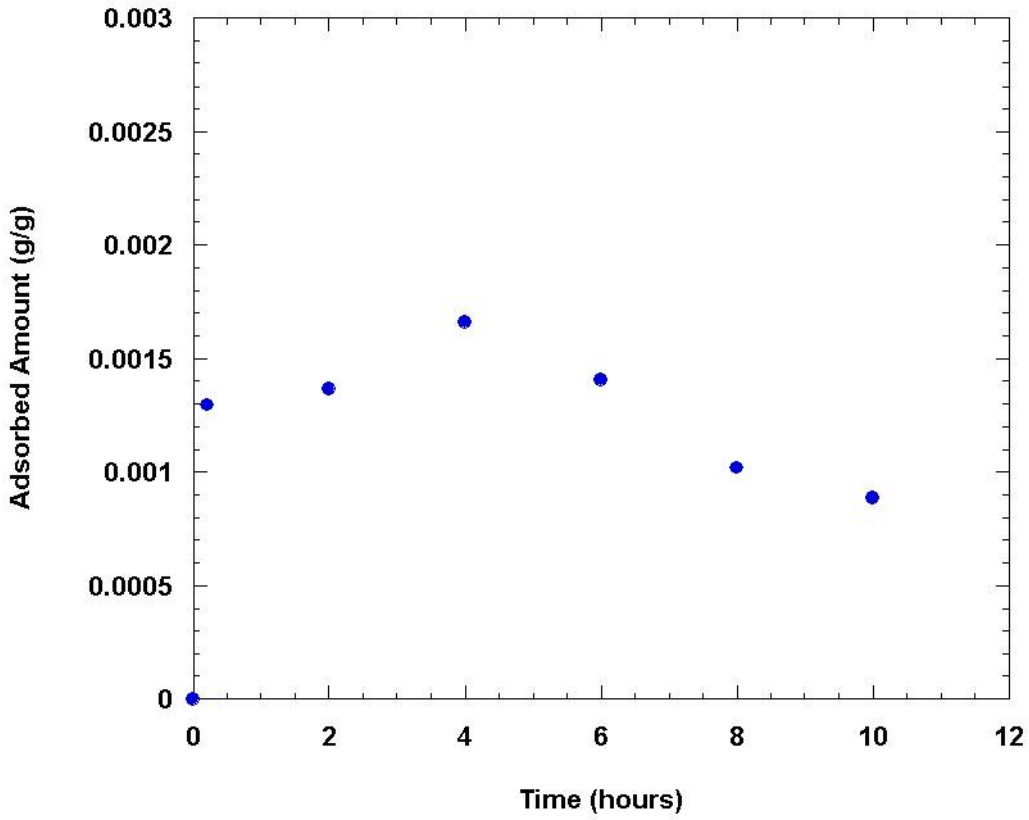

Figure 5.8: Kinetics of PEOX adsorption

The adsorption isotherms for PEOX on MCC from deionized water at room temperature and after the addition of salt and heat are shown in Figure 5.9.

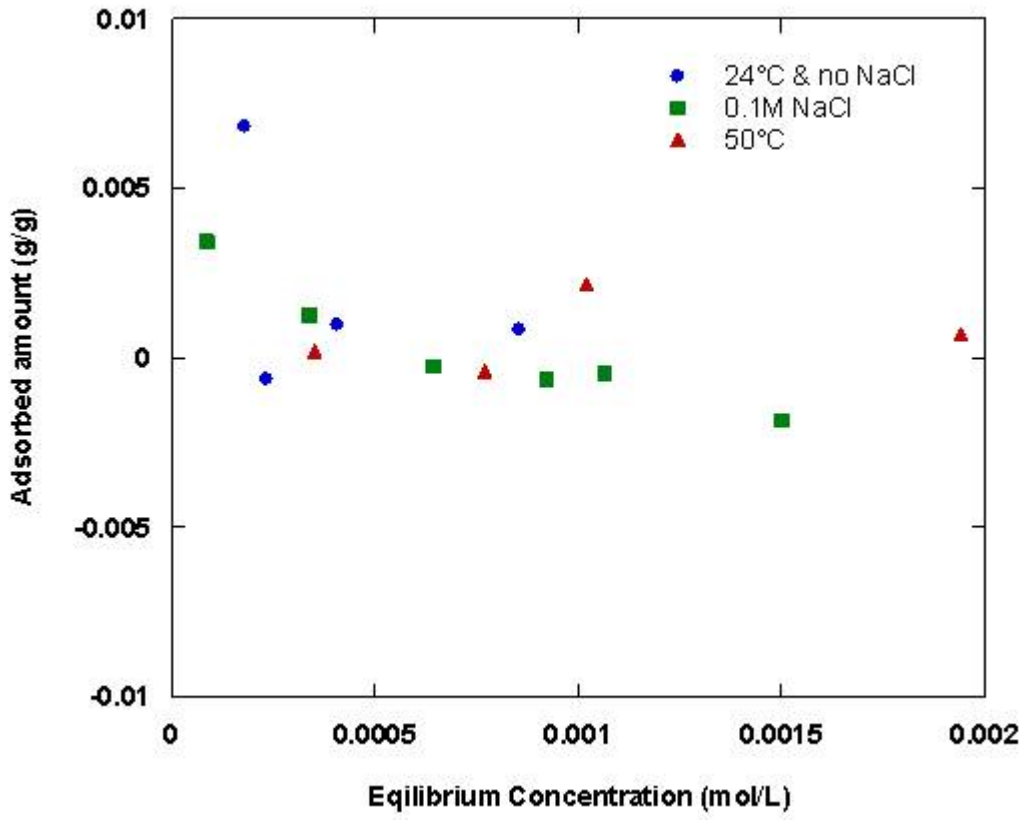

Figure 5.9: Adsorption isotherm of PEOX a. room temperature (24$\pm$1°C) in deionized water b. room temperature in 0.1M NaCl solution and c. 50°C in deionized water.

PEOX was not found to adsorb significantly on MCC even with the addition of NaCl or with increased temperature even after taking into account the experimental error resulting from MCC residues. In order to be useful as a wet-end additive PEOX will need to perform better than additives of similar cost and purpose. When compared with the adsorption of cationic starch on MCC, PEOX does not adsorb significantly. As shown in Table 5.2 the adsorbed amounts for cationic potato starch range from 2 to 30 $mg\ g^{-1}$ [11] as opposed to the less than 1 $mg\ g^{-1}$ for PEOX.

Table 5.2: Comparison of adsorption of cationic starch and PEOX on microcrystalline cellulose

	Adsorbed Amount ($mg\ g^{-1}$)	Adsorbed Amount ($mg\ m^{-2}$)
Experiment	<1	<0.05
Van de Steeg et al [10, 11]	2-30	0.1-2

5.3.3 Flocculation of MCC by PEOX

The results of the settling test of MCC suspensions treated with PEOX are shown in Figure 5.10. Increasing the concentration of PEOX decreases flocculation and promotes dispersion of MCC particles as is evidenced by the decrease in settling velocity with the addition of PEOX.

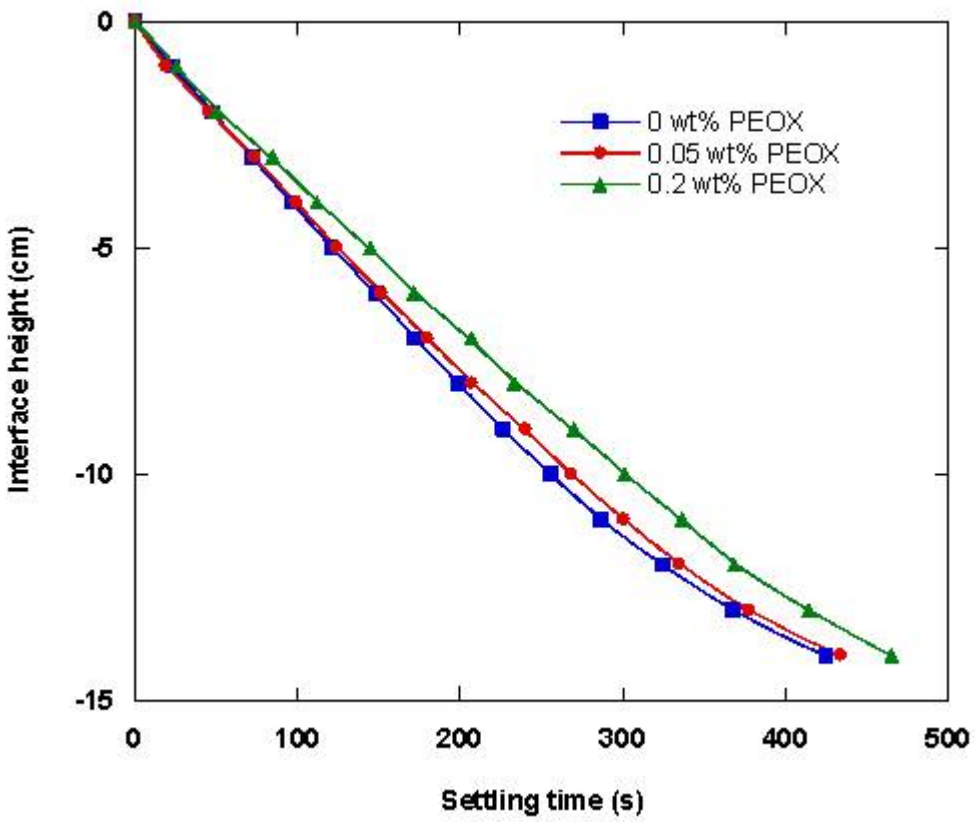

Figure 5.10: Settling curve for 10wt% MCC suspensions with added PEOX to 0.02wt% and 0.5wt%.

5.4 Conclusions

PEOX does not adsorb significantly on microcrystalline cellulose and its adsorption is not improved by the addition of salt or by applying heat to the suspension, although heat and salt reduce the ability of water to dissolve PEOX. This minimal adsorption does not completely exclude the possibility of PEOX adsorbing minimally in order to have useful effects in paper making but reduces the likelihood of such an event. It may be valuable to measure the adsorption of PEOX on cellulose fibers on which it may adsorb better than it does on microcrystalline cellulose. The effect of PEOX on cellulose is that of a dispersant which was reveled by studying setting behavior. It

does not act as a flocculant and would therefore make a poor retention aid in the wet end of paper making.

5.5 References

[1] Biswal, D. R. and Singh, R. P., "Flocculation studies based on water-soluble polymers of grafted carboxymethyl cellulose and polyacrylamide," *Journal of Applied Polymer Science*, vol. 102, no. 2, pp. 1000–1007, 2006.

[2] Graham, D., "Characterization of physical adsorption systems .3. the separate effects of pore size and surface acidity upon the adsorbent capacities of activated carbons," *Journal Of Physical Chemistry*, vol. 59, no. 9, pp. 896–900, 1955. 0022-3654.

[3] Gregg, S. J. and Sing, K. S. W., *Adsorption, surface area, and porosity.* London ; New York: Academic Press, 1982.

[4] Gustafsson, C., Lennholm, H., Iversen, T., and Nystrm, C., "Evaluation of surface and bulk characteristics of cellulose i powders in relation to compaction behavior and tablet properties," *Drug Development & Industrial Pharmacy*, vol. 29, no. 10, p. 1095, 2003.

[5] Ishimaru, Y. and Lindstrm, T., "Adsorption of water-soluble, nonionic polymers onto cellulosic fibers," *Journal of Applied Polymer Science*, vol. 29, no. 5, pp. 1675–1691, 1984.

[6] Kaewprasit, C., Hquet, E., Abidi, N., and Gourlot, J. P., "Quality measurements. application of methylene blue adsorption to cotton fiber specific area measurement. part 1. methodology," *The Journal of Cotton Science*, vol. 2, no. 4, pp. 164–173, 1998.

[7] Lindstrom, T. and Soremark, C., "Adsorption of cationic polyacrylamides on cellulose," *Journal of Colloid and Interface Science*, vol. 55, no. 2, p. 305, 1976.

[8] Sandell, L. S. and Luner, P., "Flocculation of microcrystalline cellulose with cationic ionene polymers," *Journal of Applied Polymer Science*, vol. 18, no. 7, pp. 2075–2083, 1974.

[9] Shirazi, M., vandeVen, T. G. M., and Garnier, G., "Adsorption of modified starches on pulp fibers," *Langmuir*, vol. 19, no. 26, pp. 10835–10842, 2003.

[10] Van de Steeg, H. G. M., de Keizer, A., Stuart, M. A. C., and Bijsterbosch, B. H., "Adsorption of cationic amylopectin on microcrystalline cellulose," *Colloids and Surfaces A: Physicochemical and Engineering Aspects*, vol. 70, no. 1, p. 77, 1993.

[11] Van de Steeg, H. G. M., de Keizer, A., Stuart, M. A. C., and Bijsterbosch, B. H., "Adsorption of cationic potato starch on microcrystalline cellulose," *Colloids and Surfaces A: Physicochemical and Engineering Aspects*, vol. 70, no. 1, p. 91, 1993.

[12] Van de Ven, T. G. M., "Association-induced polymer bridging by poly(ethylene oxide)-cofactor flocculation systems," *Advances in Colloid and Interface Science*, vol. 114-115, pp. 147–157, 2005.

[13] Wagberg, L. and Hagglund, R., "Kinetics of polyelectrolyte adsorption on cellulosic fibers," *Langmuir*, vol. 17, no. 4, pp. 1096–1103, 2001.

[14] Wagberg, L., Odberg, L., Lindstrom, T., and Aksberg, R., "Kinetics of adsorpton and ion-exchange rections during adsorption of cationic polyelectrolytes onto cellulosic fibers," *Journal of Colloid and Interface Science*, vol. 123, no. 1, p. 287, 1988.

[15] Winter, L., Wagberg, L., Odberg, L., and Lindstrom, T., "Polyelectrolytes adsorbed on the surface of cellulosic materials," *Journal Of Colloid And Interface Science*, vol. 111, no. 2, pp. 537–543, 1986. 0021-9797.

CHAPTER VI

CONCLUSIONS AND RECOMMENDATIONS

6.1 Conclusions

Molecular modeling has been used to understand the molecular behavior of a polymer solution system and in turn predict its applicability in various applications. More specifically this work has probed the conformation of poly(2-ethyl-2-oxazoline) in aqueous solution to determine its ability to adsorb on cellulose and its usefulness as a paper making additive. Gaining a molecular level understanding of polymer solution behavior in turn leads to prediction of macroscopic behavior and the discovery of additional uses for polymer solutions. The following conclusions may be drawn:

1. Poly(2-ethyl-2-oxazoline) does not form a rigid rod helical structure in water as was suggested by the pronounced entropy of solution.

   This was confirmed by the scaling of the intrinsic viscosity with molecular weight which corresponded with that of a random coil. Helices which collapse into a coiled tertiary structure were found through molecular simulation and these helical conformations may exist while agreeing with the random coil scaling which was obtained from viscometry measurements. This means that even with the random coil scaling in solution, secondary helical structure cannot be completely discounted. While hydrogen bonding with the carbonyl group on the PEOX side chain does determine the extent to which water molecules are organized around the polymer, this effect is not necessarily the result of a helical conformation.

2. Poly(2-ethyl-2-oxazoline) does not adsorb well onto microcrystalline cellulose

and does not act as a flocculant for microcrystalline cellulose particles.

PEOX was not found to have a rigid helical structure but both the folded helical structure and more random structures examined are fairly compact accounting for a smaller loss of entropy upon adsorption. Without the rigid predicted structure, however, it is not surprising that PEOX does not adsorb well on microcrystalline cellulose. Its adsorption is also not improved by increasing the electrolyte concentration or temperature although, heat and salt reduce the ability of water to dissolve PEOX.

Poor adsorption reduces the likelihood of PEOX adsorbing well enough on cellulose to be a useful paper making additive. Settling experiments reveal that PEOX is not a good flocculant for microcrystalline cellulose but acts as a dispersant.

3. Poly(2-ethyl-2-oxazoline) forms a random coil conformation in aqueous solution

We originally hypothesized that PEOX formed a conformation other than a random coil which was stabilized by hydrogen bonds and only in water. This investigation has shown that in fact helical conformations exist which could be present in solvents other than water. Although the structure may not be entirely stabilized by water molecules, the side chain carbonyl groups of PEOX provide opportunity for hydrogen bond bridges and complex networks of water. Comparing this folded helical conformation to a random coil conformation reveals that the random coil produces a lower energy system in water and can account for the network of water molecules which would explain the negative entropy of mixing. A stronger electrostatic interaction exists between water and the helix and water molecules are more constrained around the polymer chain according to the displacement of molecules during dynamics simulation.

The conformation with secondary helical structure is similar to a folded peptide or poly(N-substituted glycine) (peptoid) and may be present in both water and in organic solvents such as THF since it is a conformational phenomenon and not dependent on inter chain hydrogen bonding. Although these helices are a structural possibility, random coils are more energetically favorable in vacuum and in aqueous solution.

As was mentioned, the scaling of the intrinsic viscosity with molecular weight corresponded with that of a random coil although molecular simulation revealed that helical conformations may exist while agreeing with the random coil scaling which was obtained from viscometry measurements.

PEOX was found, through viscosity measurements to collapse in the presence of sodium chloride. This effect may be explained by the screening of hydrogen bonds with an electrolyte which reduces water's solvation abilities leading to PEOX salting out.

The greater understanding of PEOX structure obtained from this work will enable more educated use of poly(oxazolines) in their current applications and possibly inspire additional applications. The investigation of cellulose adsorption is an excellent case study of this effect because the conclusion that PEOX did not form a rigid rod in turn predicted that adsorption would be limited.

6.2 Recommendations

1. The effect of changes in pH of PEOX adsorption should be investigated, since as with temperature and electrolyte concentration pH changes may have interesting effects on conformation.

2. Circular dichroism of PEOX is not feasible because of the lack of a chiral group. The substitution of the ethyl group on the side chain with a large group, such

as a phenyl group, which would create a chiral center should facilitate closer examination of poly(oxazoline) structure [1]. This additional group, however, may be expected to alter molecular structure rather than function as an simple label. In fact, in peptoids, added large chiral groups are often what stabilize secondary helical structure. As shown in the molecular simulations of this study, helical structures have lower bonded energy values than more random structures. Altered side groups with sufficient steric influence may actually stabilize helical configurations.

3. Synthesis of PEOX samples with narrow molecular weight distributions could be done in order to attain static light scattering data for PEOX in water. This will provide radius of gyration as well as second virial co-efficient values in order to better characterize PEOX structure. In addition the effects of salt and temperature on the structure could be analyzed.

4. Adsorption of PEOX on cellulose may be improved by the use of a cofactor, as is the case with poly(ethylene oxide), or may enhance other retention aid systems. An investigation into potential cofactors is recommended.

5. The adsorption of a nonionic polymer depends on its properties as well as the type of cellulose fibers. A variety of cellulose fibers are used in various papermaking processes and a study should be done using a range of fibers with varying properties to assess the adsorption of PEOX on the various types.The adsorption of PEOX on a range of cellulose fibers should be measured since adsorption may occur to a greater extent on other forms of cellulose.

6. Despite the poor adsorption of PEOX on cellulose and the results of settling experiments, flocculation studies to examine floc size to confirm that no improvements are made to cellulose particle agglomeration by PEOX. This may

be particularly necessary if adsorption studies on other forms of cellulose reveal a greater tendency to adsorb.

7. As a paper making additive the dispersant properties of PEOX and their possible implications should be examined

6.3 References

[1] Oh, Y. S. and Yamazaki, T. and Goodman, M., "Syntheses and circular dichroism (CD) spectra of optically active polyoxazolines and their model compounds," *Macromolecules*, vol. 25, no. 23, pp. 6322–6331, 1992.

‘